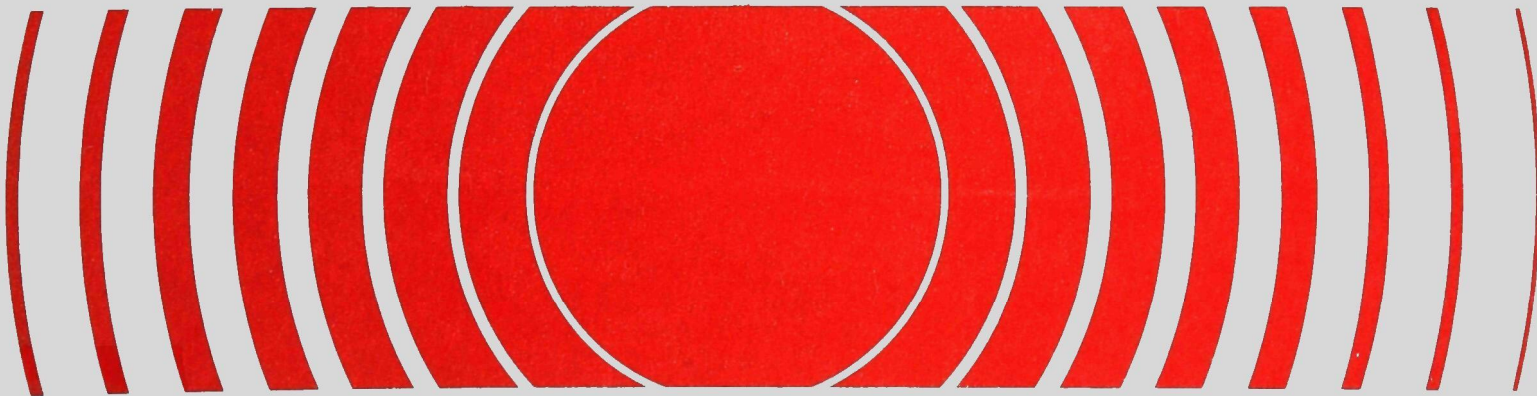




Radiological Data Analysis in the Time and Frequency Domain

Prepared for EPA by
AUBURN UNIVERSITY AT
MONTGOMERY UNDER EPA
CONTRACT No. 68-02-3049



RADIOLOGICAL DATA ANALYSIS IN THE
TIME AND FREQUENCY DOMAIN

by

Dr. Donald A. Chambless
Department of Mathematics
Auburn University at Montgomery
Montgomery, AL 36117

Contract No. 68-02-3049

EPA Project Officer: Dr. Jon A. Broadway

Prepared for
Environmental Protection Agency

DISCLAIMER

This report was furnished to the Environmental Protection Agency by Auburn University at Montgomery, Montgomery, Alabama, in fulfillment of Contract No. 68-02-3049. The contents of this report are reproduced herein as received from the contractor. The opinions, findings, and conclusions expressed are those of the author and not necessarily those of the Environmental Protection Agency. Mention of company or product names is not to be considered as an endorsement by the Environmental Protection Agency.

TABLE OF CONTENTS

	Page
I. INTRODUCTION.....	1
II. SUMMARY.....	4
III. CONCLUSIONS.....	11
IV. RECOMMENDATIONS.....	13
V. SECTION 1: NOISE REDUCTION VIA FREQUENCY DOMAIN ANALYSIS.....	16
VI. SECTION 2: GENERAL CONSIDERATIONS IN RESOLUTION IMPROVEMENT.....	29
VII. SECTION 3: QUADRATURE METHODS AND SINGULAR VALUE ANALYSIS.....	32
VIII. SECTION 4: GENERAL PHILOSOPHY OF REGULARIZATION METHODS.....	35
IX. SECTION 5: DISCRETE IMPLEMENTATIONS OF REGULARIZATION.....	37
X. SECTION 6: CONTINUOUS/DISCRETE REGULARIZATION.....	43
XI. SECTION 7: THE PROBLEM OF D.L. PHILLIPS.....	49
XII. SECTION 8: APPLICATION TO Ge(Li) SPECTROMETER DATA.....	92
XIII. BIBLIOGRAPHY.....	138

INTRODUCTION

The accurate measurement of levels of environmental pollutants is a matter of central importance to the United States Environmental Protection Agency. However, the level of radioactivity encountered in samples of man-related nuclide pollutants is typically exceedingly low, and the highly sensitive state-of-the-art instrumentation employed in detection work becomes (because of its very sensitivity) affected not only by the radiation of interest but also by many other background radiation effects, as well as random effects. Currently, then, it may often be desirable to apply data enhancement techniques (of an analytical nature) to the raw instrumentation data.

There are two types of enhancement of the data which may be considered in any given application. First of all, any instrument data record typically shows the presence of two signal components: a deterministic component, which reflects the "genuine" informational content of the data record, and a random component which results from stochastic behavior of the basic phenomena. Usually one would like to separate these "signal" and "noise" components and retain only the former. It is often possible to partially achieve this objective using methods described in Section 1. Secondly, even assuming that a noise-free data record from the analyzer has been produced, there still may be an unsatisfactory level of resolution of the recorded signal due to simple inadequacy of the resolving capacity of the detector and instrument system. In such a case, if quantitative measurements are to be obtained then resolution improvement of the record through analytical means must be achieved; this is, both in principle and practice, a much more difficult proposition, as the details of this report

will amply demonstrate.

This report contains an outline of work accomplished under EPA Contract Number 68-02-3049 during the year beginning with September 27, 1978. Under the provisions of this contract, into which Auburn University at Montgomery and the Eastern Environmental Radiation Facility ("EERF") of the U. S. Environmental Protection Agency entered, the author was contracted to devote approximately two-thirds of the year mentioned to an investigation of the characteristics of gamma radiation data from Ge(Li) spectrometers and the applicability of data enhancement techniques (of the two types outlined above) to this data. Under the provisions of this contract the author travelled the short distance from the university to EERF after completing classes, office hours, etc. Thus the actual contract work was largely accomplished at the laboratory site, with immediate access to not only the instrumentation of interest but also the computing and library facilities of EERF and, most importantly, the continual coordination and supervision of the Project Officer. It is felt that this was a most efficient manner of administering the project, both in terms of minimizing costs and maximizing the effectiveness of the technical supervision. In particular, the contract overhead rate was only twenty per cent.

Work done jointly by the author and the Project Officer during their investigations related to the contract research topic have resulted in a number of accomplishments. These are summarized in the following:

- (1) D.A. Chambless and J.A. Broadway, Fourier Transform Methods for Analysis of Ge(Li) Spectral Data, Presented to the Health Physics Society, Atlanta, GA, July 6, 1979.
- (2) D.A. Chambless and J.A. Broadway, Digital Filtering of Speckle

Interferometric Data, Presented to the Society for Experimental Stress Analysis, San Francisco, CA, May 23, 1979.

- (3) Jon A. Broadway and Don A. Chambless, Spectral Resolution Improvement via Regularization Methods and Singular Value Decomposition, Presented to the Health Physics Society, Philadelphia, PA, July 11, 1979.
- (4) D.A. Chambless and J.A. Broadway, Digital Filtering of Speckle-Photography Data, Published in Experimental Mechanics, Vol. 19, pp. 286-289, August, 1979.
- (5) J.A. Broadway and D.A. Chambless, Resolution Improvement of Gamma Radiation Spectrometer Data, Presented to the International Symposium on Ill-Posed Problems: Theory and Practice, Newark, DE, October 2, 1979.
- (6) J.A. Broadway and D.A. Chambless, Constrained Regularization Methods for Spectral Resolution Improvement (manuscript in preparation).

Finally, it should perhaps be noted that the original proposal submitted contained also a proposal for an optional one-year extension of the contract effort. At this writing, the Office of Radiation Programs has exercised its option and effected such an extension. Therefore, the work begun under this contract arrangement will be continued for another two-thirds man-years and a report pursuant to that work and extending the work reported herein will be forthcoming in September 1980.

SUMMARY

As mentioned in the Introduction, the work conducted in this contract effort consisted primarily of feasibility studies concerned with the reduction of noise levels and the improvement of resolution of radiation spectra recorded by Ge(Li) gamma spectrometers. The methods investigated in the course of this work included a number of techniques already recognized in the literature as well as some not yet appearing (to the knowledge of the author). Closely related problems in other fields ranging from photographic enhancement to forensic science to historical document restoration have been considered in certain instances. These efforts were made so as to allow comparison of the methods considered under this contract activity with other existing methods and to provide a background of results with "well-known" problems for consideration.

The noise reduction problem is considered in Section 1 of the main body of this report. In this section the foundations of a frequency domain approach to noise suppression are described. Under the assumptions concerning the data detailed in this section, considerable increase of signal-to-noise ratio is often achieved through the application of the methods described, especially when the deterministic component of the composite signal represents a function which can be well approximated by low order trigonometric polynomials. On the other hand, if a signal should be qualitatively characterized as, say, the superposition of a linear background and a low order trigonometric polynomial plus noise then one would expect that the removal of the linear trend (through standard least squares methods) would be necessary as a preprocessing procedure before the filtering methods of Section 1 are applied; this expectation is based on the fact

that the linear carrier signal is not at all well approximable through lower order Fourier expansions.

In any case, the methods of Section 1 are found to be very inexpensive to implement due to the availability of very efficient ("fast") Fourier transform algorithms. In actual application, the speed and convenience of the use of the techniques are very dependent upon access to efficient graphics equipment and software. Unhappily, there has been no opportunity for such use of high-speed graphics during the course of this study, and so the number of applications actually included herein is rather small. Nonetheless, some rather striking results were obtained, as a comparison of Figures 1.1 and 1.5, for example, reveals, and the quality of these enhancements has been recognized through the publication of [6].

In Section 2 the mathematical generalities concerning the problem of attempting to analytically enhance an analyzer data record by correcting for limitations in instrument resolution characteristics are given and the specific conceptual problems of interest are stated. In Section 3 the futility of straightforward quadrature approaches to this exceedingly difficult problem is suggested (although specific indication of this is delayed until Section 7), and the singular value decomposition of a matrix is formulated and its importance discussed. In particular, the singular value analysis approach to the solution of ill-posed linear problems, which has found considerable popularity among those investigators considering the processing of photographs [23, 24], is motivated and described.

The major concentration of effort in this contract endeavor came to be the study and application of the family of "regularization" methods [22, 27-30] for the solution of ill-posed linear operator equations. The

general conceptual framework of regularization methods is given in Section 4, and a number of discrete implementations of regularization are formulated in Section 5. All of the methods of Section 5 are basically matrix-theoretic. Some employ the difference operator in order to allow (discrete) considerations of the first (or higher) derivatives of the functions of interest to be included while the most basic form of discrete regularization does not. Later (in Section 7) the effect of this higher generality is examined. Although there appears to be some advantage in including consideration of one or more derivatives in regularization calculations, there was not a generally marked improvement in the quality of the results noticed while, on the other hand, the cost of doing "differential regularization" was significantly higher. It is known that more efficient algorithms for these advanced methods can be developed (with an additional expenditure of time) but there seemed to be no justification for embarking on such an effort at this point.

In Section 6 a form of regularization [32] ("CDR regularization") which represents a very significant conceptual advance over the discrete methods of Section 5 is discussed at some length. During the course of this contract year this was actually the first form of regularization which was considered, and considerable time and effort were devoted to this aspect of the project. In particular, the method was discretized (as any computational method must eventually be) and applied to model problems such as those in Sections 7 and 8. Results from these efforts showed a striking improvement over the singular value analysis (and harmonic analysis) solution attempts which had been previously conducted. Similarly, the subsequent discrete regularization calculations (using Simpson's rule

to perform quadratures as previously) were not nearly of the quality of the results using the methods of Section 6. Sometime later it was discovered that Simpson's rule itself was causing significant degradation of the results obtained through singular value analysis or discrete regularization (as compared to those achieved by means of the simple rectangle rule, for example). Of course, one ordinarily thinks of Simpson's rule as being generally more accurate than the rectangle rule for most usual types of functions, and hence an adequate explanation of this phenomenon is not immediately apparent. (An indication of the reason for this is given in Section 7.) In any case, the CDR method was found to give results of about the same quality with either quadrature rule and therefore appears much more powerful (for the types of problems being considered) than the methods of Sections 3 or 5. A fairly extensive effort was made to lower the initially high cost of the CDR computations and a good deal of success was achieved in this regard; details are given in Section 6.

Sections 7 and 8 are devoted to outlining an indication of typical results obtained with resolution enhancement problems during the course of this contract effort. Two basic types of problems were considered. The first problems, which are discussed in Section 7, are derivatives of the original problem of D. Phillips which was considered in his 1962 paper [22]. In this model problem, which has come to be a classic example in the literature of the field, the resolution improvement of noisy pulse-like data is considered. Since the data of this problem is somewhat typical of the gamma spectral data of ultimate interest in this contract effort and since, also, this problem of Phillips is one of the few prototypes of the field, there was a considerable amount of effort devoted to "sorting out" the

methodology considered during the contract year by means of analytical investigation of Phillips' problem. It was in the course of this work that the sensitivity of the calculations to the selection of the quadrature rule was noticed. Clear indication of this phenomenon is included in Section 7. It is of considerable interest to note that the degradation generally introduced by Simpson's rule was largely overcome by the DER and CDR methods described in Sections 5 and 6, respectively. On the other hand, all of the methods considered (with the notable exception of the simple quadrature and Fourier deconvolution methods) were found to be reasonably capable of handling Phillips' problem when the rectangle rule is used for quadratures.

In Section 8 the second basic type of resolution improvement problem is considered. Here Ge(Li) spectral data from radium sources as recorded by a Nuclear Data ND100 spectrometer are investigated by means of the methodology of Sections 5 and 6 in two basic situations. In the first group of calculations the data used were realized by the superposition of 5% random noise on the impulse response of the spectrometer (as defined by the data record resulting from a monochromatic radium energy line); this was referred to as the "spectral data". The other group of calculations was performed using data from a different radium peak; this data was called the "cross-spectral data". It should be pointed out that although Ge(Li) spectrometers are not generally thought of as shift-invariant devices, it was felt that this was a reasonable assumption herein due to the small energy ranges considered in Section 8.

With both of these sets of data it was found to be exceedingly difficult to produce a result sharply approximating the ideal discrete pulse for which one might hope under perfect circumstances. The instability of the

basic problem per se is such that even a few per cent noise superposed on the impulse response causes extreme computational difficulty and results closely approximating the ideal one seem impossible to obtain without some further modification of the problem statement beyond that provided by the various regularization techniques. Two such modifications were considered, the first representing a "compromise" problem statement and the other involving the imposition of constraints on the computed solution.

The compromise used was effected by selecting a Gaussian pulse with half-width significantly smaller than that of the impulse response of the analyzer and then modifying the problem statement such that the ideal solution of the modified problem* consists of this selected Gaussian. Philosophically, one may view this as solving for a certain moment of the solution instead of the solution, per se. This "data spreading" method was found to increase the stability of the calculations in Section 8 while not causing any large increase in the computational costs. The relevant comparison can be drawn from Figures 8.8 and 8.11, for example. On the other hand, a second modification of the problem was constructed by explicitly incorporating the a priori knowledge of nonnegativity of the solution. Very striking improvements in the stability and sharpness of the results obtained were found to be gained through this type of consideration as Figures 8.38 and 8.40 reveal. There was no remaining time in which to

*C. Nelson of the Environmental Analysis Division, Office of Radiation Programs, suggested that such a modification be considered.

conduct further calculations of this type and thus spectra larger and more complex than those indicated in Section 8 have not yet been considered at this writing. The conduct of such larger scale investigations will be an early topic in the work of the year of continuation of this contract effort.

CONCLUSIONS

Two types of enhancement procedures for Ge(Li) gamma spectral data have been considered under this contract effort: noise reduction techniques and resolution improvement methods. In the case of noise reduction the results of Section 1 (as observed, for example, by comparison of Figures 1.6 and 1.7) show that very significant increases in signal-to-noise ratio can be obtained by means of fast (and inexpensive) frequency domain procedures (under certain hypotheses concerning data and noise characteristics). One does have to make a significant effort in software development in this regard and high-speed graphics equipment is an almost essential component when processing data using this methodology. In this regard it is implicit, of course, that the analyzer being used is calibrated to sample along a sufficiently fine energy grid so as to allow the difference between signal and noise characteristics to be discerned in the frequency domain. The results shown in Section 1 were obtained using high gain settings over a limited energy band. Since analyzers with larger storage capacity are becoming available, it should become a routine matter to use high gain calibrations over broad energy ranges, and increasingly successful separation of signal and noise in Ge(Li) data should become possible.

In Sections 7 and 8 the extremely unstable nature of the resolution improvement problem is clearly revealed and some promising developments are in evidence. The family of regularization methods has been found to offer some promise for controlling the degrading effects of noise, roundoff error, etc., and, in particular, the CDR method outlined in Section 6 appears to be especially capable of resisting the oscillatory effects of noise. In all of these methods there appear in the basic formulation one

or more parameters which effect the compromise between the considerations of residuals and size or smoothness. For the present time the inclusion of these parameters appears to be indispensable but one would, of course, prefer that such need not be chosen in an interactive fashion. There is some encouraging evidence in the literature [32-34] which suggests that one may eventually be able to devise mathematical routines which allow a good selection of the smoothing parameters from the data of the problem. This would have the most desirable effect of eliminating human interaction with the program and permit routine production-like application of the methods to take place.

The imposition of nonnegativity constraints which was further required in order to stabilize the resolution improvement calculations in Section 8 seems to be completely necessary at the present time. Without the use of such a priori information none of the methods considered thus far is capable of yielding significant levels of resolution improvement of the spectral analyzer data without incurring degradation (due to noise effects) unacceptable for the applications eventually desired. Happily, this causes only minor inconvenience and small additional expense in conducting computations. It should be noted that the principle of imposing nonnegativity constraints in order to achieve a higher level of numerical stability should find beneficial applications in a wide variety of physical measurement and data transmission problems in which positive-valued intensity data are the subject of concern. Larger scale calculations with these methods will be conducted during the coming year of extension of this contract endeavor.

RECOMMENDATIONS

An overall analysis of the results of work conducted under this contract effort suggests certain general recommendations concerning the direction of work dealing with improvement of techniques for processing of gamma radiation data. First of all, continued progress in the power of the Ge(Li) analyzers is of central concern in regard to the problem of enhancing gamma data since increased analyzer power is reflected in an increased ability to define the photopeaks distinctly and thereby allow successful separation of signal and noise (through methods such as those described in Section 1). A somewhat paradoxical consequence of these observations, which has not yet been adequately considered in the literature of nuclear detection, is that although the achievement of very high levels of system resolution typically leads one to anticipate that a photopeak will be recorded in only a few (perhaps one) data channels, the requirement for computational tractability necessitates that photopeaks be instead recorded in a significantly larger number of channels. Similar comments apply to the resolution improvement methods in Sections 5 and 6. Therefore, it is important to include the instrumentation capability, both in terms of system resolution (keV at FWHM) and system gain (keV per channel), explicitly when discussing any path to progress in gamma data reduction techniques.

In regard to mathematical and computational aspects of continued work, it would seem that the constrained regularization methods represent the most versatile and promising family of techniques for resolution improvement of the gamma spectral data among those methods considered thus far. Thus it is recommended that the methods of Sections 5 and 6 be tested on a larger scale using, in particular, more complex gamma spectra as the subject data. In order to make such increased level of complexity of test

computations practicable it will be necessary to make a software conversion of all procedures from the M-LAB language to a less versatile but more inexpensive language such as FORTRAN. This unfortunate situation is due to the small size of the matrix calculations permitted by M-LAB and, especially, due to the exorbitantly high cost of using this program on the ADP, Inc. network. In the course of this work the capabilities and limitations of the data spreading and constrained regularization techniques should be investigated more thoroughly and alternate methods of stabilizing the calculations considered if necessary.

Throughout this contract work only single step and finite iterative methods (singular value analysis) have been considered. This is in accordance with the major emphasis of the literature of the field of resolution improvement problems in general. There are, however, certain iterative procedures which could be advantageous, and it is recommended that these be given some consideration. In this case it is anticipated that M-LAB computational costs may prove to be not unduly excessive and thus this path of quick feasibility study of iterative schemes is recommended.

For many types of early stage software development processes the M-LAB program can be extremely beneficial. The matrix capabilities are so convenient and facility with the language so easy to acquire that initial feasibility studies concerning linear methods can often be conducted extremely quickly. It is very unfortunate that the use of M-LAB is currently confined to the PDP-10 family of computers and it is recommended that support be given to the structuring of an M-LAB program in a more portable compiler.

Finally, due to the basically visual nature of the enhancement task

addressed in this contract work, graphics capability is a simple necessity. As mentioned previously, the lack of high speed graphics capability at the laboratory site has constituted a severe limitation and major obstacle of progress of the contract work. Therefore it is recommended that the Eastern Environmental Radiation Facility be fully supported in its attempt to acquire quality high speed graphics with large color screen capability and the associated software services. This equipment would also, of course, prove extremely beneficial in countless other aspects of the work of the laboratory besides those related to gamma data reduction.

SECTION 1. NOISE REDUCTION VIA FREQUENCY DOMAIN ANALYSIS

In this report, the term "linear filter" is used to refer to a process L which operates upon a given input signal f to produce the output signal $g = Lf$ in accordance with the following model:

$$g(e) = \int_{-\infty}^{\infty} h(e, E) f(E) dE ; \quad (1.1)$$

here the kernel function h is characteristic of the particular linear filter in question. In this section the additional hypothesis that h is a difference kernel will be stipulated; thus $h(e, E) = k(e-E)$ for some function k . Under this latter hypothesis (1.1) becomes an equation of convolution type and one often writes $g = k*f$ to represent this situation. If $k(x) = 0$ for all $x < 0$ then the process L is called "realizable" since then the output signal level $g(e)$ (at a given energy level e) is dependent only on the behavior of the input signal at energy levels less than e . Although this assumption of realizability is almost always made in usual filtering work concerned with time-variant signals, it is not applicable to the present endeavor and, in fact, none of the filters which are of interest here are such realizable ones. General background on linear filters can be found in [2, 17, 18]; work related to that in this section has appeared in [3, 16, 33].

The Fourier transformation concept holds the key to the filter design process which has proved fruitful in this work. If $g = k*f$ and capital letters are used to denote the respective Fourier transforms then one has $G = KF$ [2]. Specifically, if

$$G(\epsilon) = \int_{-\infty}^{\infty} g(e) \exp(-2\pi i \epsilon e) de$$

then

$$G(\epsilon) = K(\epsilon) F(\epsilon) ; \quad (1.2)$$

thus the unwieldy convolution process originally indicated can be replaced by the much more tractable multiplication operation, as indicated, by passing to the "frequency" domain via the Fourier transform.

It is assumed that the signal f , representing the output from a spectral analyzer, is the sum $f = d + n$ where d is the desired "pure" spectral information and n is the noise superposed on d due to random variations in the analyzer behavior, etc. Again following the above convention with respect to capitol letters and Fourier transforms one obtains $F = D + N$ (due to the linearity of the transform). It is to be expected that $F(\epsilon)$ is approximately equal to $N(\epsilon)$ for larger values of ϵ ; this is due to the expectation that $D(\epsilon)$ will be negligibly small for large ϵ due to the highly correlated nature of d . This expectation forms the basis of the following procedure for increasing the signal-to-noise ratio.

The impulse response k of the filter is constructed by means of the following considerations relative to its transform K :

- (1) For small values of ϵ , $K(\epsilon) = 1$
- (2) For large values of ϵ , $K(\epsilon) = 0$
- (3) Beginning at a specified "cutoff frequency" ϵ_c , the values of K change from 1 to 0 along some very smooth curve.

(This last consideration is motivated by the desire to avoid introducing oscillation related to the Gibbs phenomenon in the graph of the output signal g .) Then forming the product $G = KF$ (which is equivalent to performing the convolution $g = k*f$) will sharply attenuate the values $F(\epsilon)$

for ϵ significantly larger than ϵ_c while retaining those values $F(\epsilon)$ corresponding to $\epsilon < \epsilon_c$. By interactive choice of ϵ_c and the transition parameter described below, one hopes in applying this method to increase the signal-to-noise ratio of f while suffering no significant loss of resolution (This enhanced version of f is the g above.)

Details of the Filter Construction and Application

Given the data signal f (as recorded by the spectral analyzer) one first chooses evenly spaced samples f_j thereby determining the sample vector $\vec{f} = [f_0, f_1, \dots, f_{N-1}]$. Then, in principle, the discrete Fourier transform ("DFT") $\vec{F} = [F_0, F_1, \dots, F_{N-1}]$ defined by

$$F_j = \sum_k f_k \exp(2\pi i j k / N)$$

is determined. (This is one of a number of trivially different forms of the DFT which could be used.) Due to the large computational times incurred in the indicated formulation of the DFT (for large N) the actual computation is carried out by means of a fast Fourier transform ("FFT") [26]; this is true of all transforms and inverse transforms referred to in this report and no further explicit mention of this point will be made.

The numbers F_j are complex but the object of interest in the present context is the plot of the quantities $|F_j|$ (the complex modulus) versus the index ("frequency number") j ; in some instances it may be more appropriate to plot the logarithm of the modulus in lieu of the modulus due to the large range of values typically of interest. If the hypothesis that f is the sum of a highly correlated signal d and a noise signal n is satisfied then one will typically observe a transition from the higher

power associated with the smaller frequency numbers to lower levels of power at the larger frequency values. This region of transition is the likely location of the optimum values of the cutoff parameter [18]; the specific choice finally settled upon for a given set of data is accomplished interactively.

The final filter design consideration involves the specific manner in which the transition of the values of K from 1 to 0 takes place. The method which was finally selected for use calls for this transition to occur along a cumulative normal distribution curve with standard deviation given by the parameter σ . Thus, given the choices of the parameters ϵ_c and σ the (piecewise continuous) description of K is given by

$$K(\epsilon) = \begin{cases} 1 & \text{if } \epsilon < \epsilon_c \\ 0 & \text{if } \epsilon > \epsilon_c + 6\sigma \\ 1 - \frac{1}{\sqrt{2\pi}\sigma} \int_{-\infty}^{\epsilon} \exp\left[-\frac{1}{2\sigma^2}(x - \epsilon_c - 3\sigma)^2\right] dx & \text{else.} \end{cases} \quad (1.3)$$

In the program written to accomplish the filtering process the discrete sampling of K is accomplished using a "look-up table" to obtain approximate values of the cumulative normal distribution curve ordinates.

Finally, the DFT \vec{G} of the enhanced version \vec{g} of \vec{f} is obtained by forming the products $G_j = K_j F_j$, and \vec{g} is then determined by means of the inverse DFT as

$$g_j = \frac{1}{N} \sum_k G_k \exp(-2\pi i j k / N).$$

Under the indicated hypothesis, \vec{g} will comprise an enhancement of \vec{f} having increased signal-to-noise ratio. The optimum values of ϵ_c and σ are found

interactively; one finds that the results obtained are normally quite insensitive to small variations in these parameters.

This methodology was first applied to the 1024 channels of light intensity data indicated in Figure 1.1. (This data was kindly provided by W. F. Ranson; it resulted from work conducted in the preparation of [25]). The behavior of the 513 values of the discrete Fourier transform F of this data is indicated by Figure 1.2. In this figure one may observe the expected tendency for the modulus (which is associated with the power of the signal) to steadily decrease with increasing frequency number until a "leveling off" is eventually experienced in the vicinity of approximately frequency number 15 to 25. This behavior suggests that the cutoff frequency ϵ_c for the filter to be applied to this data be chosen in the region from 15 to 25. After some experimentation the value $\epsilon_c = 15$ was chosen as appropriate. (The results finally obtained are quite insensitive to small changes in ϵ_c .) Similarly the standard deviation σ specifying the sharpness with which the transition in the values of K occurs was selected interactively. The value $\sigma = 2$ was found to be adequate but, again, the results are very insensitive to perturbations in the values of σ . The transfer function K corresponding to this choice of the parameters ϵ_c and σ is indicated graphically in Figure 1.3, and the modulus of the corresponding result G from (1.2) is shown by Figure 1.4. This G represents the result of the filtering process in the transform domain, and its inverse DFT g (Figure 1.5) thus comprises the end product of the smoothing process.

The noise reduction technique was also applied to a noisy gamma photopeak; the raw data is shown in Figure 1.6. In this case there were 60 channels of data and thus 31 Fourier transform values (figures detailing

the intermediate steps have not been included in this instance). The same sort of consideration of the modulus of the transform as was previously employed suggests that cutoff frequency number be taken at channel 6. In this case a simple truncation of the subsequent values of the transform was sufficient to yield very acceptable results. The results of this smoothing is shown in Figure 1.7. The results achieved in these two examples (and in other applications which were not included here due to their entirely similar nature) are especially good because of several factors. First of all, the modeling assumption that the raw data signal f should consist of a very smooth deterministic component d with a much smaller amplitude, highly erratic noise signal n superposed is especially well satisfied in these example problems as is rather clearly revealed by the plots of raw data (Figures 1.1 and 1.6). Secondly, the signal d (which may be assumed to be accurately approximated by the result g indicated in Figure 1.5 and 1.7, respectively) is one which lends itself especially nicely to approximation by trigonometric polynomials of low degree, and thus the Fourier approach is exceedingly appropriate. In any case, the noise reduction technique outlined in this section has been amply demonstrated to be a powerful tool for certain types of data, and this fact has been recognized by the appearance of the article [6].

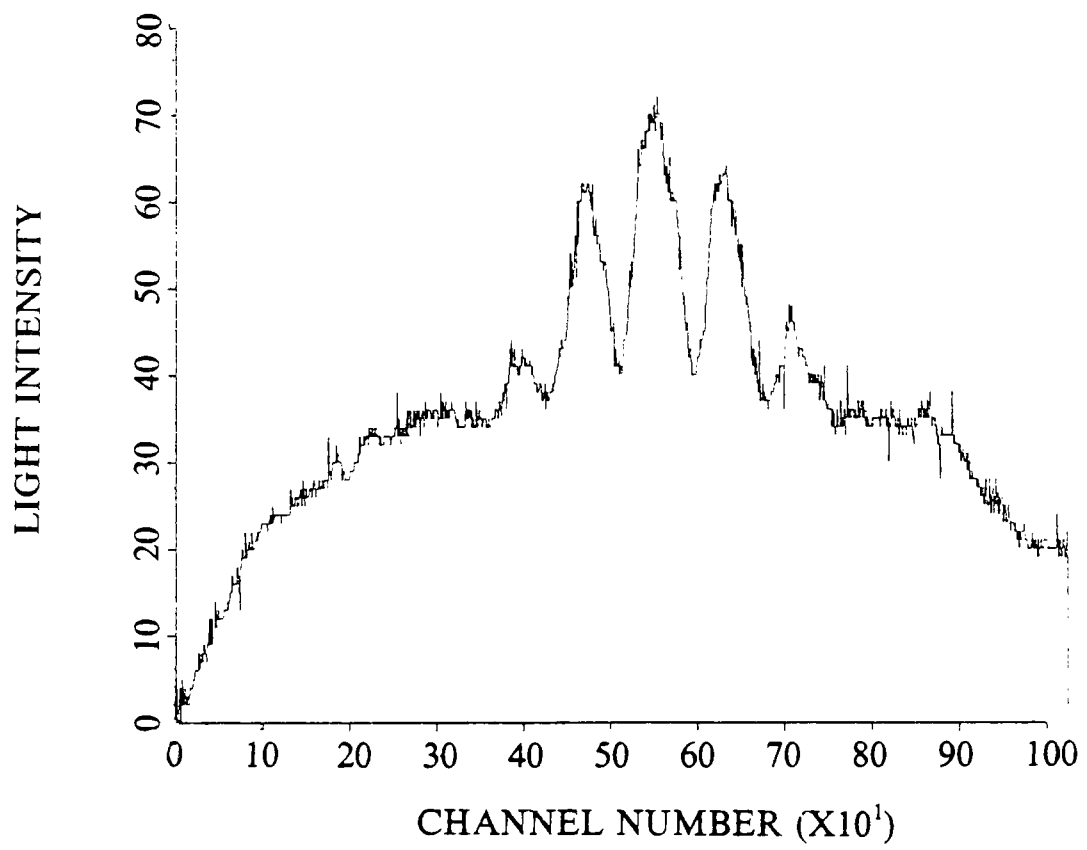


Figure 1.1 Light intensity data (from [25]).

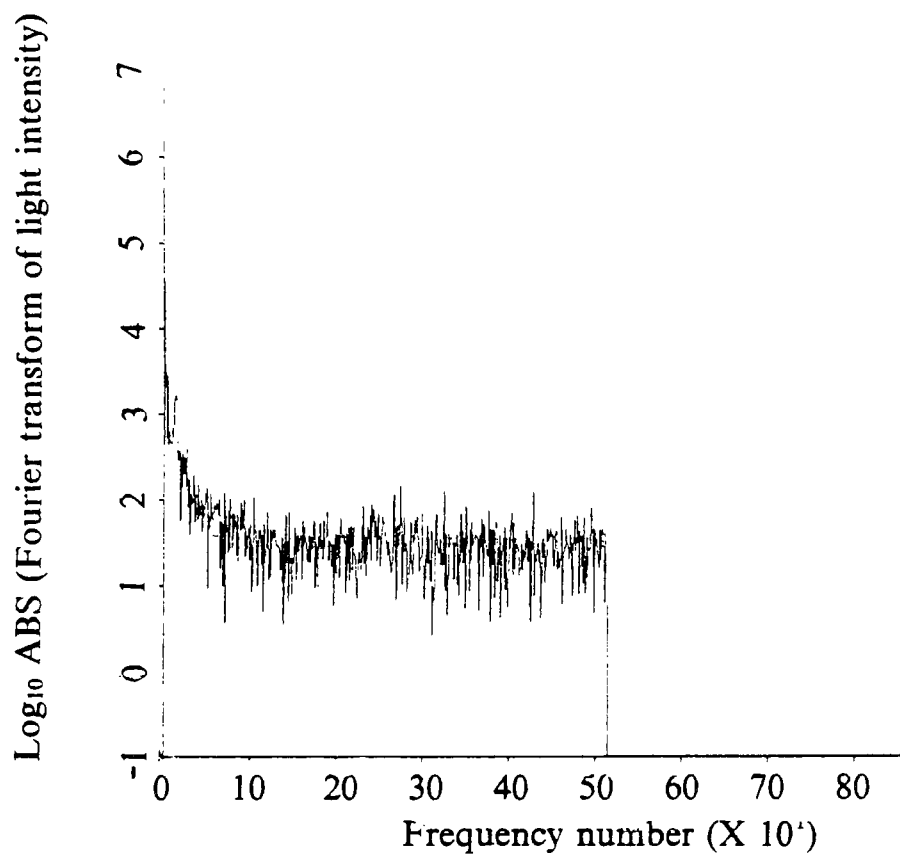


Figure 1.2 Modulus of the transform of data from Figure 1.1

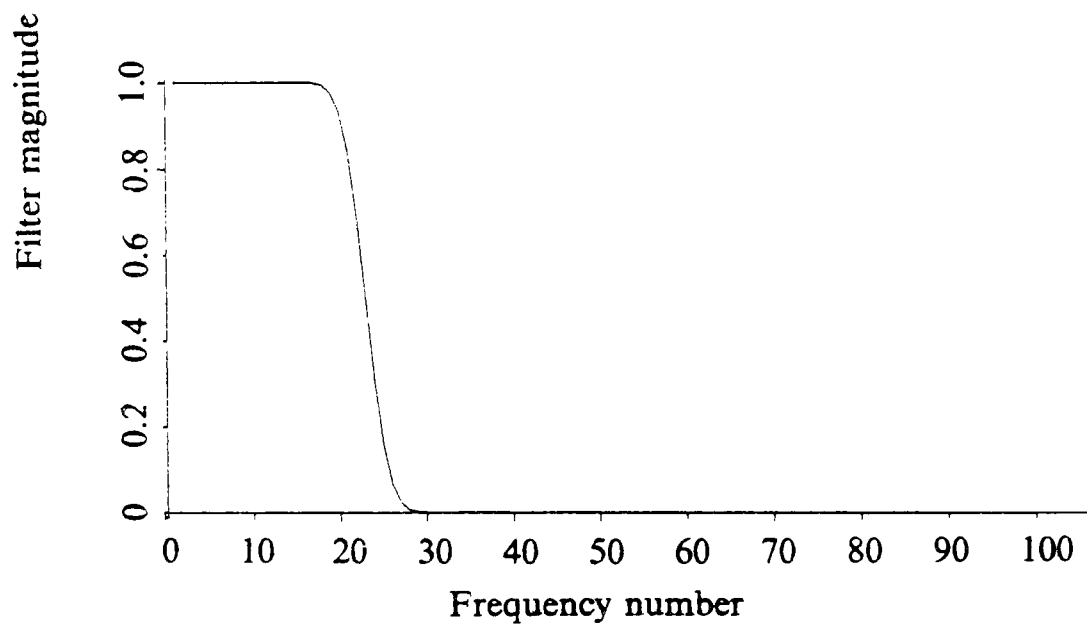


Figure 1.3 Filter function chosen for the enhancement.

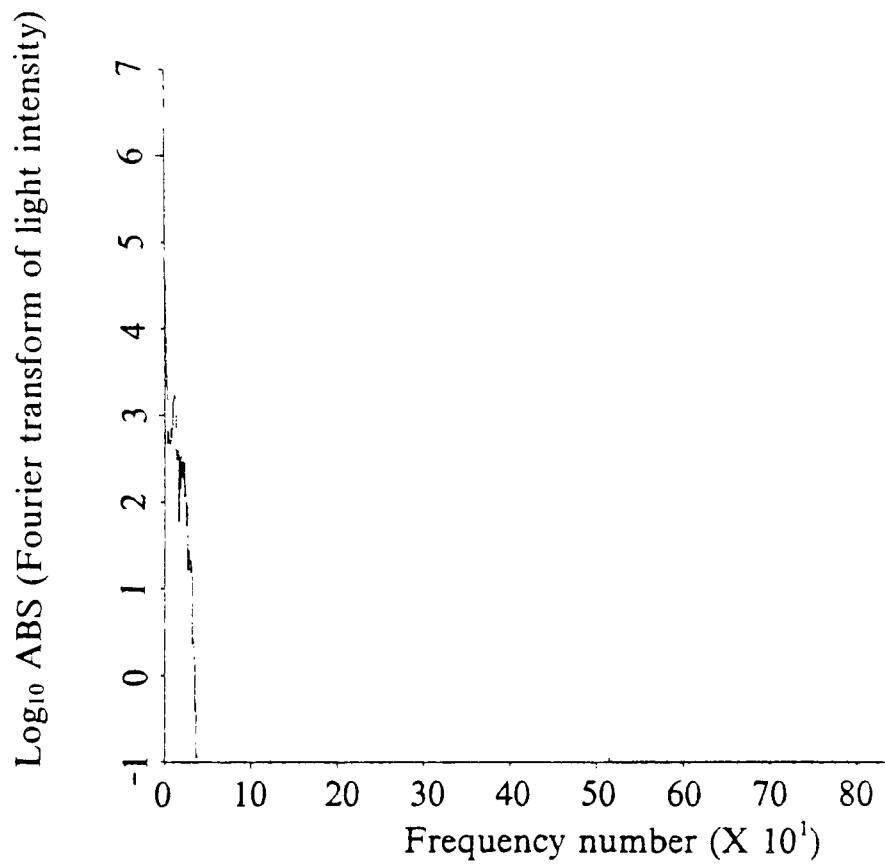


Figure 1.4 Attenuation of transform shown in Figure 1.2.

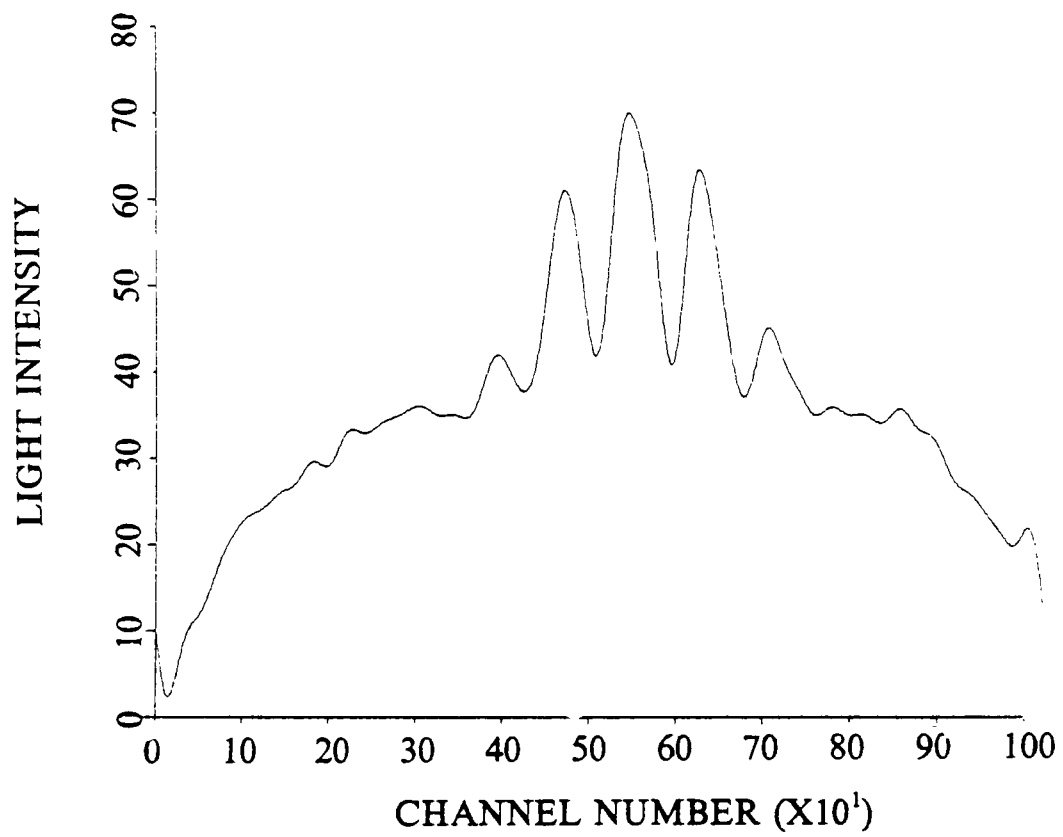


Figure 1.5 Result of enhancement of data in Figure 1.1.

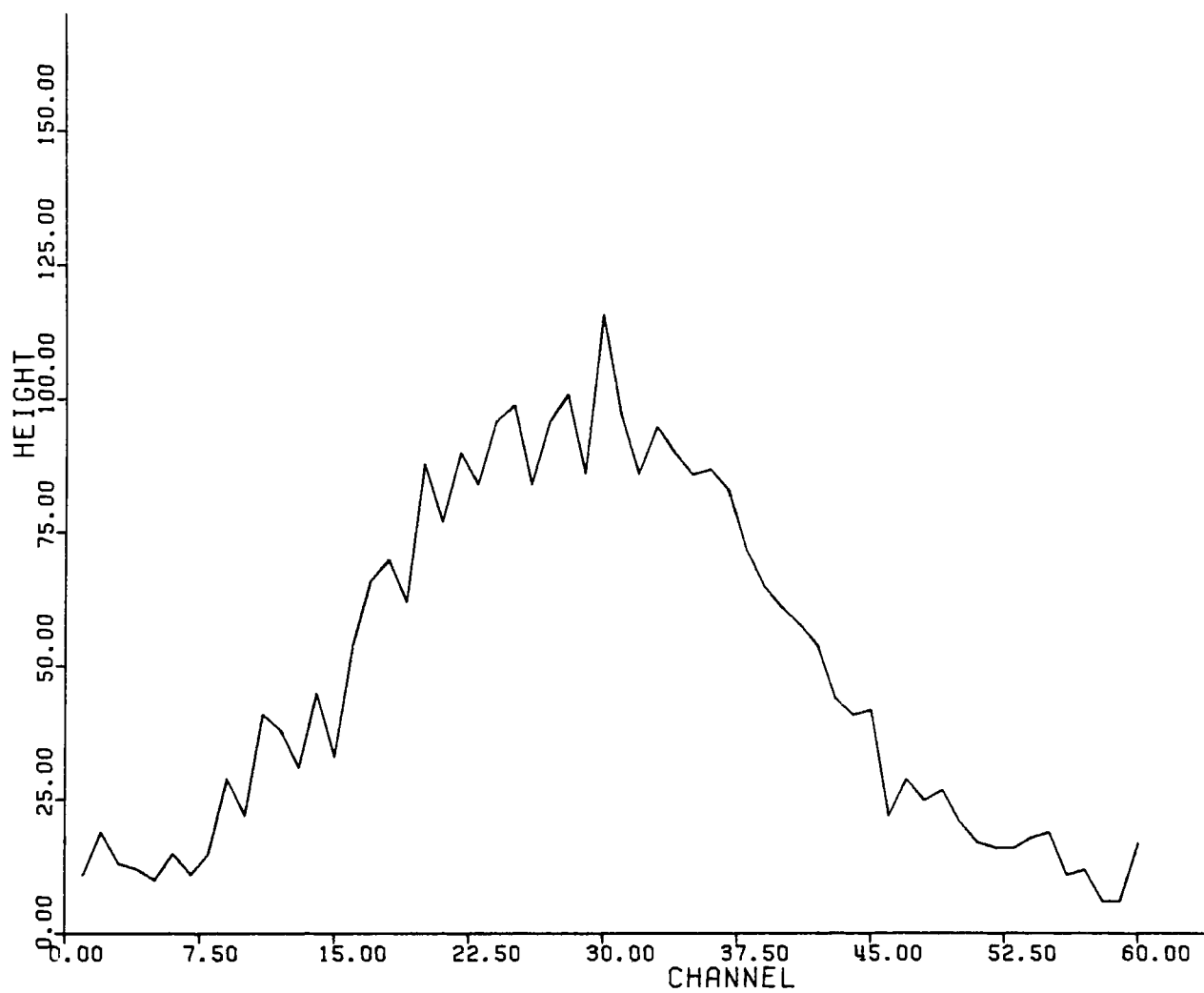


Figure 1.6 Raw photopeak data from a radium energy line.

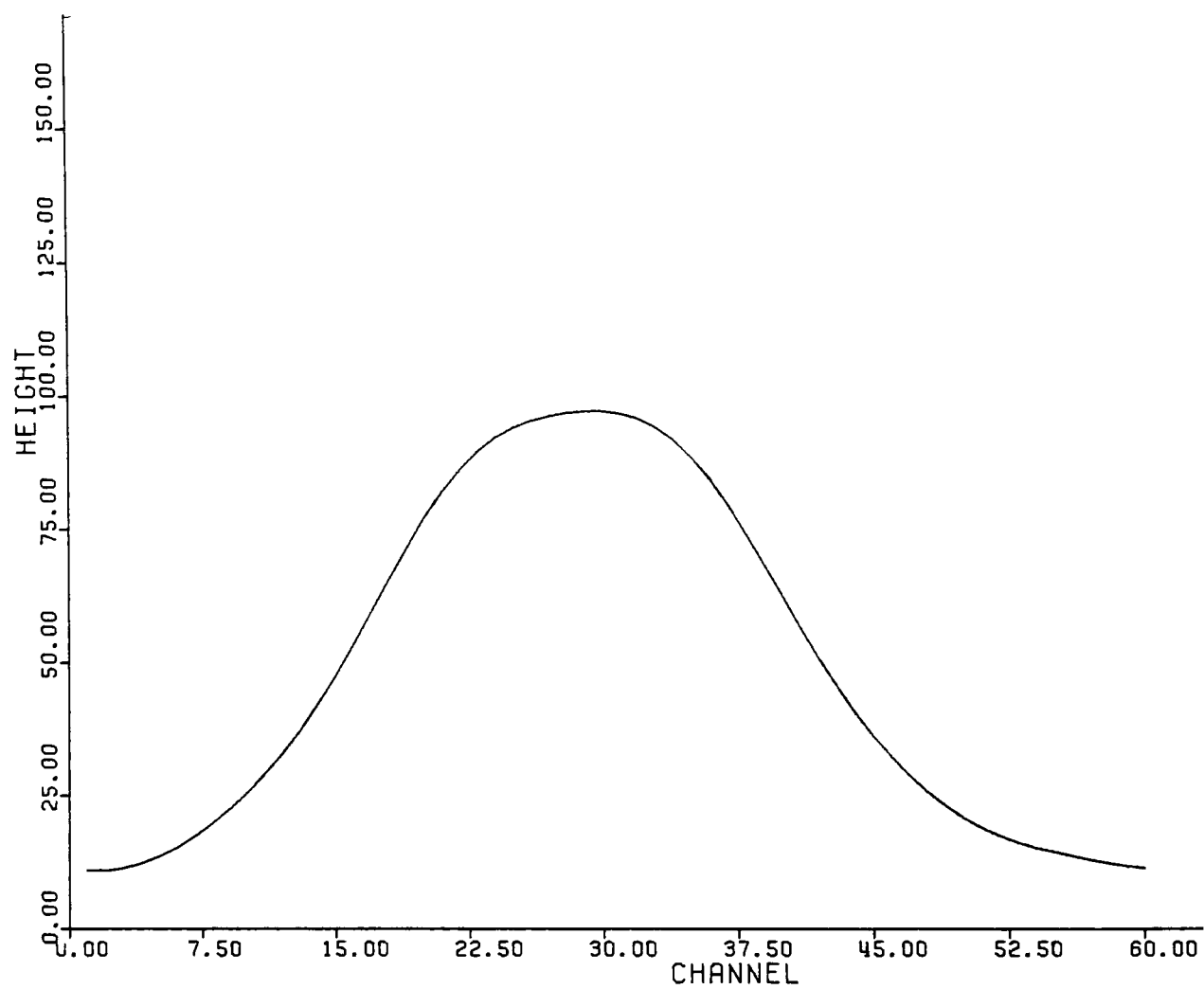


Figure 1.7 Result of enhancement of data in Figure 1.6.

SECTION 2. GENERAL CONSIDERATIONS IN RESOLUTION IMPROVEMENT

The operational characteristics of a radiation spectrometer are usually modeled by the equation*

$$g(e) = \int_0^U h(e, E) f(E) dE \quad (2.1)$$

where $g(e)$ is the recorded intensity of the radiation at energy level e , $f(E)$ is similarly representative of the incident radiation, and h is a function determined by the particular spectrometer (including its settings and calibration, etc.). Often one makes the further assumption that h is a difference kernel (i.e., $h(e, E) = k(e-E)$ for some function k); it is well-known, however, that this assumption is likely to be a good approximation over only a limited energy range. With this assumption the equation becomes one of convolution type and one may often write $g = k*f$ (or some similar notation) to denote this convolution process.

Equations such as (2.1) are categorized as "Fredholm integral equations of the first kind." There is a large amount of literature devoted to the problem of generating reliable approximate solutions of such equations and, in this literature, the many perversities of this problem are evident. The essential point, however, is easily seen by examining the following considerations [22].

For any integrable kernel h it can be shown that the values of the function g_m given by

*In practical applications there is typically no loss of generality in specifying a finite upper limit U for the indicated integral.

$$g_m(e) = \int_0^v h(e, E) \sin(mE) dE$$

approach 0 as m becomes large. This means, assuming that the map of f onto g given by (2.1) is one-to-one, that replacing the data g by $g + g_m$ (for some large m) yields an equation whose solution differs from that of (2.1) by the signal $\sin(mE)$. Thus an extremely small perturbation g_m in the data of the problem gives rise to a very significant oscillatory disturbance in the (theoretically correct) solution.

In practice, of course, one will never have data g which agrees exactly with that which the analyzer model would describe for the given incident signal f . Furthermore, even if such "exact" data were available, computer roundoff errors will be incurred in any practical calculation. Even though these errors will generally be small ones, the result of their presence will often be a very significant (usually oscillatory) disturbance of the true solution f . This difficulty causes any "straightforward" attempt to achieve an approximate solution to (2.1) to be generally unsatisfactory, and thus methods which are (at first glance) quite unintuitive are entirely predominant in this field. The next several sections will discuss the various methods which have been applied to the spectral resolution improvement problem of (2.1). The following notation and specific problem statement will be relevant to a reading of these sections.

Consider the linear operator \mathcal{H} defined by

$$(\mathcal{H} f)(e) = \int_0^v h(e, E) f(E) dE ; \quad (2.2)$$

then the formal problem associated with (2.1) can be stated as

Problem P*: Given g and h , solve the operator equation $Uf = g$ for f .
On the other hand, any practical computational version of this problem would have to be phrased more nearly as

Problem P: Given noisy samples from g and samples from h , estimate sample values of f given that $Uf = g$.

In the course of this contract effort a great deal of literature related to the solution of problems similar to that given in (2.1) was surveyed and the many techniques for solution of problems such as Problem P presented in this literature were considered vis-a-vis the enhancement problem for gamma radiation spectral data. In the following sections the main types of solution procedures are described and implemented on prototypical example problems (in Section 7 and Section 8). In particular, the necessity for some type of stabilizing procedure and even a priori assumptions (based on physical interpretation of the problem) will become evident

SECTION 3. QUADRATURE METHODS AND SINGULAR VALUE ANALYSIS

The most immediate (and least successful) method for Problem P involves choosing quadrature weights w_j and replacing (2.1) by

$$g_i = \sum_{j=1}^N w_j h_{ij} f_j, \quad 1 \leq i \leq M \quad (3.1)$$

where g_i is an approximate observation of $g(e_i)$, $f_j = f(E_j)$ and $h_{ij} = h(e_i, E_j)$. (Here the e_i and E_j are the sample points.) This can be written

$$\vec{g} = A\vec{f} \quad (3.2)$$

where $A = [A_{ij}]$ is the $M \times N$ matrix determined by $A_{ij} = w_j h_{ij}$, M is the number of samples of g observed and N is the number of quadrature nodes E_j .

In this context $M \geq N$ will always hold, and it will be further assumed that A has rank N although more will be said concerning this assumption later. In all sections following this one the assumption that $M = N$ will be made for simplicity.

If $M = N$ then one has $\vec{f} = A^{-1}\vec{g}$ as the formal solution. More generally, when $M \geq N$ the usual least squares criterion would be the natural sense in which to consider the solution of the possibly overdetermined system $A\vec{f} = \vec{g}$. In either case, one may use the concept of the singular value decomposition [19] of a matrix to computational advantage. Under this decomposition A becomes factored into the form UDV' where U is an $M \times N$ matrix with orthonormal columns, D is an $N \times N$ diagonal matrix whose diagonal entries are the (positive) singular values of A , and V is an $N \times N$ orthogonal matrix; here the prime ($'$) symbol is used to denote the transposition operation. The normal equations for the system $A\vec{f} = \vec{g}$ are $A'A\vec{f} = A'\vec{g}$. The latter is a non-

singular system of N equations in the indeterminants f_1, \dots, f_N but the coefficient matrix $A'A$ is expected to be very ill-conditioned and thus the solution of this system must be approached with great care. Using the singular value decomposition $A = UDV'$ and changing the variables \vec{f} to $\hat{f} = V'\vec{f}$ and the data \vec{g} to $\hat{g} = U'\vec{g}$, one obtains the diagonal system $D\hat{f} = \hat{g}$. This can be easily solved for \hat{f} ; \vec{f} is then available from $\vec{f} = V\hat{f}$.

Reliable solutions are generally not available from this procedure due to the ill-conditionedness of A . The singular values σ_i of A (which comprise the diagonal entries of D - we assume, without loss of generality that they are in decreasing order) will typically approach zero rapidly as i approaches N . Since \vec{g} consists of noisy samples, one will find that the components of \hat{g} are sums of the form $d_i + n_i$ where d_i is representative of the pure spectral information and n_i results from the noise. One hopes that the d_i approach zero faster than the σ_i but the same is certainly not to be expected of the n_i . When the respective components of \hat{f} are computed from the diagonal system $D\hat{f} = \hat{g}$ the quantities $d_i/\sigma_i + n_i/\sigma_i$ result. For larger values of i the ratio n_i/σ_i will tend to increase wildly and hence the noise component of the data will dominate the solution.

This analysis of the situation suggests also the following possible remedy. If \vec{v}_j is the j th column of V and \hat{f} has components c_j as described, then the least squares solution to $A\vec{f} = \vec{g}$ can be expressed as $\vec{f} =$

$\sum_{j=1}^N c_j \vec{v}_j$. As mentioned above, it is anticipated that the latter summands

in this expression will be dominated by the effects of the noise component of the data \vec{g} and thus one may wish to consider deleting some of these. The term "singular value analysis" refers to the process of inter-actively considering the behavior of the partial sums $\vec{f}_k = \sum_{j=1}^k c_j \vec{v}_j$,

$k = 1, 2, \dots N$. In this regard the positive integer k can be considered as a "smoothing parameter" with smaller values of k giving high signal-to-noise ratio but low resolution level while the larger values of k yield the reverse compromise situation. It should be observed that this process amounts to the truncation of the last $N-k$ singular values of A thereby producing a computational version of A having rank k .

This technique was applied to several relevant resolution enhancement problems during the course of this contract effort. The program of Golub and Reinsch [12] was used to perform the singular value decompositions of the various matrices as required while the software otherwise necessary was implemented on the M-LAB program of the ADP, Inc. Network. Typical results obtained by this means are indicated in detail in Sections 7 and 8.

SECTION 4. GENERAL PHILOSOPHY OF REGULARIZATION METHODS

There are a number of methods in the literature which may be loosely identified as "regularization methods." Roughly speaking, each of these methods attempts to provide a compromise between the residual in (2.1) on the one hand, and the size of some norm of the solution f , on the other. (This norm may be a reflection of the size of f or one of f 's derivatives, or some combination of these.)

The philosophy of regularization methods is fairly well revealed by the statement of the following problem.

Problem R: Given the operator K , the data g (possibly contaminated by noise), the norm $||\cdot||_R$, and the number $\lambda \geq 0$, determine $f = f_\lambda$ so as to minimize the expression $||g - f||_2^2 + \lambda^2 ||f||_R^2$. Here the expression $||\cdot||_2$ refers to the L_2 (RMS) norm given by

$$||f||_2 = \left[\int_0^v f^2(E) dE \right]^{1/2}.$$

In this class of methods the "smoothing parameter" λ is often chosen interactively (as was true for the singular value analysis parameter k of the previous section). However, there has also been some fairly recent work [32] in which the choice of this regularization parameter is made by means of specific considerations concerning the data \vec{g} and assumptions relative to the characteristics of the noise which is contained within this data signal. Due to the fact that the noise models considered thus far in this type of work are not appropriate for the noise encountered in

the spectral data from the analyzers of interest in this contract endeavor and to the preliminary nature of the work reported herein, these methods for the choice of the "optimum" value of λ were not actively considered in the computations which were carried out. The interested reader is referred to [32, 33, 34] and the references contained therein.

In Section 8 it will be demonstrated that the application of the a priori knowledge of the nonnegativity of the functions being considered can have a most powerful effect on the quality of the solutions obtained. Thus one may find it beneficial to modify the statement of Problem R to require the minimization of the indicated form among functions f which have no negative values. In such a case as this the problem of attempting to select the "optimum" value of the regularization parameter is one of active current research interest.

Section 5. Discrete Implementations of Regularization

In this report the term "discrete regularization" (the terminology of this field is not at all standardized) will be used to refer to a form of regularization in which the quantities in the statement of Problem R (Section 4) are all calculated using discrete operations. In this section several methods based on the discrete regularization concept will be formulated and their application to sample problems studied.

Euclidean Regularization

The term "Euclidean Regularization" ("ER") will be applied to methods based on the following idea. Considering again the discretized version $\vec{g} = A\vec{f}$ of (2.1) (which one obtains by applying a quadrature formula to the indicated integral) one may consider the problem: given $\lambda \geq 0$, minimize the expression

$$||\vec{g} - A\vec{f}||_E^2 + \lambda^2 ||\vec{f}||_E^2 \quad (5.1)$$

by properly selecting $\vec{f} = \vec{f}_\lambda$. In this (discrete) context the norm $||\cdot||_E$ is that of the Euclidean length in N-space, i.e., $||f||_E$ is defined as

$$\left[\sum_i f_i^2 \right]^{1/2}$$

This problem may be solved rather efficiently [31] by realizing that the terms $||\vec{g} - A\vec{f}||_E^2$ and $\lambda^2 ||\vec{f}||_E^2$ can be thought of as the total square residuals in the linear systems $A\vec{f} = \vec{g}$ and $\lambda I\vec{f} = \vec{0}$, respectively. It follows, therefore, that the minimization problem stated above is identical with that of determining the least squares solution to the linear system

$$\begin{bmatrix} A \\ \lambda I \end{bmatrix} \vec{f} = \begin{bmatrix} \vec{g} \\ \vec{0} \end{bmatrix}$$

and hence the solution, in principle, is available from the associated normal equations

$$\begin{bmatrix} A' & \lambda I \end{bmatrix} \begin{bmatrix} A \\ \lambda I \end{bmatrix} \vec{f} = \begin{bmatrix} A' & \lambda I \end{bmatrix} \begin{bmatrix} \vec{g} \\ \vec{0} \end{bmatrix}$$

which can be written as

$$[A'A + \lambda^2 I] \vec{f} = A'g. \quad (5.2)$$

It is advantageous to write A (again as in Section 3) in the form UDV' . Then $A'A + \lambda^2 I = V[D^2 + \lambda^2 I]V'$, and so if one sets $\vec{f} = V\hat{f}$ and $\vec{g} = U\hat{g}$ then (5.2) can be written

$$[D^2 + \lambda^2 I] \hat{f} = D\hat{g}. \quad (5.3)$$

Due to the diagonal character of this latter system the components of \hat{f} are immediately available by performing the obvious divisions; then one easily calculates $\vec{f} = \vec{f}_\lambda$ by the multiplication of V and \hat{f} . In this way repeated calculation of \vec{f}_λ (for the various values of λ which one may want to consider in a typical interactive situation) can be very quickly and inexpensively generated.

Differential Euclidean Regularization

Other forms in which discrete implementations of regularization may be advantageously cast involve formulations dependent upon the difference operator Δ given by $(\Delta \vec{f})_i = f_{i+1} - f_i$. It should be observed that Δ is a linear transformation from N space onto $(N-1)$ space and, thus, that the second order operator Δ^2 given by $\Delta^2 \vec{f} = \Delta(\Delta \vec{f})$ maps N space linearly onto $N-2$ space. Δ and Δ^2 are, of course, often used in constructing discrete approximations to the first and second derivatives, respectively, of a function whose samples f_i at equally spaced grid points have been determined.

Due to the widely observed fact that approximate solutions to (2.1) are often subject to pathological oscillation, it may be helpful to regularize the solution of the discrete approximation $A\vec{f} = \vec{g}$ in one of the following ways. First, one may consider the optimization problem: given A , g and δ , $\lambda \geq 0$, minimize the expression

$$||\vec{g} - A\vec{f}||_E^2 + \lambda^2 ||\vec{f}||_E^2 + (\lambda\delta)^2 ||\Delta\vec{f}||_E^2 \quad (5.4)$$

One could view this as the method which results from the replacement of the second Euclidean norm in (5.1) by the norm $||\cdot||_\delta$ given by $||\vec{f}||_\delta = [||\vec{f}||_E^2 + \delta^2 ||\Delta\vec{f}||_E^2]^{1/2}$. Thus, this "First Order Differential Euclidean Regularization Method" ("DER1") is concerned with the minimization of $||\vec{g} - A\vec{f}||_E^2 + \lambda^2 ||\vec{f}||_\delta^2$ (given \vec{g} , A and λ , $\delta \geq 0$) and hence results from a small, formal (although important) alteration of (5.1). The same sort of consideration as was given to the ER optimization problem now shows that the DER1 solution to $A\vec{f} = \vec{g}$ can be realized as the least squares solution to the system

$$\begin{bmatrix} A \\ \lambda I \\ \lambda\delta\Delta \end{bmatrix} \vec{f} = \begin{bmatrix} \vec{g} \\ \vec{0} \\ \vec{0} \end{bmatrix} \quad (5.5)$$

where, in this context, " Δ " now denotes the matrix of the linear transformation Δ relative to the standard bases of the Euclidean spaces of dimension N and $N-1$, respectively. (Specifically, then the j th column of the matrix Δ is the image $\Delta\vec{e}_j$ of the j th column of the $N \times N$ identity matrix I under the transformation Δ .)

To solve this problem one may write the singular value decomposition of the $3N-1$ by N coefficient matrix of the system (5.5) as UDV' . In this case, the three factors are functions of the parameters λ and δ ; U is $3N-1$ by N with orthonormal columns while D and V are both N by N . If \vec{f} is formally set to be $\hat{V}\hat{f}$ and \hat{g} is defined as the product of U' and the vector

on the right hand side of (5.5) then the normal equations for (5.5) can be transformed to the diagonal system $\hat{D}\hat{f} = \hat{g}$. (Here $U^t U$ yields the N by N identity matrix due to the fact that the columns of U are orthonormal.) Then the coordinates of \hat{f} can be easily found by division and $\vec{f} = \vec{f}_{\lambda, \delta}$ generated as the product $V\hat{f}$.

Another type of differential Euclidean regularization which can sometimes be used to advantage in suppressing oscillation in the solution of (2.1) employs consideration of the growth of the second order difference $\Delta^2 \vec{f}$ in the formulation of the solution. This "Second Order Differential Euclidean Regularization Method" calls for replacing the problem of solving $A\vec{f} = \vec{g}$ with that of minimizing the expression

$$||\vec{g} - A\vec{f}||_E^2 + \lambda^2 ||\vec{f}||_E^2 + (\lambda\epsilon)^2 ||\Delta^2 \vec{f}||_E^2 \quad (5.6)$$

In a manner completely analogous to that used following (5.4), one could consider this "DER2" method to consist of the minimization of the quantity $||\vec{g} - A\vec{f}||_E^2 + [\lambda ||\vec{f}||_E^\epsilon]^2$ where the norm $||\cdot||^\epsilon$ is defined by $||\vec{f}||^\epsilon = [||\vec{f}||_E^2 + \epsilon^2 ||\Delta^2 \vec{f}||_E^2]^{\frac{1}{2}}$.

The solution $\vec{f} = \vec{f}_\lambda^\epsilon$ to $A\vec{f} = \vec{g}$ (given A, \vec{g} and $\lambda, \epsilon \geq 0$) is, of course, the least squares solution to the system

$$\begin{bmatrix} A \\ \lambda I \\ \lambda \epsilon \Delta^2 \end{bmatrix} \vec{f} = \begin{bmatrix} \vec{g} \\ \vec{0} \\ \vec{0} \end{bmatrix} \quad (5.7)$$

where, here, Δ^2 denotes the N-2 by N matrix whose columns are the respective images of the second order difference operator on the standard basis vectors for N space. This is a system of 3N-2 equations in the indeterminant coor-

dinates of \vec{f} and, using exactly the same sort of procedures as was followed in deriving the DER1 solution, one can transform the normal equations for (5.7) to a diagonal form such as $\hat{D}\vec{f} = \hat{g}$. Then the solution $\vec{f} = \vec{f}_\lambda^E$ is available as the product $\hat{V}\hat{f}$. (Here, of course, the singular value decomposition of interest is that of the coefficient matrix of (5.7) into the form UDV' where, in this instance, U is a $3N-2$ by N matrix with orthonormal columns.)

Obviously, many other variations along the lines which have been illustrated here could be similarly formulated and implemented, but there does not seem to be any justification in the context of the present study for persisting further in this. It seems intuitively clear that the differential Euclidean regularization methods yield a significant generalization of Euclidean regularization and that in some types of problems this added generality may bring welcome improvement of quality to the solution. It should also be clear that this increased capability has not been achieved without the cost of additional computational inconvenience. The singular value decompositions must now be performed on matrices which have almost three times the number of entries as previously; also, there are now two regularization parameters to consider instead of the previous one. Furthermore, the differential methods (as implemented) require that a singular value decomposition be performed for each choice of the smoothing parameters whereas the Euclidean method needs only one such decomposition (for a given coefficient matrix A). Therefore the cost incurred in typical interactive computations with these three discrete regularization methods is normally significantly lower when using the first of them (Euclidean regularization), although it would be possible to reduce the cost of the differential methods by employing constructions due to Elden or van Loan [31] (as mentioned in

the Summary).

Finally, it should be observed that any of these regularizations can be implemented with one or more constraints imposed. In Section 8 it is demonstrated that Euclidean regularization with nonnegativity constraints can be a very attractive alternative.

Section 6. Continuous/Discrete Regularization

The term "Continuous/Discrete Regularization Method" ("CDR") will be used to refer to a practical computational method [32] based on a theoretical formulation which represents a compromise between the exact solution of (2.1) (which would be normally totally impracticable) and the discrete regularization methods. The basic idea of this method and the approach to its solution are indicated in the following.

If \mathcal{H} denotes the linear integral operator defined in (2.2) then given (noisy) approximate observations $g_i \approx g(e_i)$, $1 \leq i \leq N$ and $\lambda > 0$ one considers the problem of minimizing the expression

$$\frac{1}{N} \sum_{j=1}^N \left[(\mathcal{H}f)(e_j) - g_j \right]^2 + \lambda \int_0^V f^2(E) dE \quad (6.1)$$

by appropriately selecting the function $f = f_\lambda$. If \vec{r} denotes the vector of residuals given by $r_j = (\mathcal{H}f)(e_j) - g_j$ and $||\cdot||_2$ denotes the usual L_2 functional norm (defined in Section 4), then the problem becomes that of minimizing $||\vec{r}||_2^2 + N\lambda ||f||_2^2$ and hence the mixture of discrete and continuous considerations becomes apparent. The solution f of this problem can be determined (in closed form) by considerations which will now be briefly outlined. (The kernel h of (2.2) is assumed to satisfy the hypothesis stipulated in [32].) If the functions h_k are defined by $h_k(E) = h(e_k, E)$ then the solution $f = f_\lambda$ can be written as the linear combination $f = \sum_{k=1}^n c_k h_k$. Therefore the problem becomes that of determining the scalars c_1, \dots, c_N which minimize the function ϕ given by the expression

$$\Phi(c_1, \dots, c_N) = \sum_{j=1}^N \left[\left(\sum_{k=1}^N c_k h_k \right) (e_j) - g_j \right]^2 + N\lambda \left\| \sum_{k=1}^N c_k h_k \right\|_2^2.$$

The quantities c_k of interest can, in principle, be determined from the extremal conditions requiring that all the partial derivatives of Φ be zero when evaluated at the points c_1, \dots, c_N .

In determining the solution to these equations the following notation is employed. \vec{g} and \vec{c} denote the N vectors whose components are the observations g_i and the coefficients c_i being sought, respectively. Also, the N by N matrix M is that given by

$$M_{ij} = \int_0^1 h(e_i, E) h(e_j, E) dE. \quad (6.2)$$

Then the extremal conditions are reflected by the system $M(\vec{M}\vec{c} - \vec{g} + N\lambda\vec{c}) = \vec{0}$ and, using the assumption that M is nonsingular, this becomes

$$[M + N\lambda I]\vec{c} = \vec{g}. \quad (6.3)$$

Solutions of this system of equations for the c_k then yields the CDR solution $f = f_\lambda$ to (2.1) in the form $f = \sum c_k h_k$. This is in marked contrast to the results generated in Section 5, of course, since one is now determining not approximate samples of the solution f , but, instead, a closed form expression approximating f .

A significant computational improvement over the obvious least squares solution of (6.3) as $\vec{c} = [M + N\lambda I]^+ \vec{g}$ (where the plus sign denotes the pseudoinverse) can be achieved in the following manner. Since the matrix M is symmetric, the spectral theorem of linear algebra guarantees the existence of a decomposition of the form VDV' where V is an orthogonal matrix and D is a diagonal matrix (the diagonal entries of D are the eigenvalues of M). Using this decomposition, (6.3) can be written as $V[D + N\lambda I]V'\vec{c} = \vec{g}$ and so if one lets $\vec{c} = \hat{c}$ and $\vec{g} = V\hat{g}$ then the diagonal system

$$[D+N\lambda I]\hat{c} = \hat{g} \quad (6.4)$$

results. The entries of \hat{c} are then immediately available by division, one gets $\vec{c} = V\hat{c}$ and then generates the solution $f = f_\lambda$ in the form $f = \sum c_k h_k$. This allows extremely efficient interactive regularization iterations since, for a given kernel function h , the decomposition calculation (of M as VDV') is performed only once; then the procedure indicated by (6.3) is repeated for the various values of λ which are to be considered.

In many cases a closed form expression for the kernel function h may not be available. In such a case it will, of course, not be possible to determine the entries of the matrix M in the fashion indicated above; neither will the functions h_k be available in closed form and so the representation

$$f = \sum c_k h_k \quad (6.5)$$

must be viewed in a different light. It is assumed that one does at least have available the samples $h_{it} = h(e_i, E_t)$ for $1 \leq i \leq N$ and $1 \leq t \leq N$ and that a quadrature rule with weights w_t and nodes E_t has been selected (as a replacement for integrations in the variable E). Then the description of the entries in (6.2) will be replaced by the approximate calculation

$$M_{ij} \approx \sum_t w_t h_{it} h_{jt}. \quad (6.6)$$

Also, the availability of only the samples h_{it} will dictate that (6.5) now describe only a sampling of the solution $f = f_\lambda$. Letting f_t denote the approximation to $f(E_t)$ thus generated, (6.5) will be replaced by the equation $f_t = \sum_k c_k h_k(E_t) = \sum_k c_k h_{kt}$. This sampling of f can be notationally improved by letting $\vec{f} = \vec{f}_\lambda$ denote the vector of samples f_t and defining a matrix H whose entries are $H_{tk} = h_{kt} = h(e_k, E_t)$. Then if $\vec{c} = \vec{c}_\lambda$ is the solution to (6.3) (in which M has now been replaced by the approximation

generated as indicated in (6.6)) one has the compact description

$$\vec{f}_\lambda = H\vec{c}_\lambda \quad (6.7)$$

The notation chosen here emphasizes the fact that the matrices M and H are entirely determined by the kernel function h (and the choice of grid points e_i and E_t) and, thus, the selection of various values of λ to be considered in interactive iteration merely requires that the (inexpensive) repeated solution of (6.4) be carried out. It follows, therefore, that the cost of such application of CDR consists preponderantly of the cost of calculating the entries of the matrix M (H is obviously a trivial matter in comparison).

Since the determination of M by (6.2) will seldom be possible in applied work, the cost associated with (6.6) must be considered very seriously. During this contract endeavor the calculation of such M 's of the order of approximately 40 by 40 has required an expenditure of more than one thousand dollars on the ADP, Inc. Network. (Of course, this cost could be cut tremendously by an eventual development of Fortran routines for execution on the Comnet system.) It was possible, however, to partially solve this economic problem in a manner which will be described next.

In this discussion it will be assumed that h is a difference kernel given by $h(e,E) = k(e-E)$ where e and E take on values between 0 and U ; then $k(s)$ is defined for s between $-U$ and U and this definition may be extended to all other real s by setting $k(s) = 0$. In this situation (6.2) becomes

$$M_{ij} = \int_0^U k(e_i - E)k(e_j - E)dE.$$

For many pairs i,j the two functions multiplied here, when considered as functions of the variable E are such that the intersection of their supports is included within the interval of integration. (This condition will be

referred to as the "support hypothesis".) In such a case the formulation

$$M_{ij} = \int_{-\infty}^{\infty} k(e_i - E)k(e_j - E)dE$$

is appropriate and, using the change of variable $s = e_i - E$, this can be written as

$$M_{ij} = \int_{-\infty}^{\infty} k(s)k(s + \Delta_{ij}e)ds \quad (6.8)$$

where $\Delta_{ij}e = e_j - e_i$.

Any quadrature rule could be applied to the approximate computation of M_{ij} in (6.8) but it is of interest here to use equally-spaced nodal points s_t and equal quadrature weights $w_t = \Delta s$. Then (6.8) is replaced by

$$M_{ij} = \Delta s \sum_t k(s_t)k(s_t + \Delta_{ij}e). \quad (6.9)$$

The important fact here is that sums of the form of (6.9) can be computed extremely efficiently through the use of the FFT algorithms previously mentioned in Section 1. Specifically, letting k_t denote $k(s_t)$ it is known [2] that the sums $\frac{1}{N} \sum_t k_t k_{t+r}$ are the values of the inverse Fourier transform of the (discrete) power spectrum of the sequence k_t , $t = 1, \dots, N$ provided that the nontrivial samples from k are augmented with a sufficient number of zero samples. (Additional details concerning convolution and correlation are given in [4].) Furthermore, the power spectrum sequence required can also be efficiently found using the FFT since its values are the squares of the moduli of the (complex) discrete Fourier transform values K_t . It should also be mentioned that this indirect method of determining the M_{ij} satisfying the support hypothesis is not necessarily more efficient than the direct calculation of (6.9) for smaller numbers of nodes s_t , but for larger and larger problems the use of this technique provides increasingly more important savings. Those entries M_{ij} not satisfying the support hypothesis have been computed using (6.9) although for very large numbers

of quadrature nodes a calculation based on a convolution formulation could provide significant savings through the use of the FFT as above.

In principle the CDR method is applicable when the solution f lies in either the space L_2 of functions which are square integrable on the interval $[0,U]$ or in a reproducing kernel Hilbert space with reproducing kernel satisfying certain regularity conditions as detailed in [32]. In the next section the results of the application of this method to a well-known ill-posed problem of D.L. Phillips are presented. The high quality of these results (compared to those obtained with totally discrete methods) is apparent. Further, in Section 8, the application of this method to sample resolution improvement problems for gamma spectra is considered. In Section 8 the problems of estimating a certain moment of the incident spectrum f as well as the spectrum f itself are considered. The spectrum f is modeled as a linear combination of delta functions and thus the latter problem does not fall within the conceptual framework of the CDR method as formulated, per se. However, sample calculations of this type were performed to gain some insight concerning the robustness of the discretizations of the method as applied in Section 7, and good (comparative) results were still obtained.

Section 7. The Problem of D.L. Phillips

A classical problem in the literature of first kind Fredholm integral equations is that stated by Phillips in 1962 [22]. In fact, the methodology devised by Phillips for the approximate solution of these types of equations can be considered one of the original regularizations methods. The problem of interest is the following. First one sets k and g to be the functions defined by

$$k(x) = \begin{cases} 1 + \cos(\pi x/3) & \text{if } -3 \leq x \leq 3, \\ 0 & \text{else} \end{cases} \quad (7.1)$$

and

$$g(x) = \begin{cases} (6-x) \left[1 + \frac{1}{2} \cos(\pi x/3) \right] + \\ \frac{9}{2\pi} \sin(\pi x/3) & \text{if } 0 \leq x \leq 6, \\ g(-x) & \text{else.} \end{cases} \quad (7.2)$$

Then the problem of Phillips can be stated in the following way: determine the function f , defined on the interval $[-6,6]$ such that

$$\int_{-6}^6 h(x,s) f(s) ds = g(x), \quad -6 \leq x \leq 6 \quad (7.3)$$

where g is as given by (7.2) and where $h(x,s)$ is defined to be $k(s-x)$. It can be shown that the exact solution of this problem is the function f given by $f(s) = k(s)$; Figure 7.1 shows the comparison between g and f . It should be noted that h is a difference kernel and thus (7.3) is an equation of convolution type; therefore a number of computational "shortcuts" are available for the solution of this problem.

In Section 2 general qualitative remarks concerning the unstable nature of the first kind integral equations were made, but some useful insight may be afforded to a reader having no direct experience with such problems by considering the results of a straight-forward approach to the solution of (7.3) using the quadrature methods. To furnish such an indication of the nature of this problem the following exercise was conducted.

The integral of (7.3) was approximated through the use of both Simpson's rule and the rectangle rule (thereby furnishing the appropriate discretization of this equation); in both cases there were 41 quadrature nodes taken (equally spaced) on the interval $[-6,6]$. Furthermore, since in any real problem the data are likely to be obtained from experiment, it is not reasonable to include the exactly computed corresponding samples from g and so these sample values (which range in size from 0 to 8) were all rounded to one fixed-point decimal place accuracy. The resulting discrete problems then have the form of (3.1) and (3.2) wherein the quadrature weights w_j correspond to Simpson's rule and the rectangle rule, respectively. Here $N = 41$, and one wants to solve for the vector \vec{f} .

The singular value decomposition was used (as described in Section 3) to compute the solutions \vec{f} to the two respective equations (3.2); the results obtained for the sample values of f have been included as Figures 7.2 and 7.3. These figures show that the computed "solutions" are totally dominated by the effects of noise. (The noise results from the finite arithmetic of the computer, the truncation errors in the quadrature rules and the initial data errors due to the data rounding.) In particular, while the true solution f forms a smooth cosine bell varying between 0 and 2, the computed samples are totally wildly dispersed ranging from about -88

to 46 with Simpson's rule and -16 to 18 when using the rectangle rule. Furthermore, it is important to note that the discrete "solutions" are actually quite good in the usual sense of residuals. Thus the vector \vec{f} which is plotted in Figure 7.2 satisfies equation (3.1) to what would ordinarily be considered a very good "level of accuracy" since, for each value of i , the difference between the quantities on the two sides of (3.1) is quite small. The fact that this smallness of residuals does not reflect high accuracy of the approximate solution is characteristic of ill-conditioned linear problems. Similar comments can be also made with regard to the approximate solution indicated in Figure 7.3.

The singular value analysis described in Section 3 was carried out for the problem of Phillips using both exact data and data rounded to one fixed point decimal place; in each of these instances both Simpson's rule and the rectangle rule were used to supply the quadrature weights w_j in (3.1). To lower the cost of computation the numbers of grid points were reduced to $N = 13$. The results are indicated by Figures 7.4 through 7.14; in these figures the theoretically correct solution to the integral equation is indicated by a trace of stars(*) while the thirteen computed sample values of f are superposed by plotting zero's (0). Whenever two points are found to overlies one another (to the resolution level of the plotter used) the two symbols are superposed - this convention remains in effect throughout this report.

It is very interesting to note that Simpson's rule (which would ordinarily be considered generally superior to the rectangle rule) gives oscillatory results (Figures 7.4 through 7.7) which eventually (Figure 7.7) considerably "overshoot" the correct peak maximum. This pathology is evident

even with exact samples from g and the rounding of the data merely causes a further slight deterioration of the same qualitative features (Figure 7.8 and 7.9). On the other hand, using the rectangle rule with the same exact and rounded data gave much more regular and accurate results (Figures 7.10 through 7.13) with the optimum approximations obtained using $k = 9$ and $k = 7$, respectively. (Note that the smaller value of the optimum k when higher levels of noise are present is in accordance with the theory outlined in Section 3.) Previously, (when using Simpson's rule and exact data) the optimum value of k was also 9 but the results (Figure 7.6) were not nearly as acceptable as with the rectangle rule (Figure 7.11). The explanation is that when using the latter quadrature method the resulting eigenvectors \vec{v}_j as described in Section 3 represent discrete versions of eigenfunctions shaped much more compatibly with the solution f than is true when using Simpson's rule. For this reason most of the emphasis in the remaining computations to be discussed herein will be placed upon solutions in which the rectangle rule is used for performing quadrature calculations (whenever such are needed).

The various discrete forms of regularization discussed in Section 5 were also applied to Phillips' problem. Both types of quadrature methods were applied for comparison; also, both exact and rounded data were considered. The results obtained using Euclidean regularization (Figures 7.14 through 7.20) show that the same sort of oscillatory pathology is incurred when using Simpson's rule (Figures 7.14 through 7.17) as was previously experienced when using singular value analysis with this quadrature method (Figures 7.4-7.9). Similarly, the results obtained using the rectangle rule (Figures 7.18-7.20) are much more stable with very high quality being

obtained with zero regularization when exact data is used (Figure 7.18) with only a slight degradation occurring as a result of rounding of the data (Figure 7.20).

The alternate forms of regularization were also applied to this problem and some typical results are included (Figures 7.21-7.37). The comparisons here with previous results are quite interesting. Figures 7.22 and 7.25 show that the first order differential regularization is quite capable of suppressing the pathological oscillation in the computed solution which was previously invariably present (Figures 7.4-7.9 and 7.14-7.17) when using Simpson's rule to perform the quadratures. Unfortunately, this increased power comes at the cost of higher computational expense (as compared to the Euclidean regularization method, for example). As previously mentioned, it is possible to develop more efficient computational methods for performing DER1 regularization, but it was not felt appropriate to expend any developmental effort on this since no advantage over the ER regularization method was observed (on these types of problems) when using the rectangle rule.

Similar comments apply to the use of the second order differential regularization method (Figures 7.26-7.29). The previous pathology associated with the use of Simpson's rule is largely eliminated (Figures 7.27 and 7.29), but the computational expense is higher and no real advantage over less expensive techniques was noted when using the rectangle rule.

A considerable amount of effort was expended on the continuous/discrete regularization technique; typical results are displayed in Figures 7.30 through 7.37. It was found that the oscillation associated with the use of Simpson's rule was very effectively resisted (Figure 7.31 and 7.33) and that very nice results were also obtained if the rectangle rule was used

instead (Figure 7.35 and 7.37). Moreover, as described in Section 6, very dramatic reductions in computational costs were achieved by various means. Although only a slight increase in quality of results over the Euclidean regularization method was observed when using the rectangle rule, it is felt that the CDR method deserves further considerations.

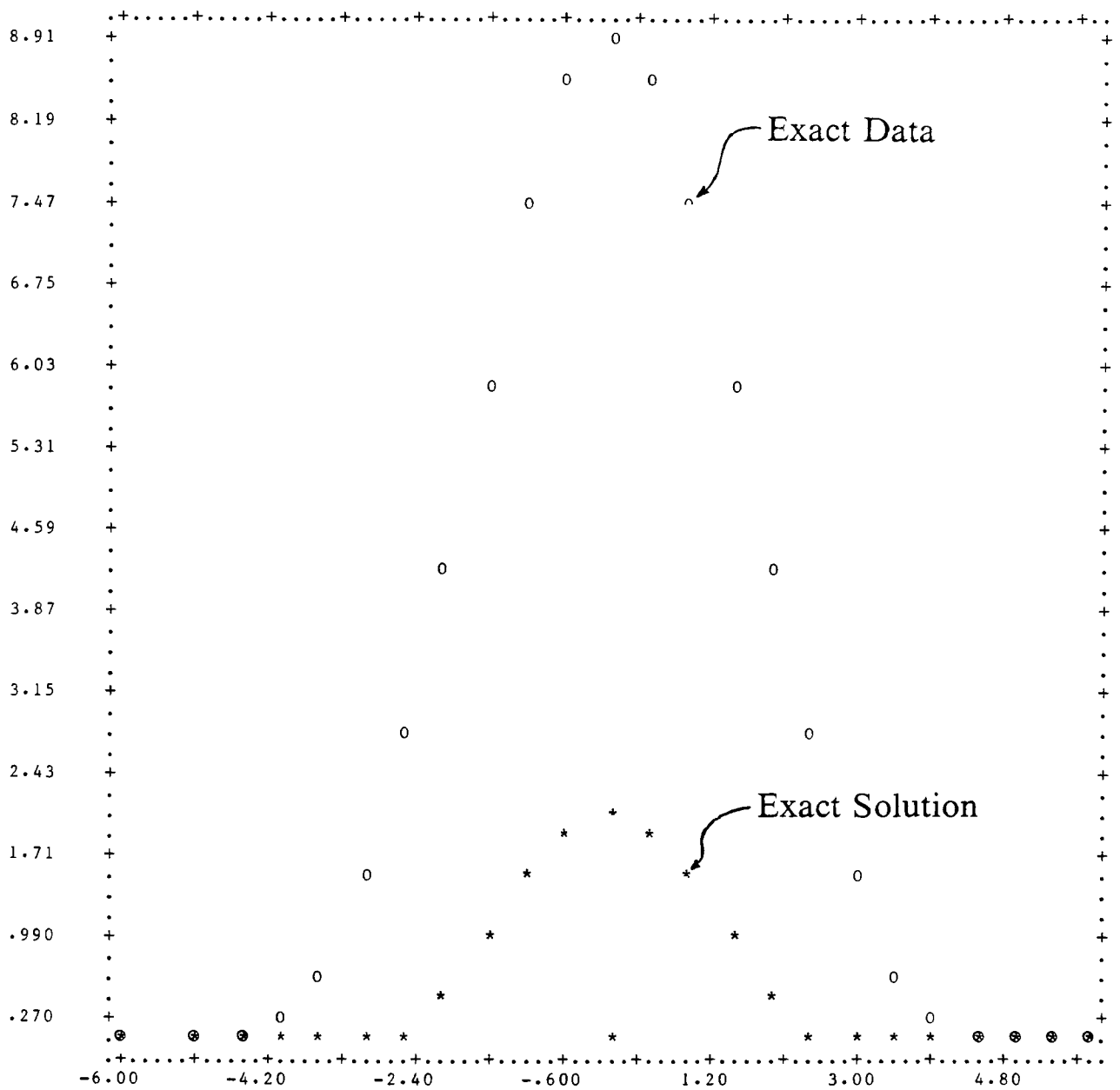


Figure 7.1 Comparison of data and solution.

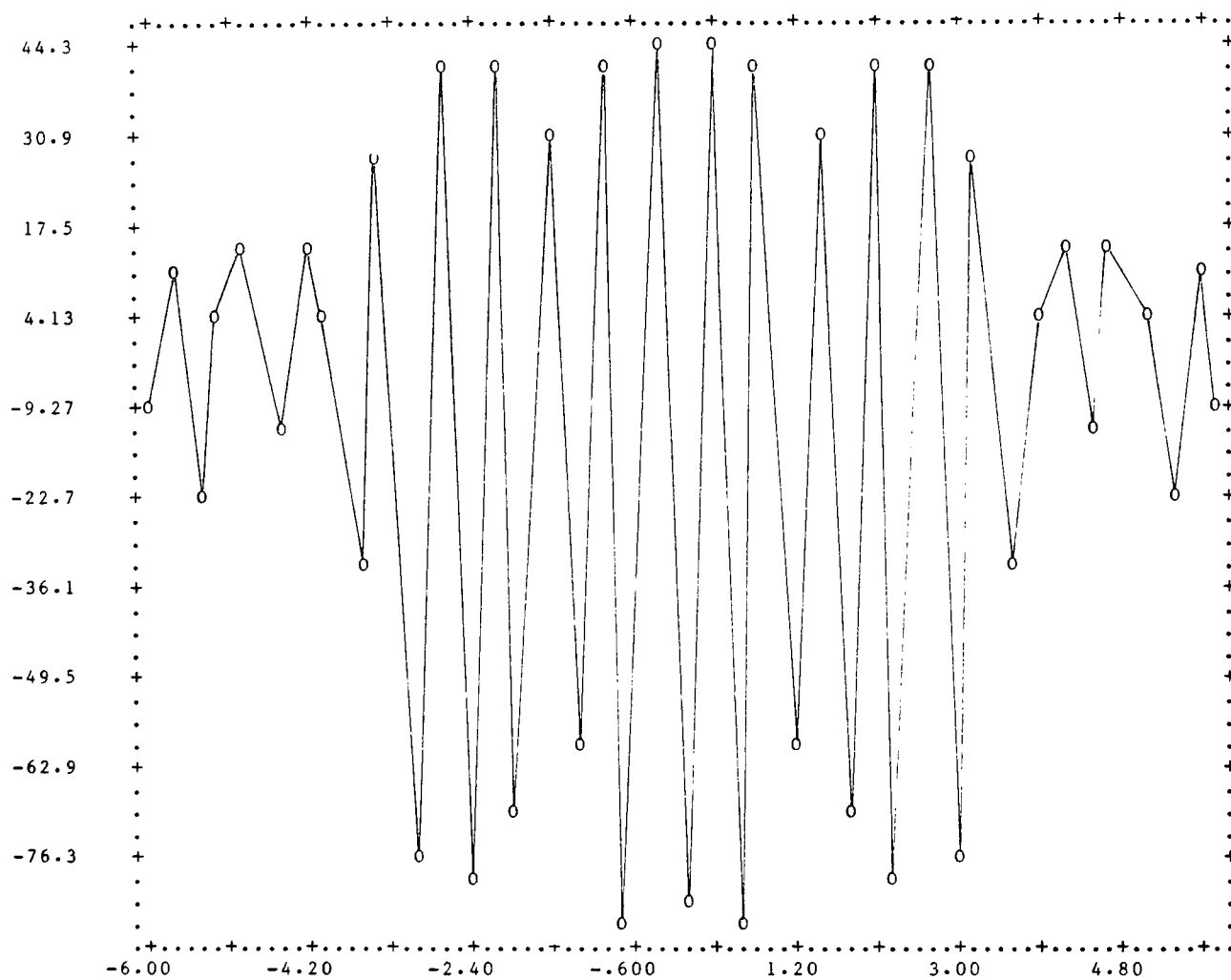


Figure 7.2 Solution by quadrature method using Simpson's rule.

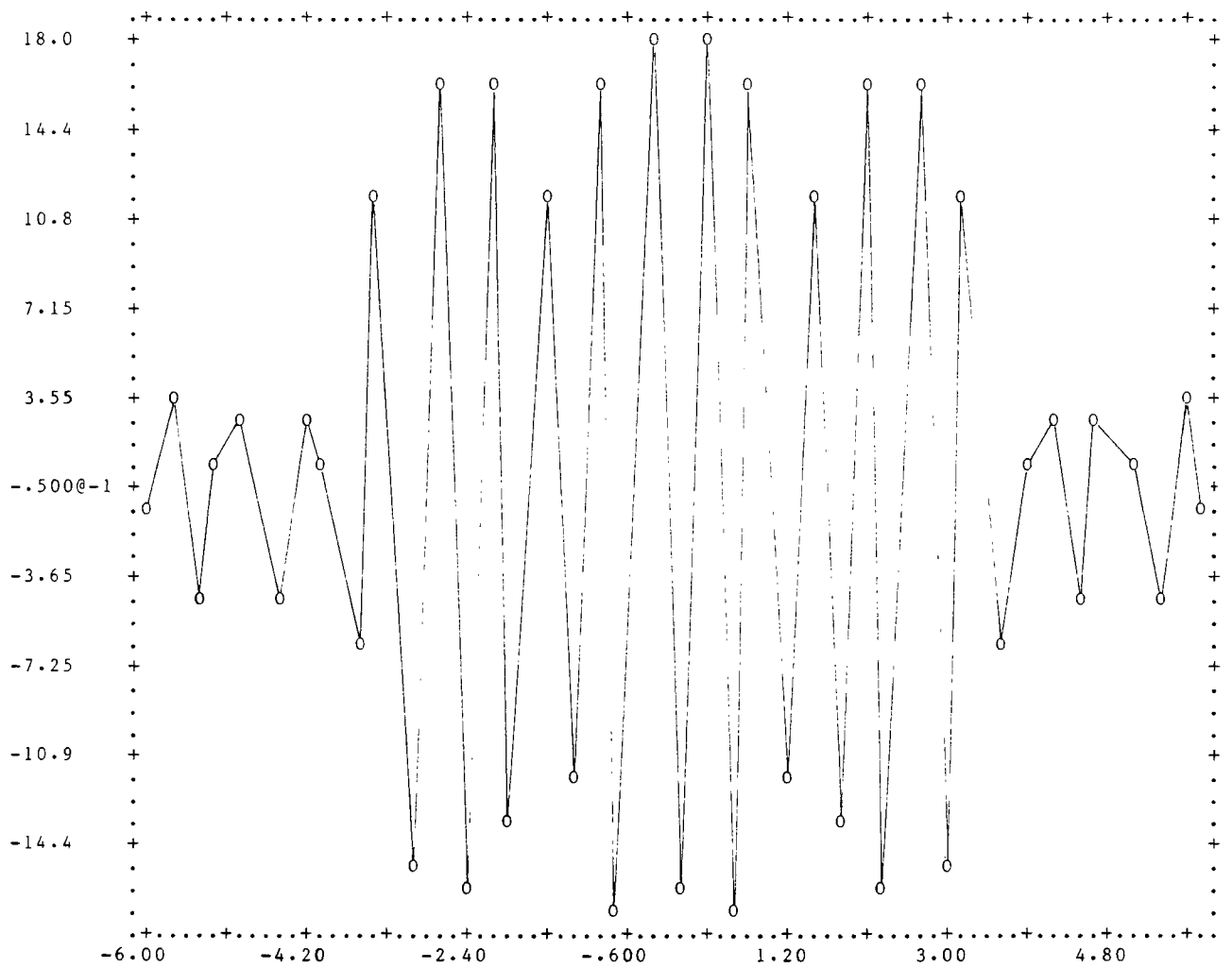


Figure 7.3 Solution by quadrature method using rectangle rule.

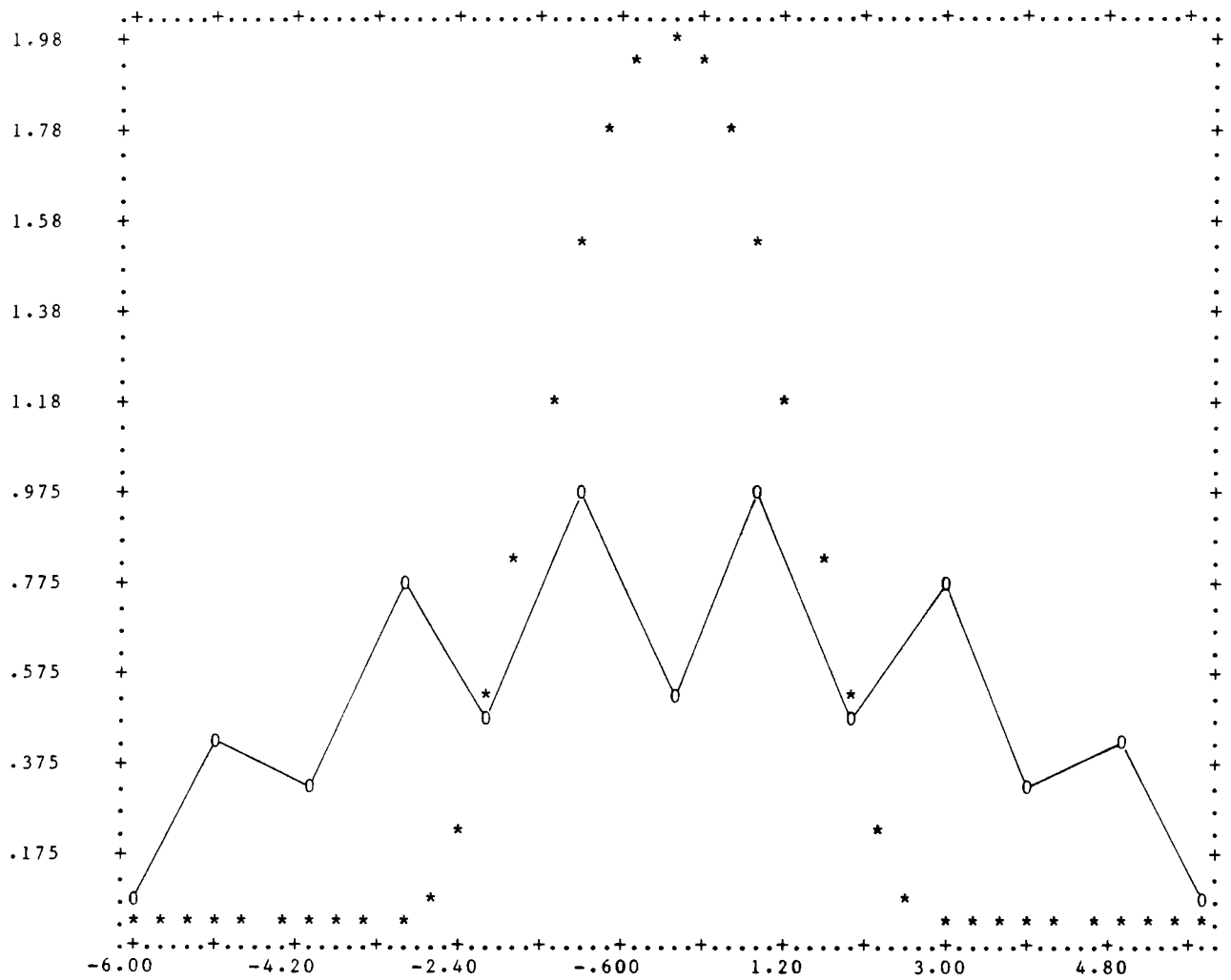


Figure 7.4 Singular value analysis with exact data and Simpson's rule; $k = 1$

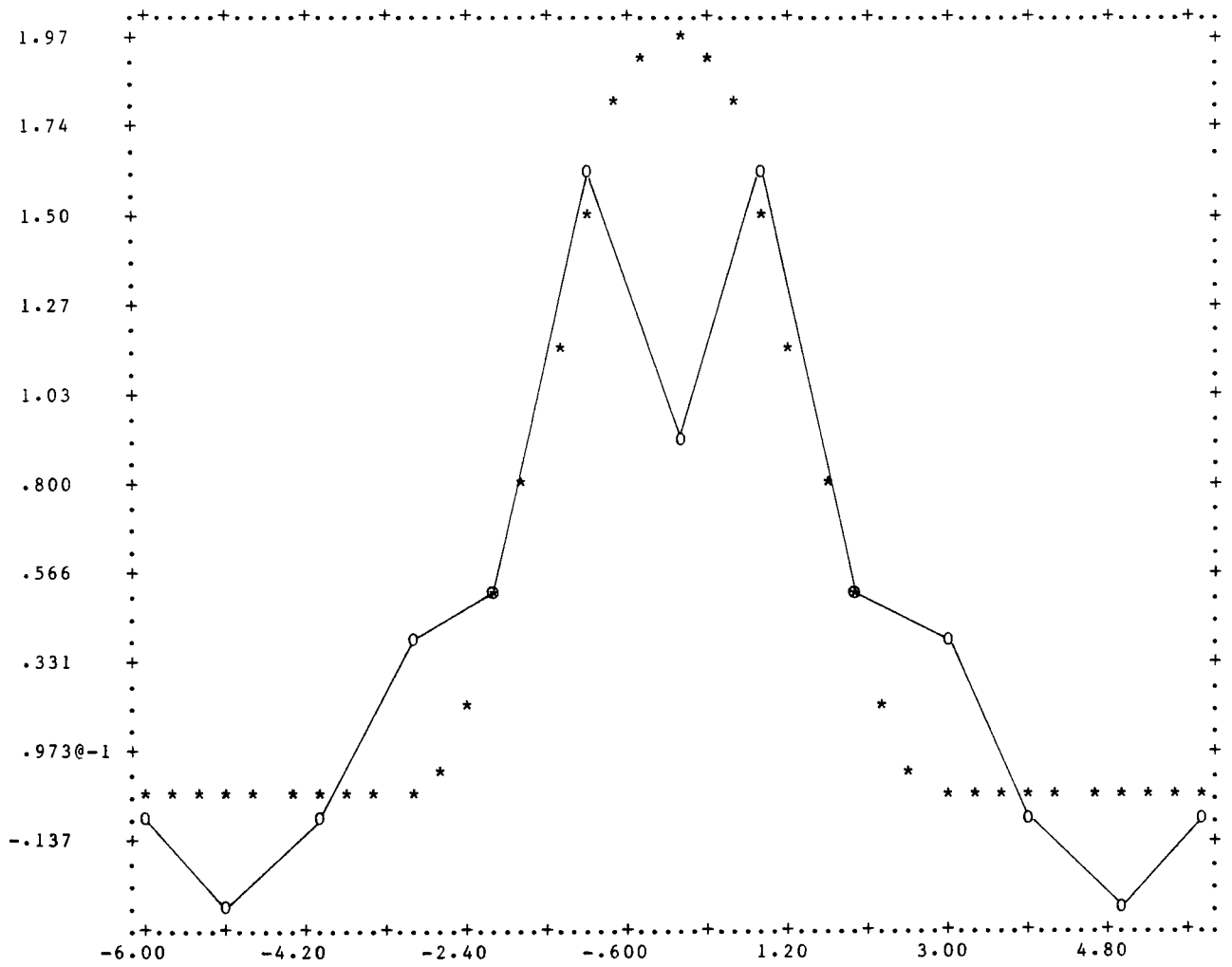


Figure 7.5 Singular value analysis with exact data and Simpson's rule; $k = 3$.

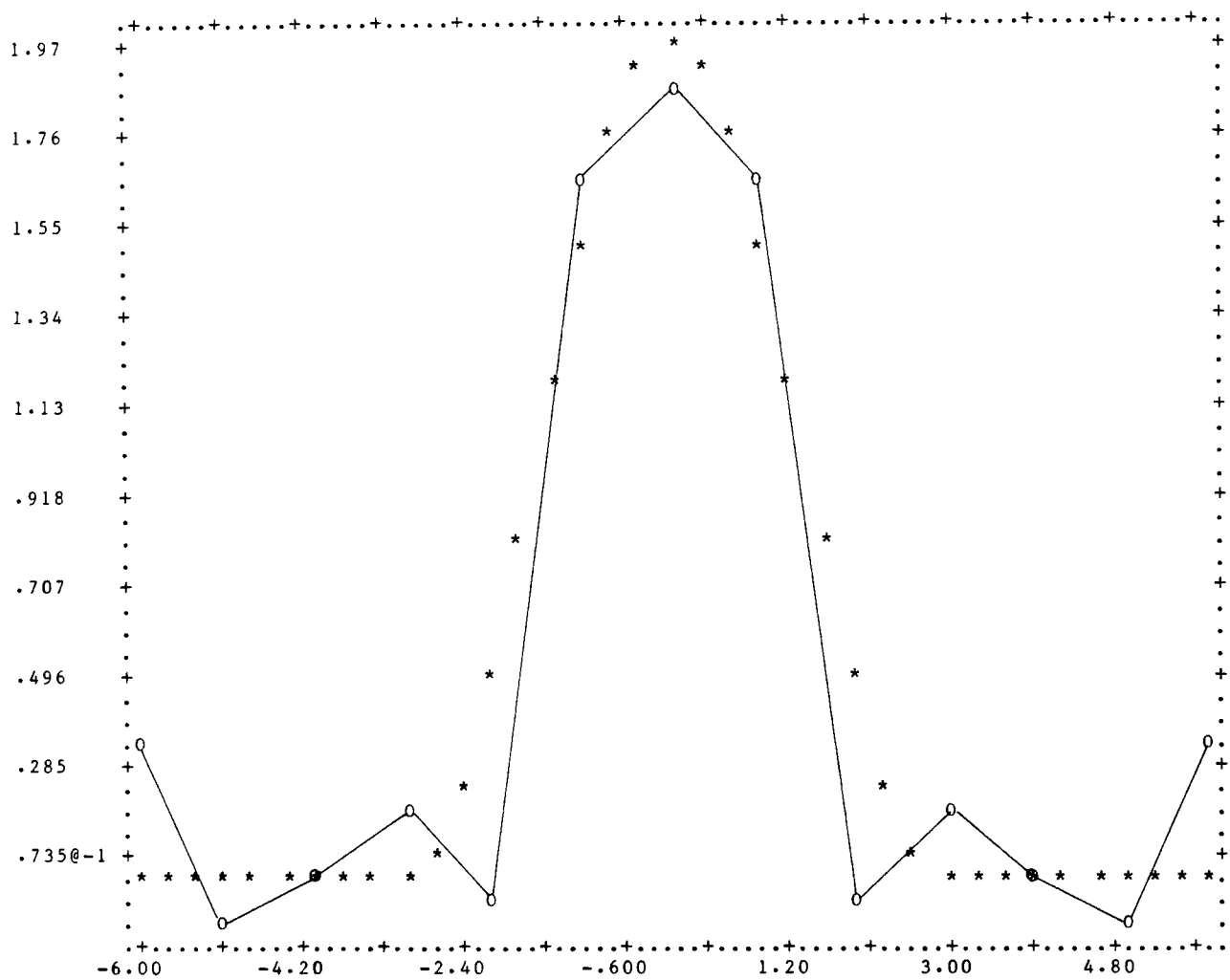


Figure 7.6 Singular value analysis with exact data and Simpson's rule; $k = 9$.

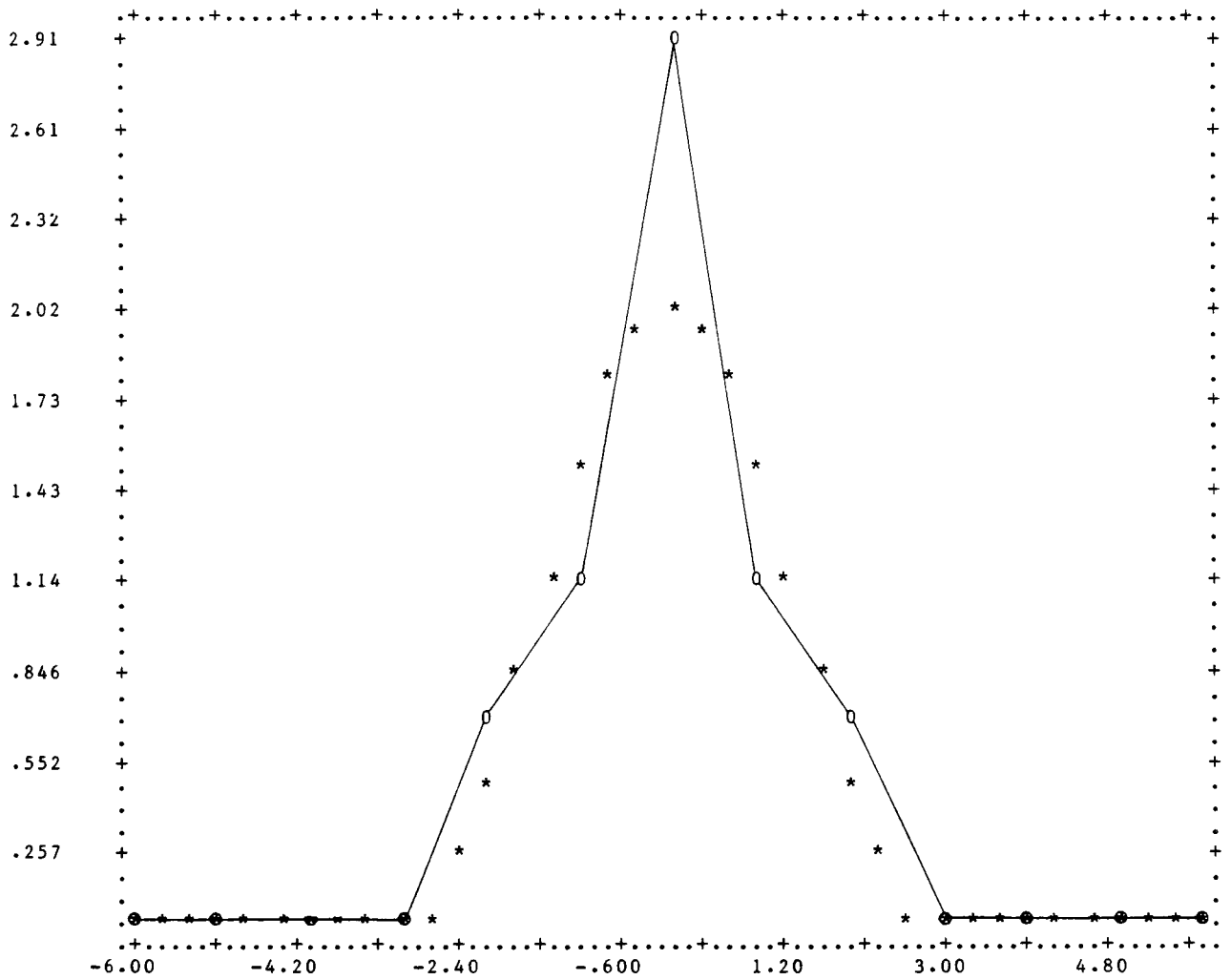


Figure 7.7 Singular value analysis with exact data and Simpson's rule; $k = 13$.

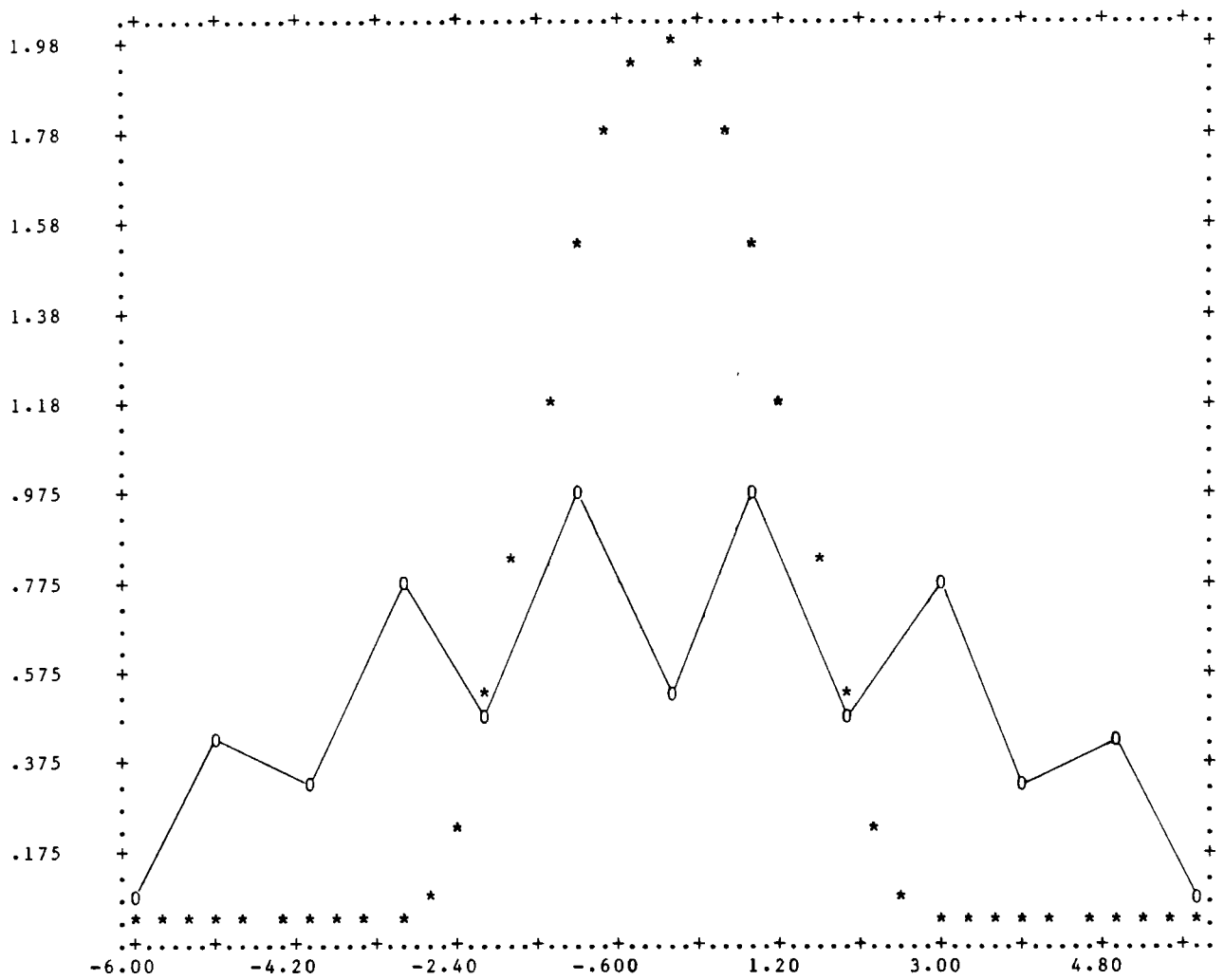


Figure 7.8 Singular value analysis with rounded data and Simpson's rule; $k = 1$.

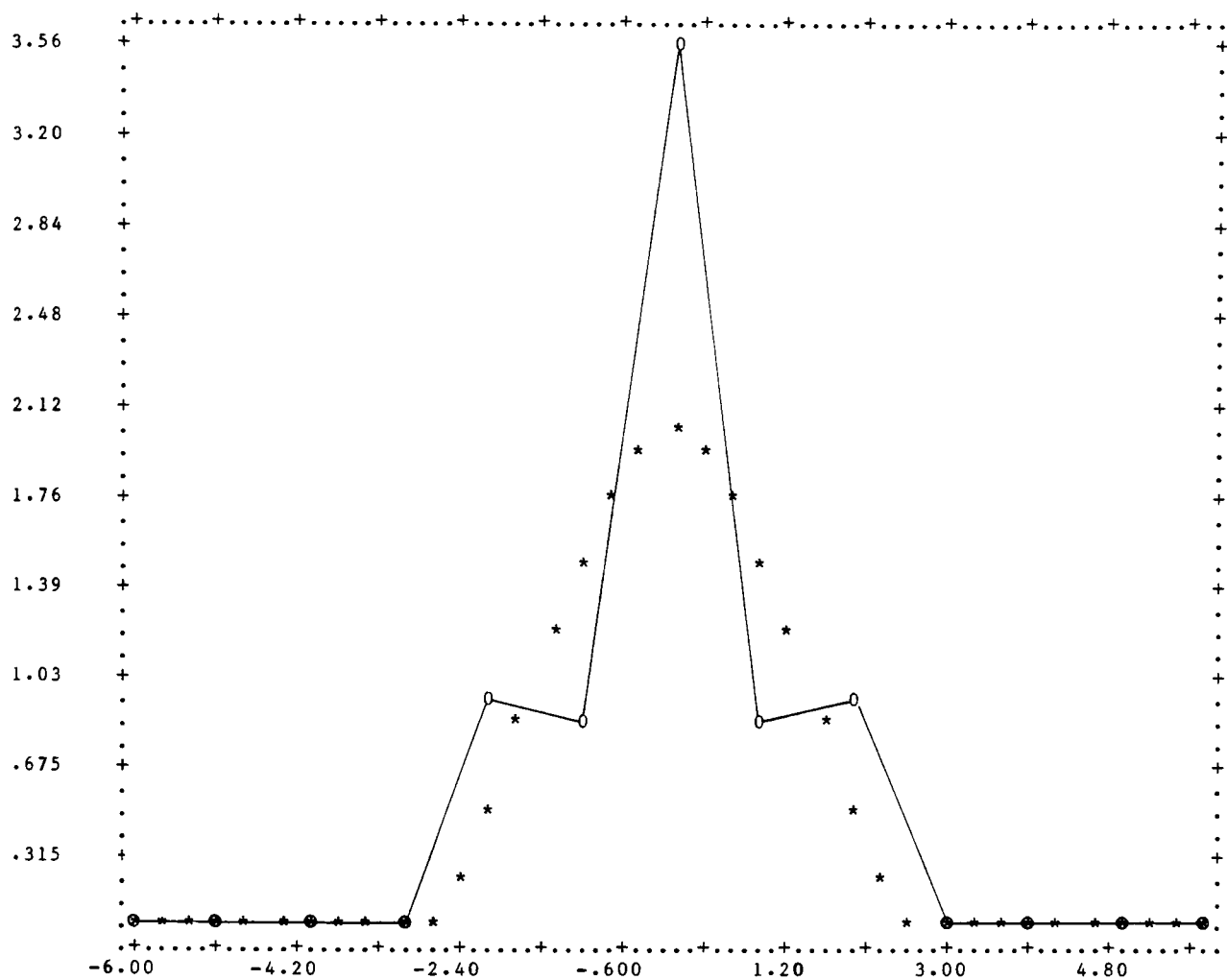


Figure 7.9 Singular value analysis with rounded data and Simpson's rule; $k = 13$.

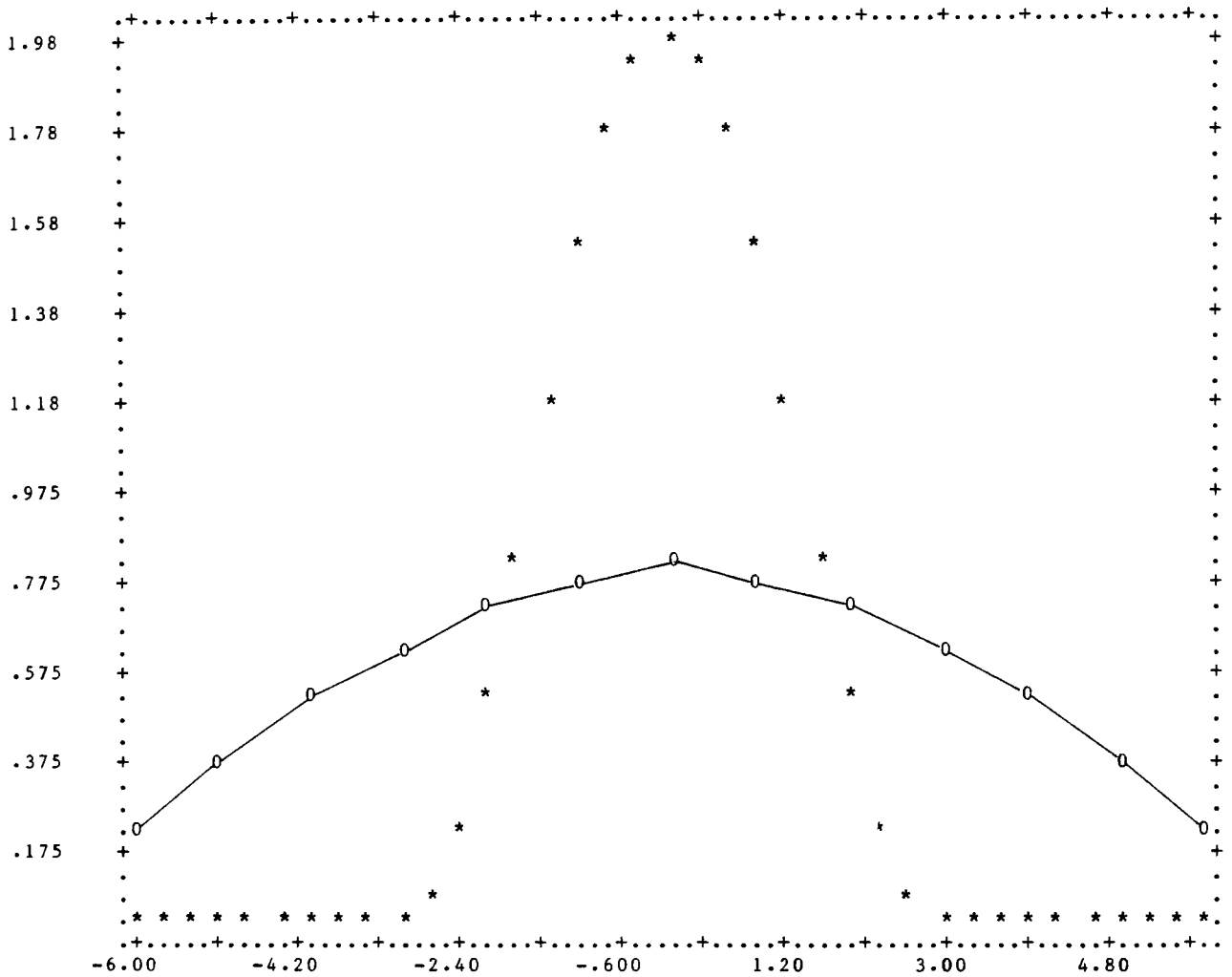


Figure 7.10 Singular value analysis with exact data and rectangle rule; $k = 1$.

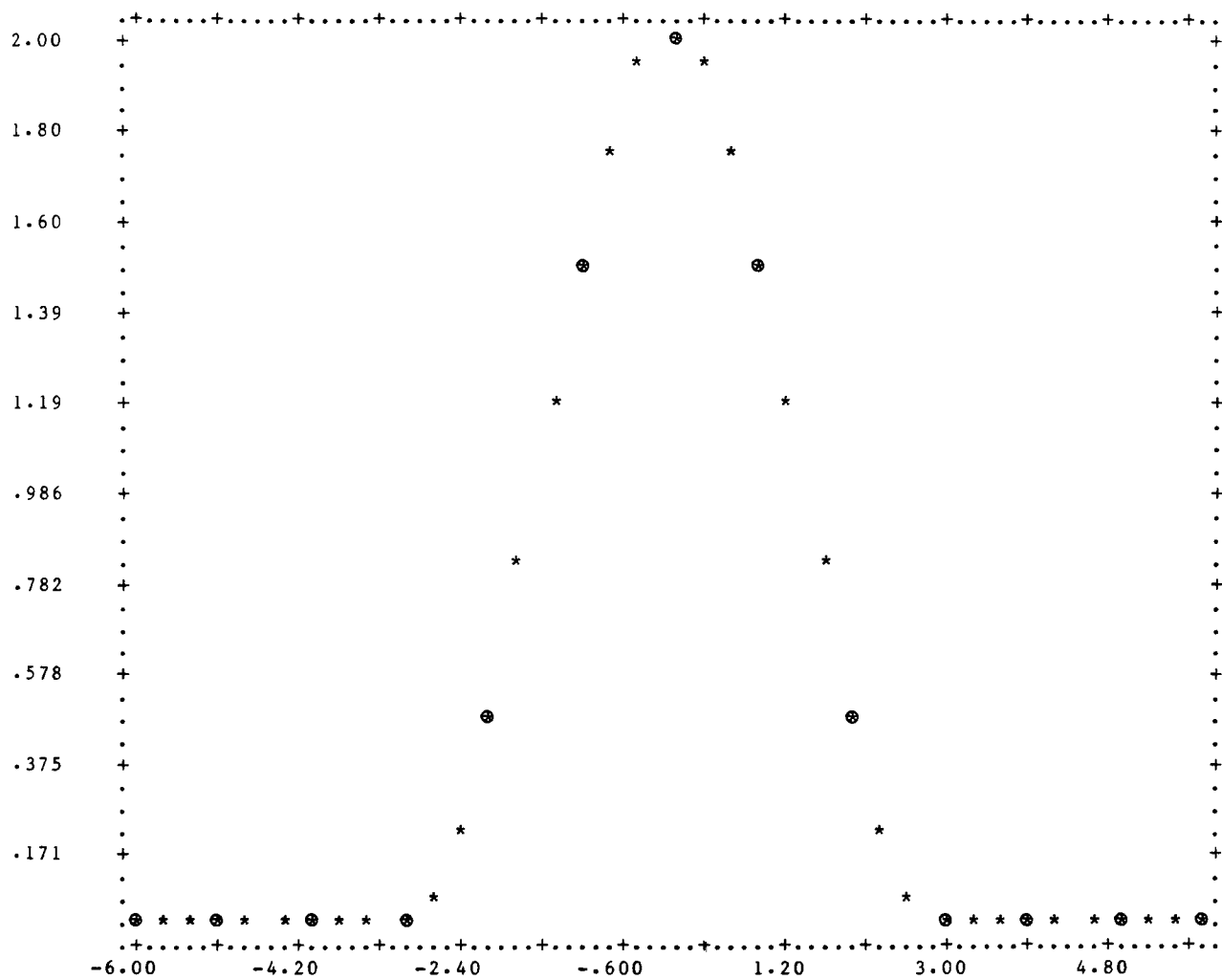


Figure 7.11 Singular value analysis with exact data and rectangle rule; $k = 9$.

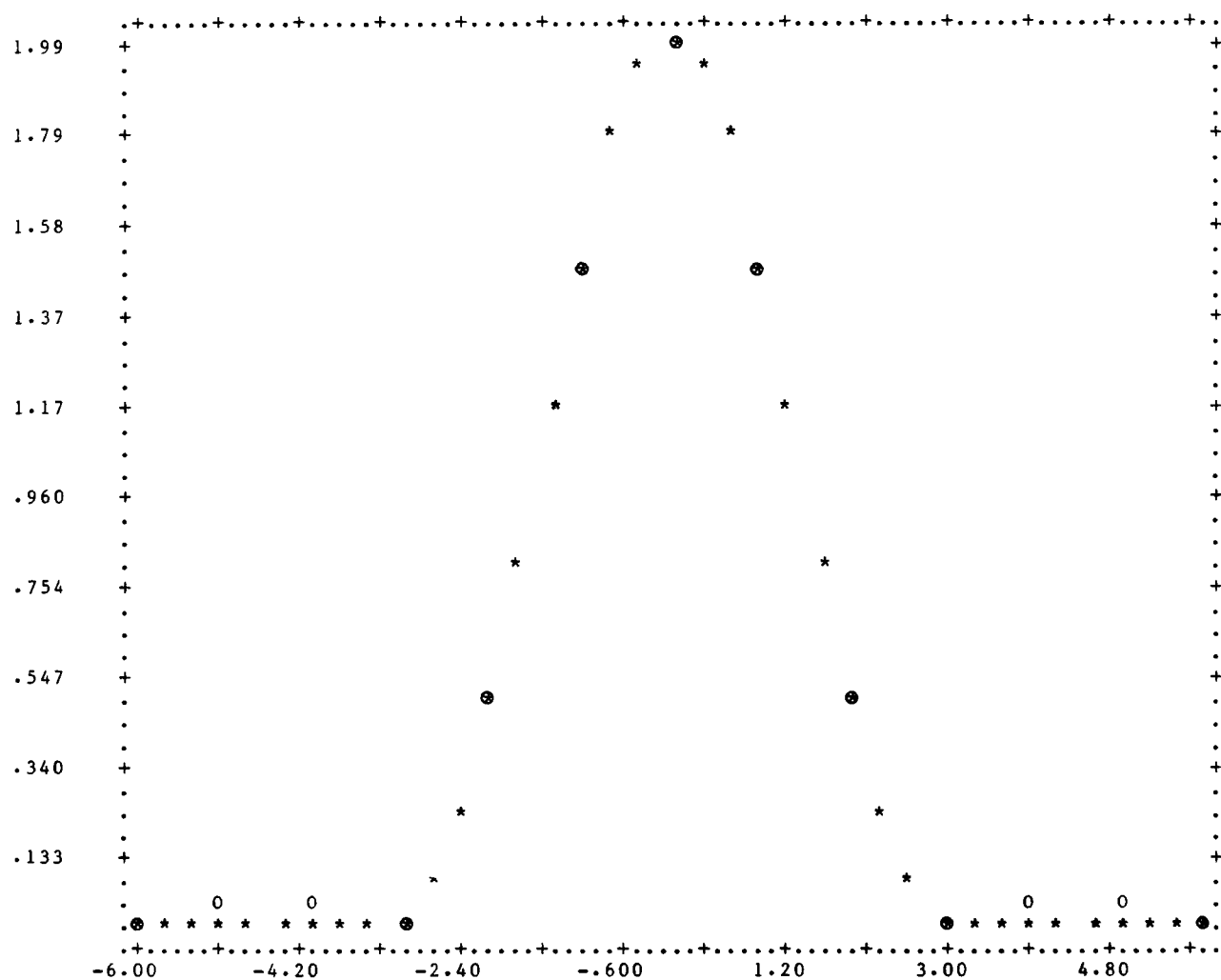


Figure 7.12 Singular value analysis with rounded data and rectangle rule; $k = 7$.

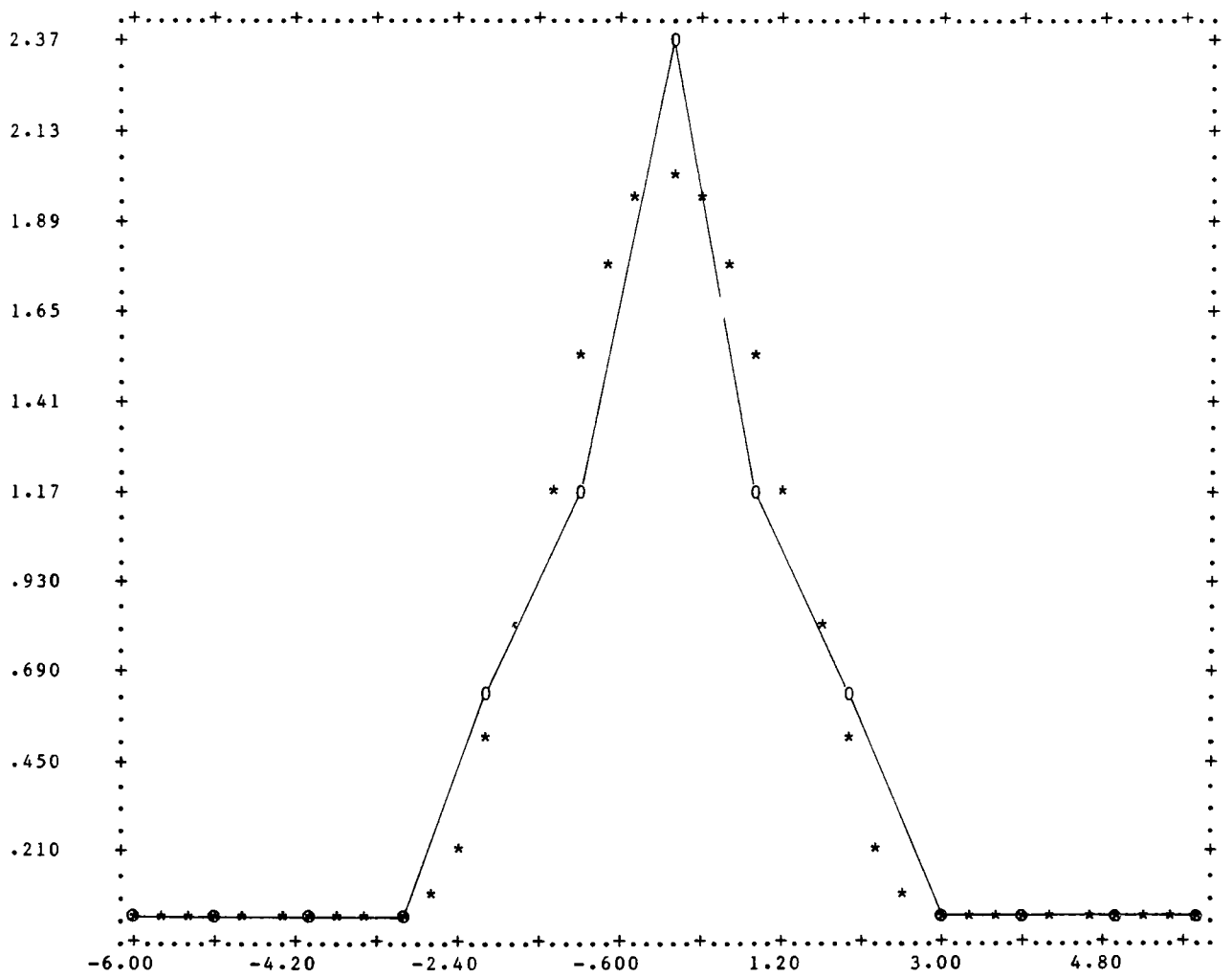


Figure 7.13 Singular value analysis with rounded data and rectangle rule; $k = 13$.

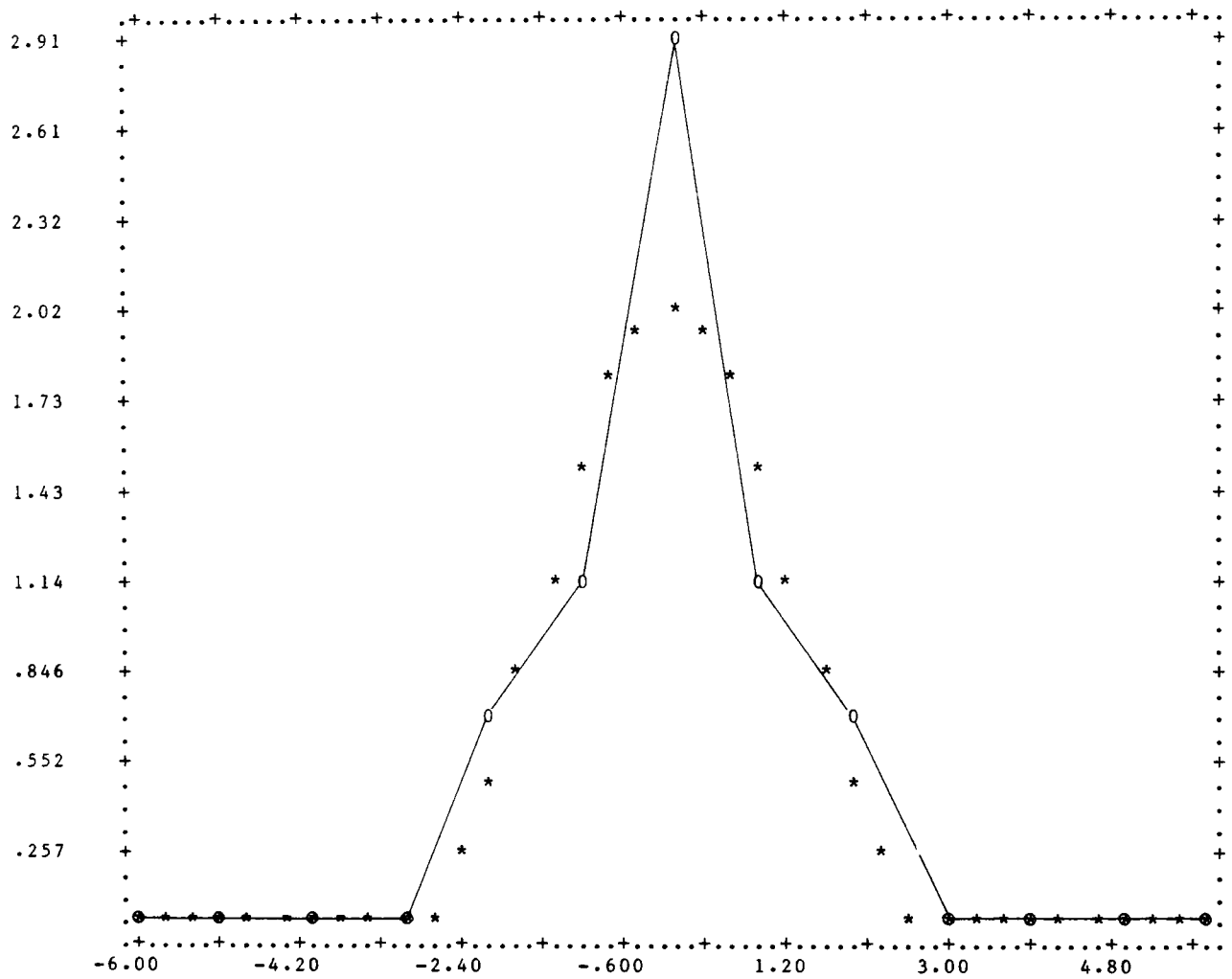


Figure 7.14 Euclidean regularization with exact data and Simpson's rule; $\lambda = 0$.

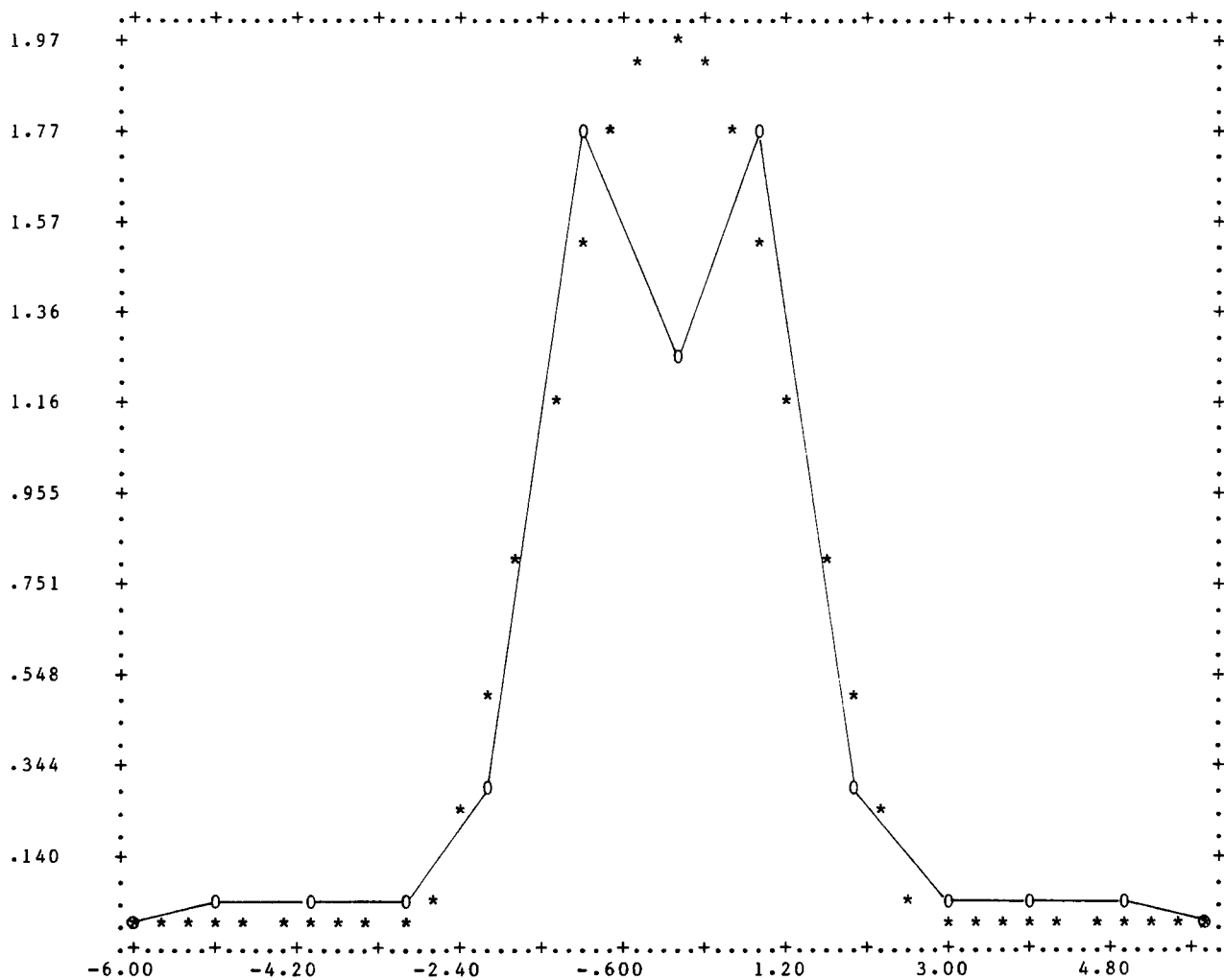


Figure 7.15 Euclidean regularization with exact data and Simpson's rule; $\lambda = .030$.

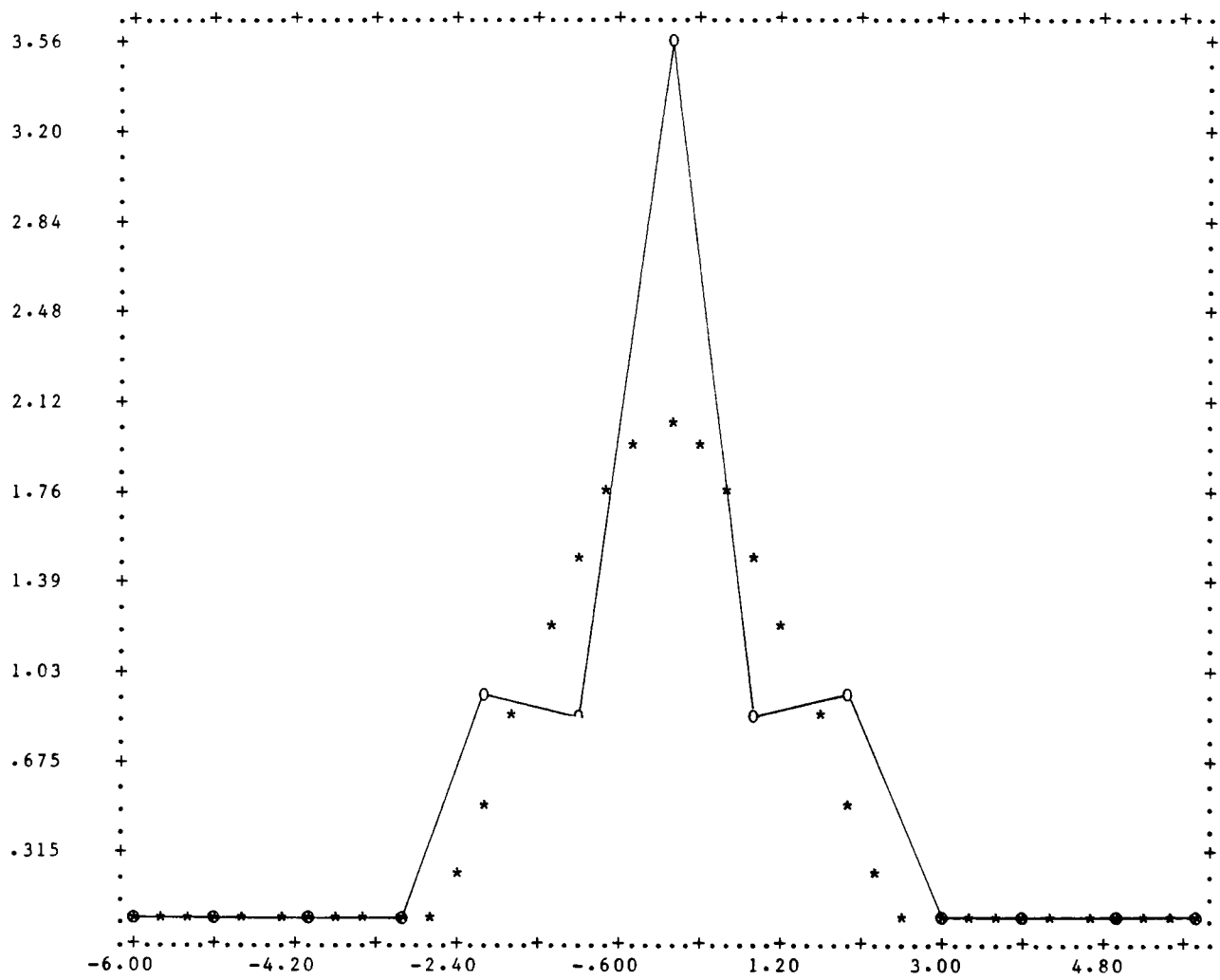


Figure 7.16 Euclidean regularization with rounded data and Simpson's rule; $\lambda = 0$.

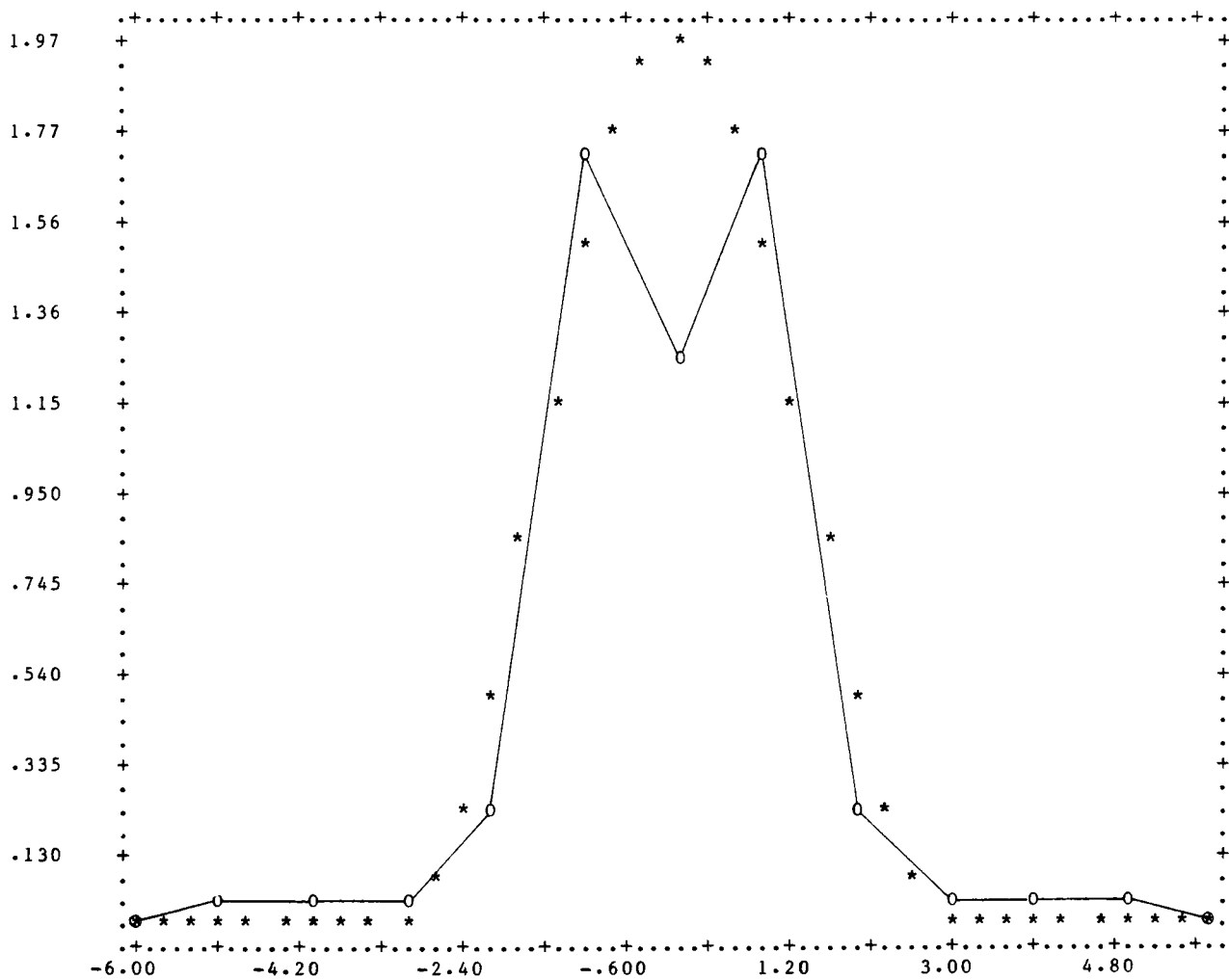


Figure 7.17 Euclidean regularization with rounded data and Simpson's rule; $\lambda = .030$.

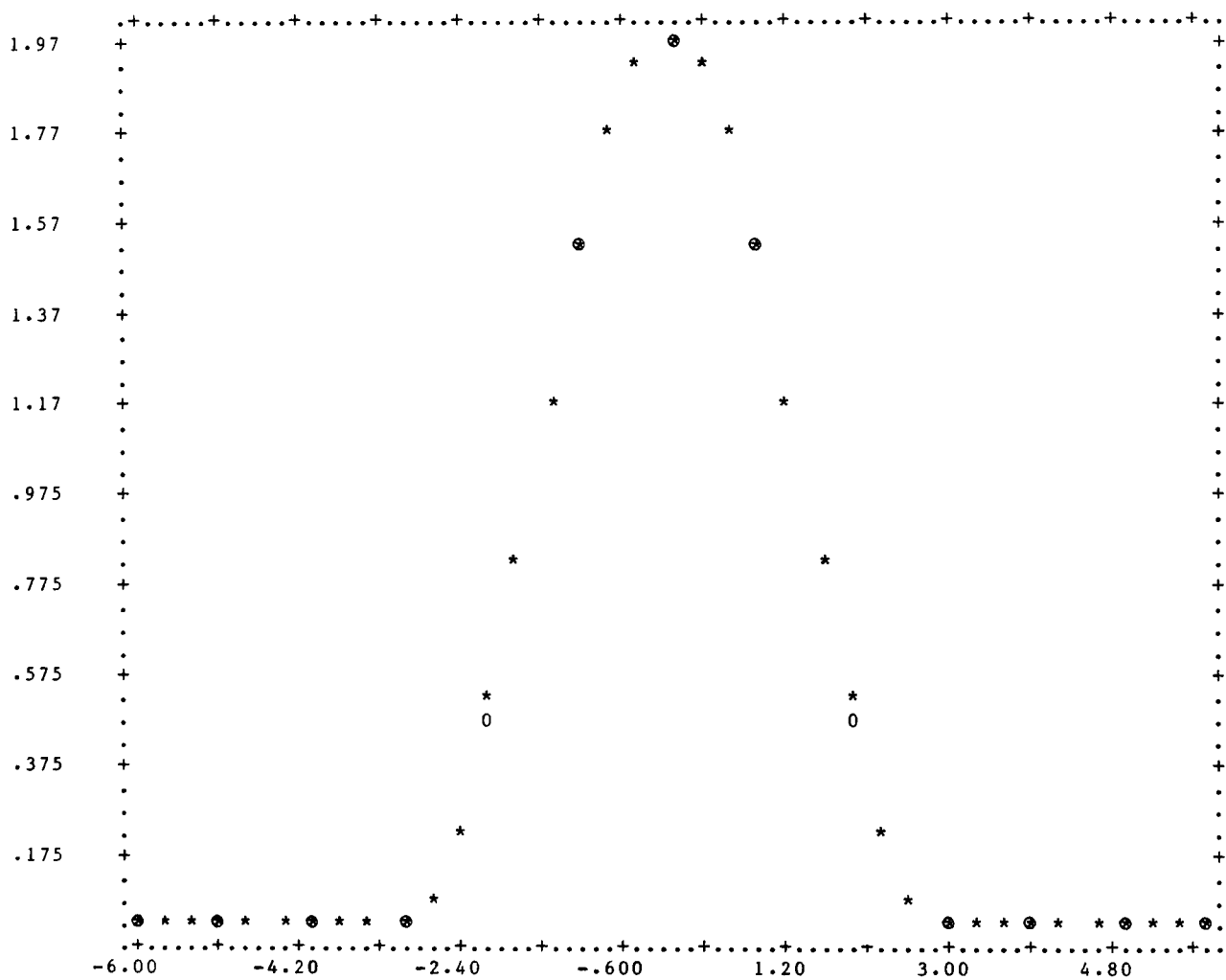


Figure 7.18 Euclidean regularization with exact data and rectangle rule; $\lambda = 0$.

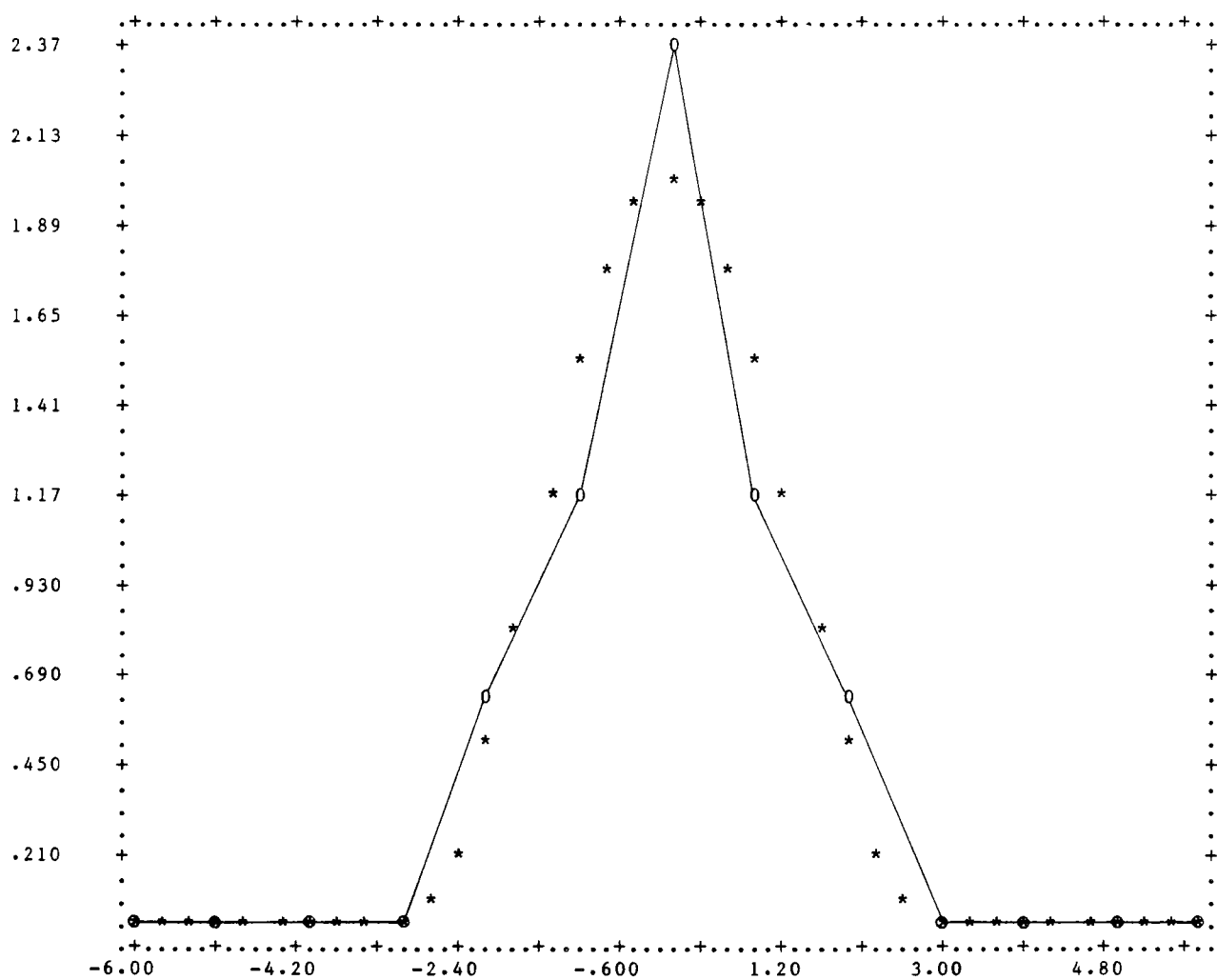


Figure 7.19 Euclidean regularization with rounded data and rectangle rule; $\lambda = 0$.

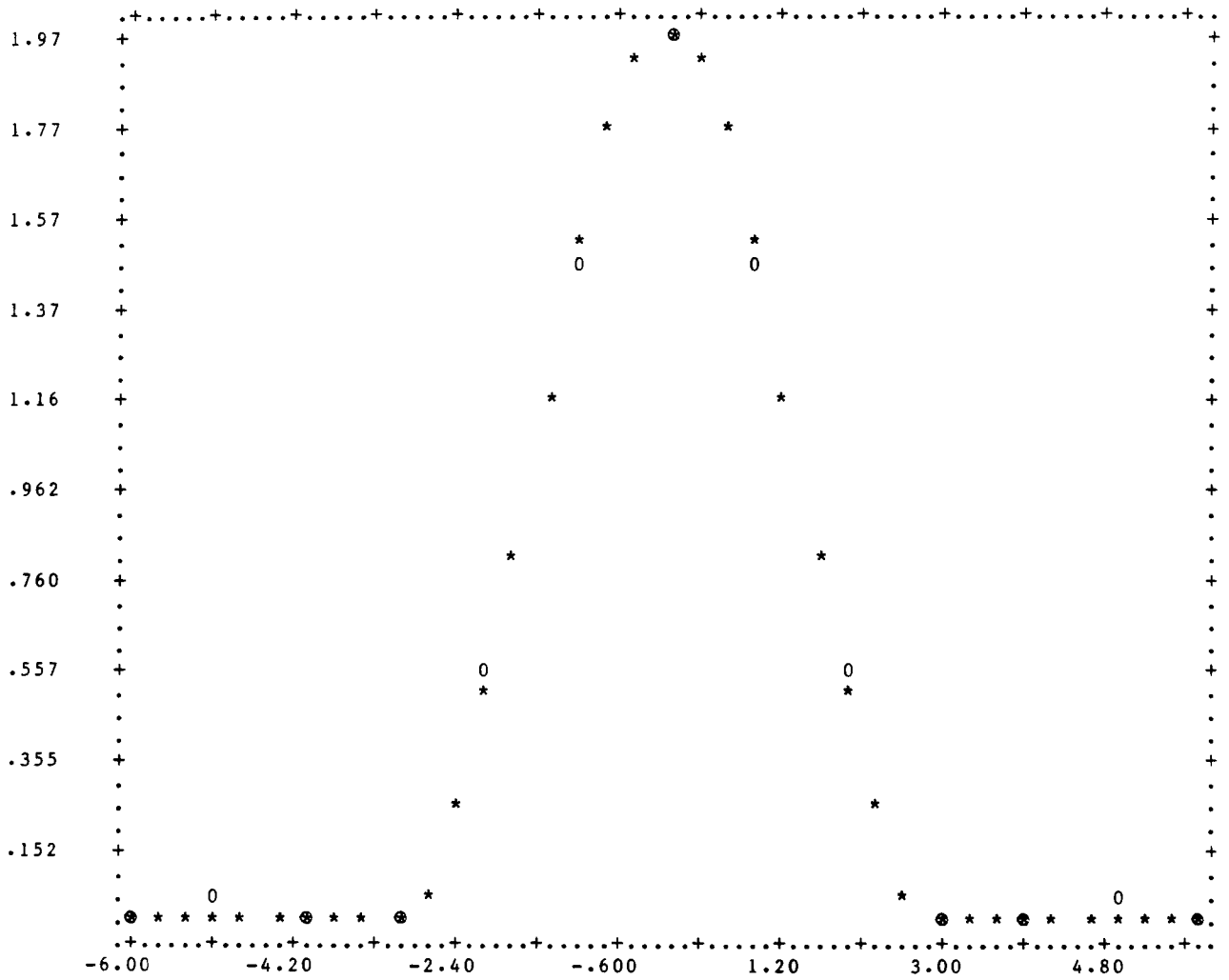


Figure 7.20 Euclidean regularization with rounded data and rectangle rule; $\lambda = .030$.

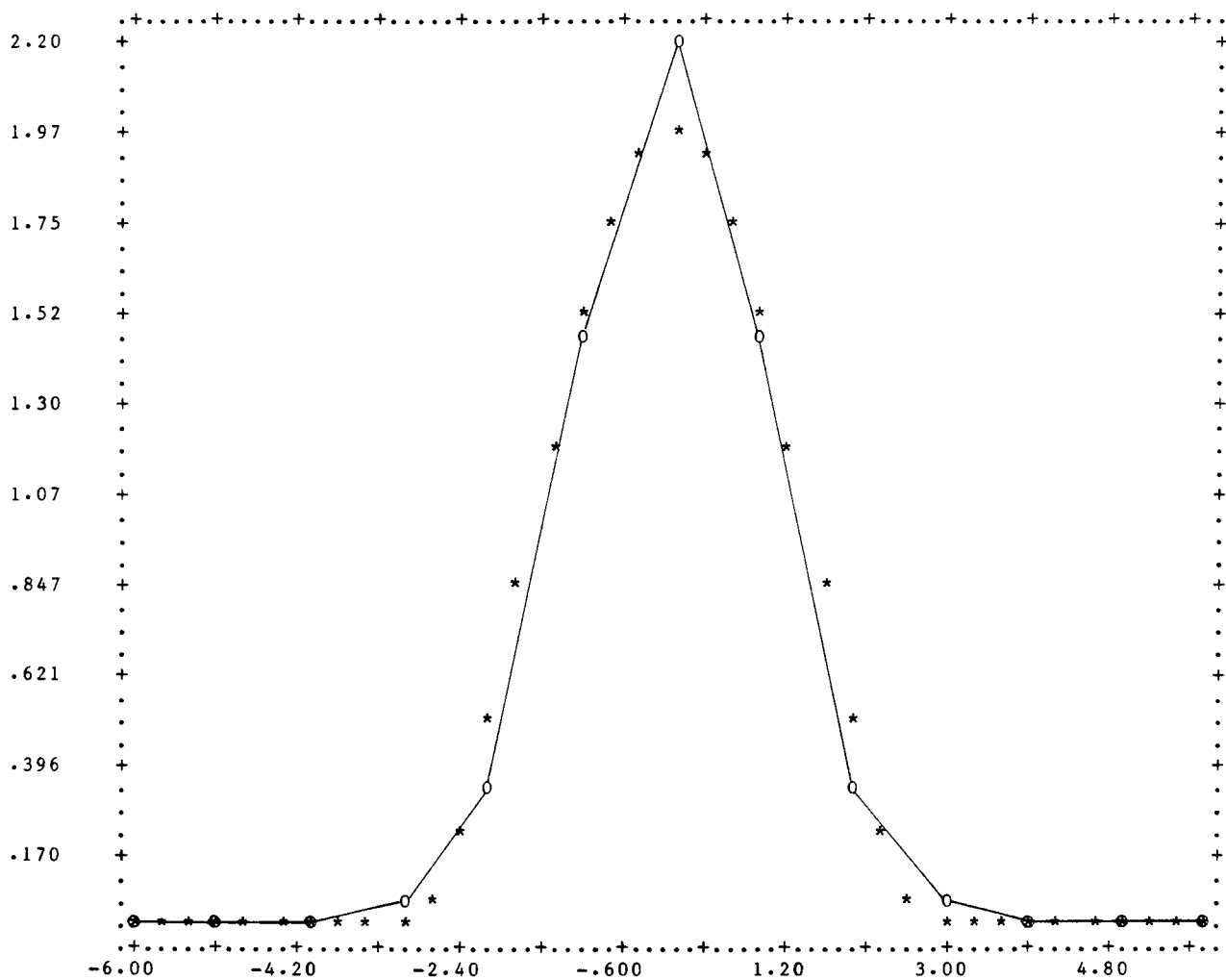


Figure 7.21 DER1 regularization with exact data and Simpson's rule; $\lambda = .050$, $\delta = 1$.

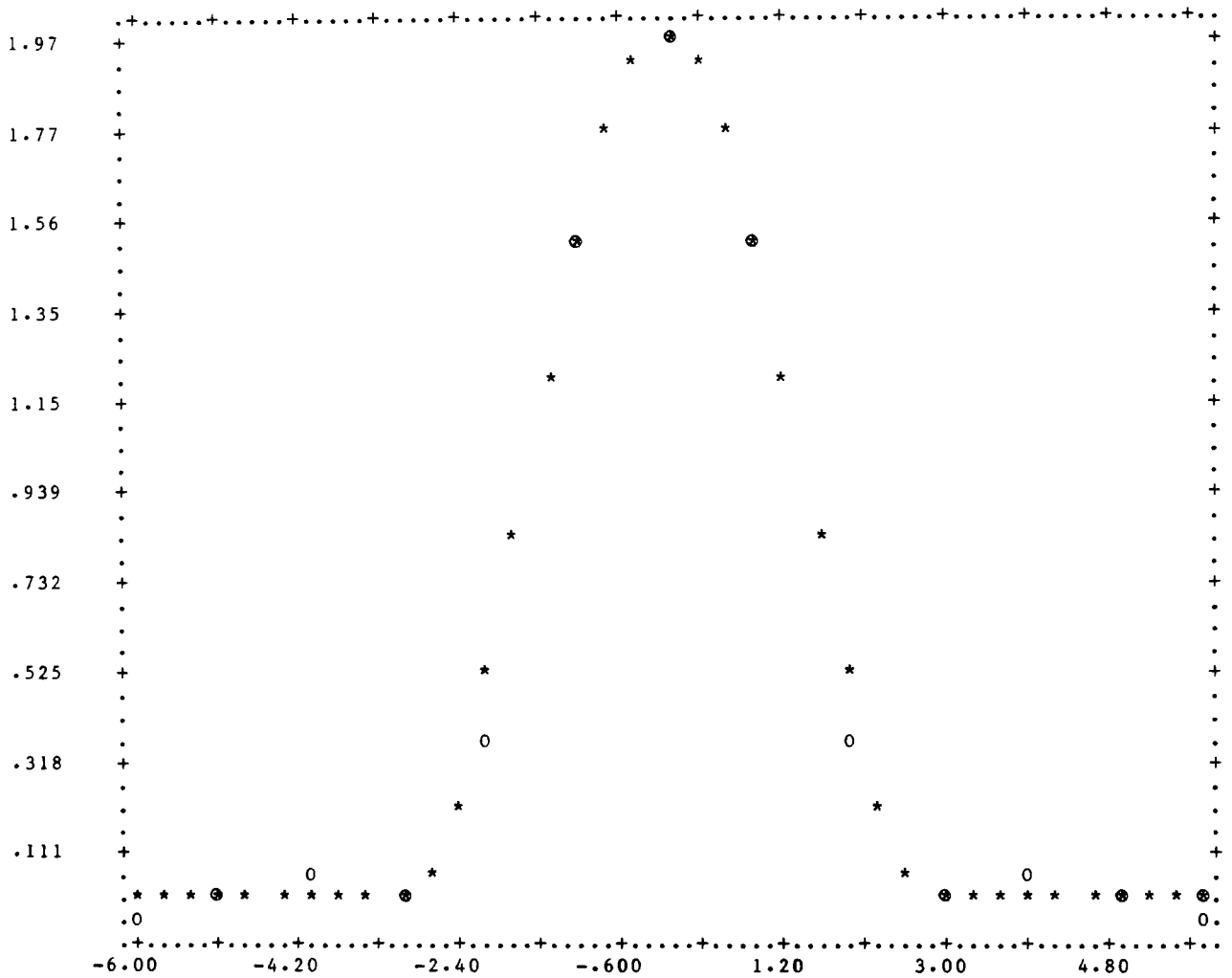


Figure 7.22 DER1 regularization with exact data and Simpson's rule; $\lambda = .100$, $\delta = 1$.

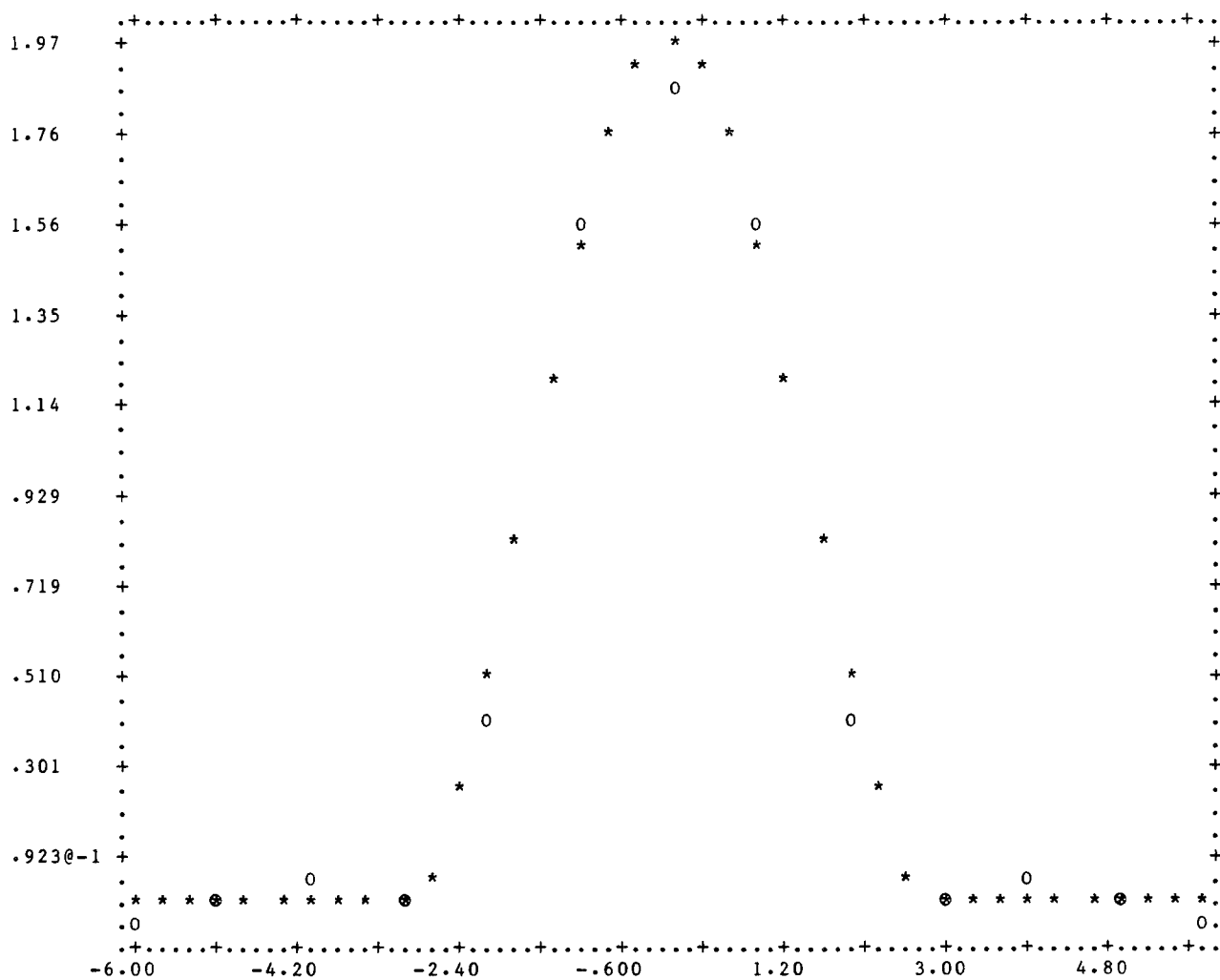
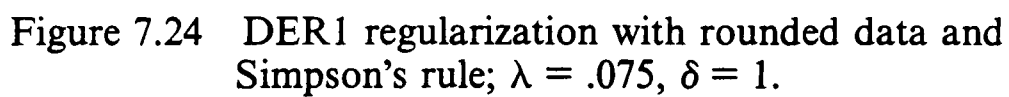


Figure 7.23 DER1 regularization with exact data and Simpson's rule; $\lambda = .150$, $\delta = 1$.



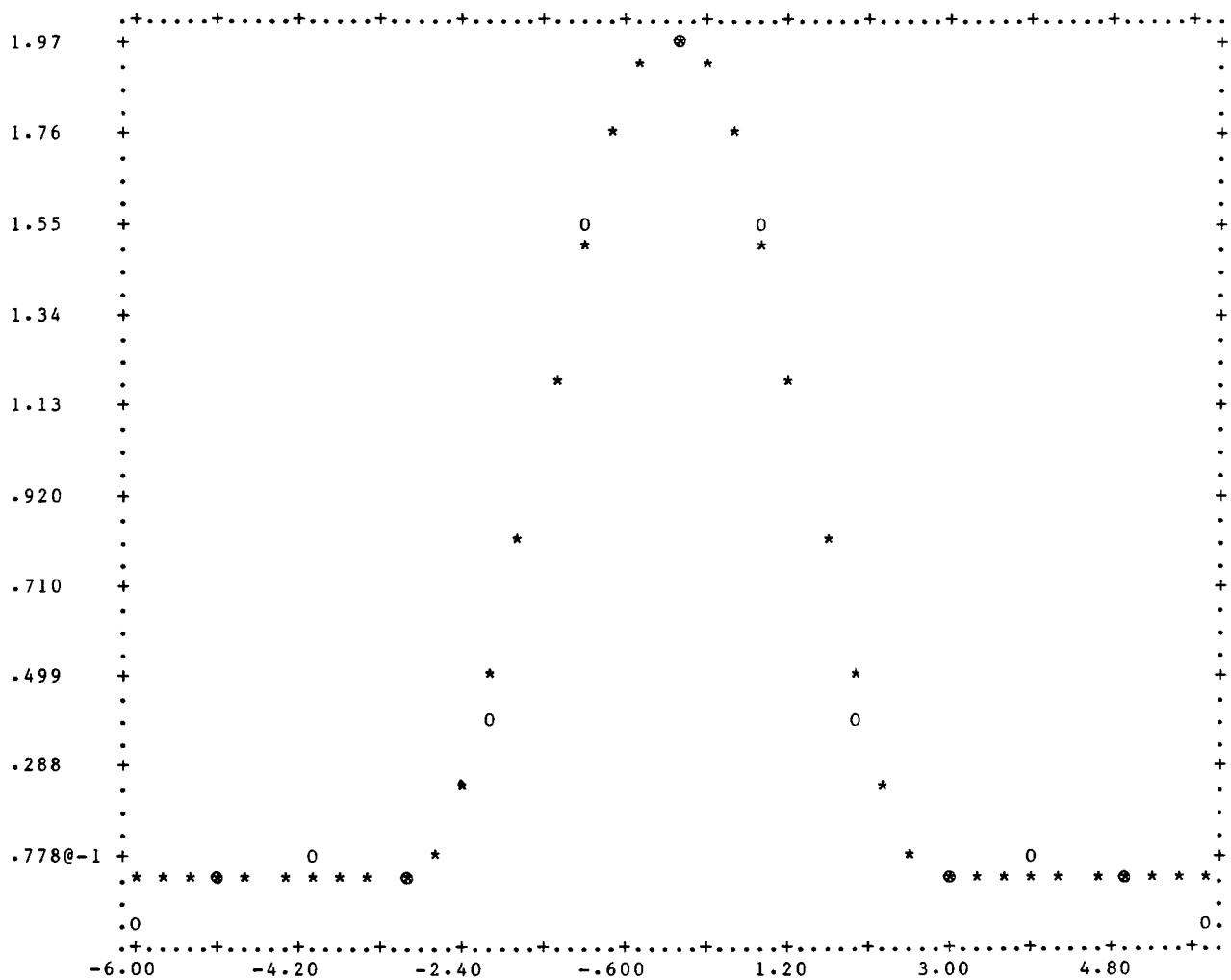


Figure 7.25 DER1 regularization with rounded data and Simpson's rule; $\lambda = .150$, $\delta = 1$.

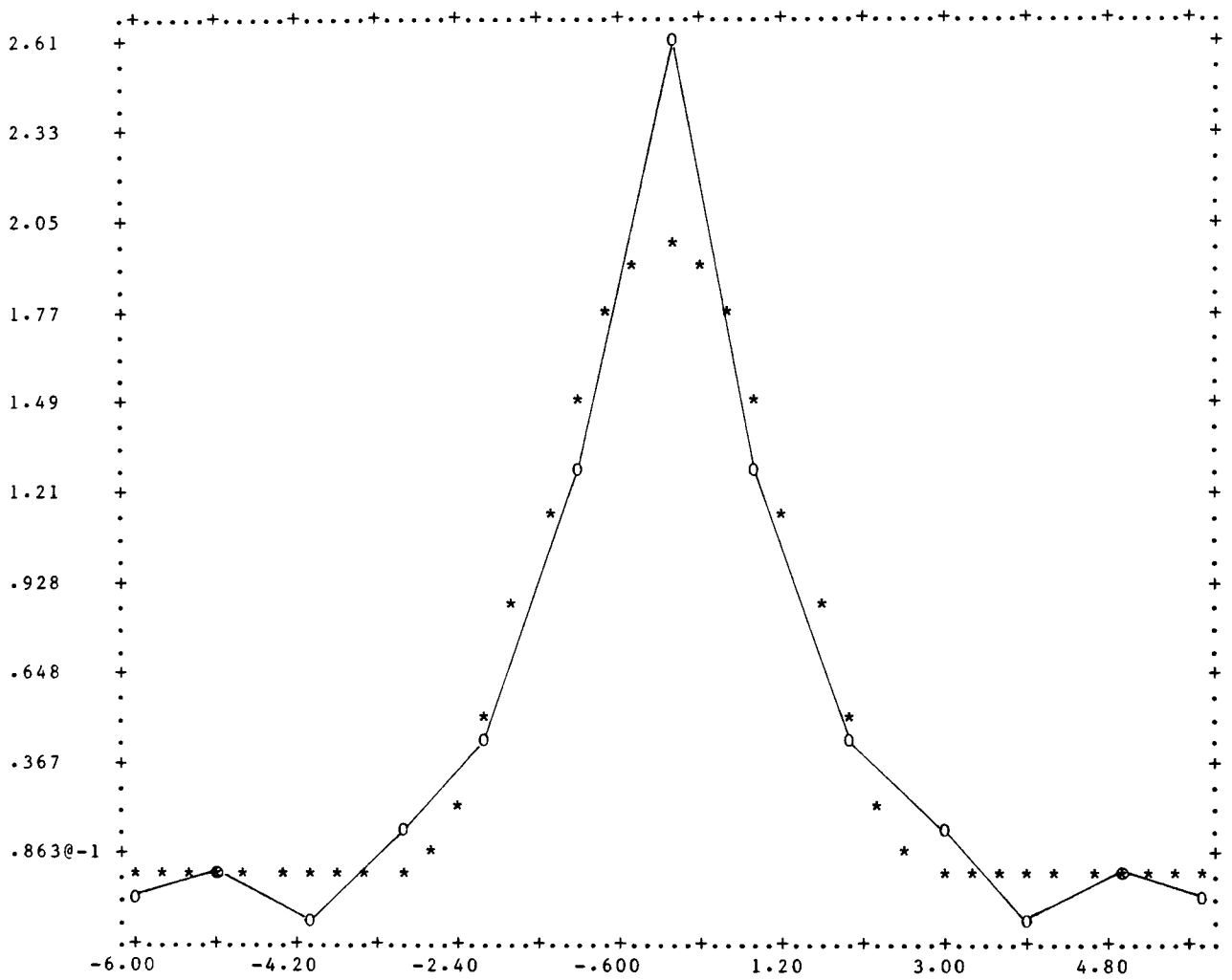


Figure 7.26 DER2 regularization with exact data and Simpson's rule; $\lambda = .010$, $\epsilon = 1$.

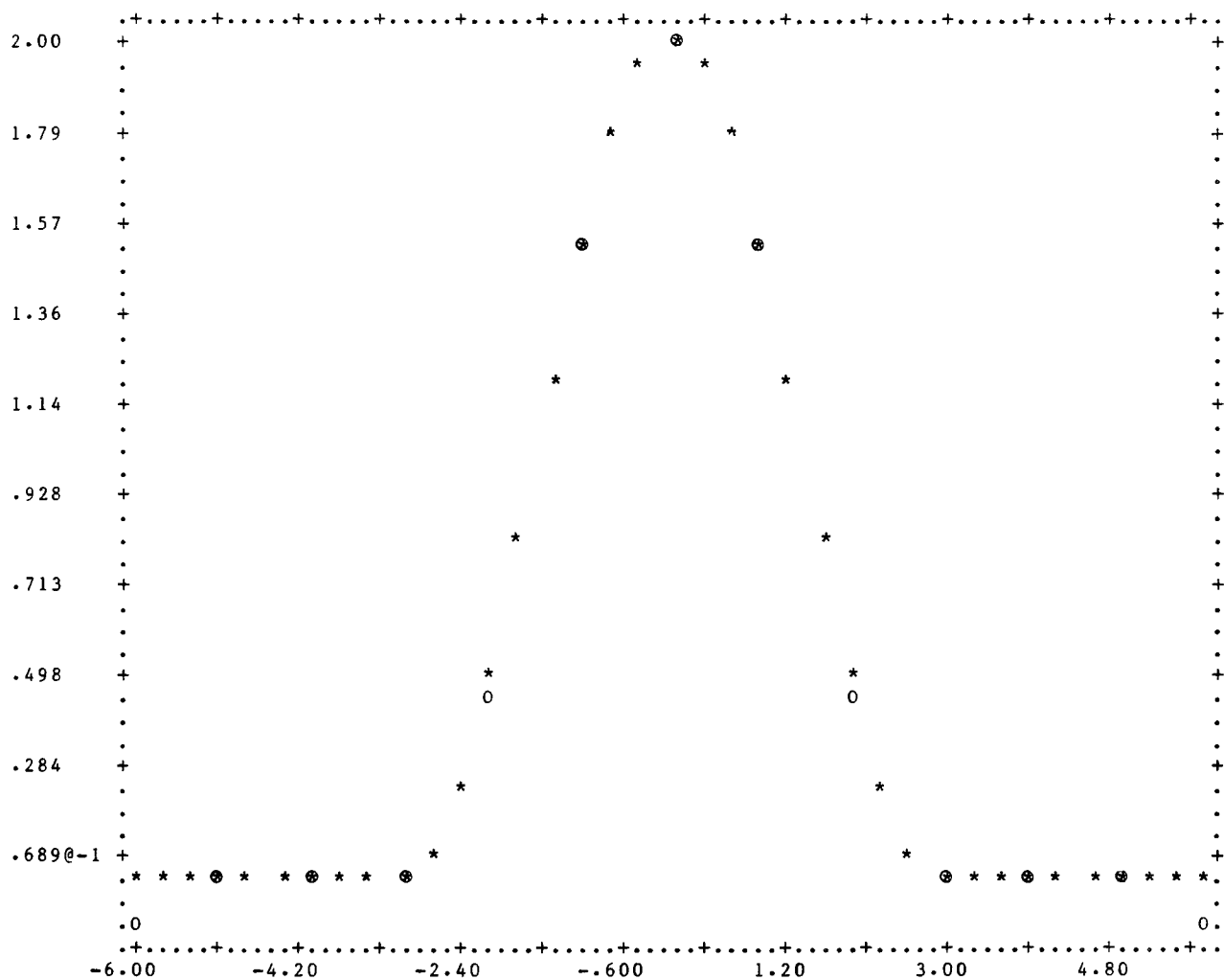


Figure 7.27 DER2 regularization with exact data and Simpson's rule; $\lambda = .100$, $\epsilon = 1$

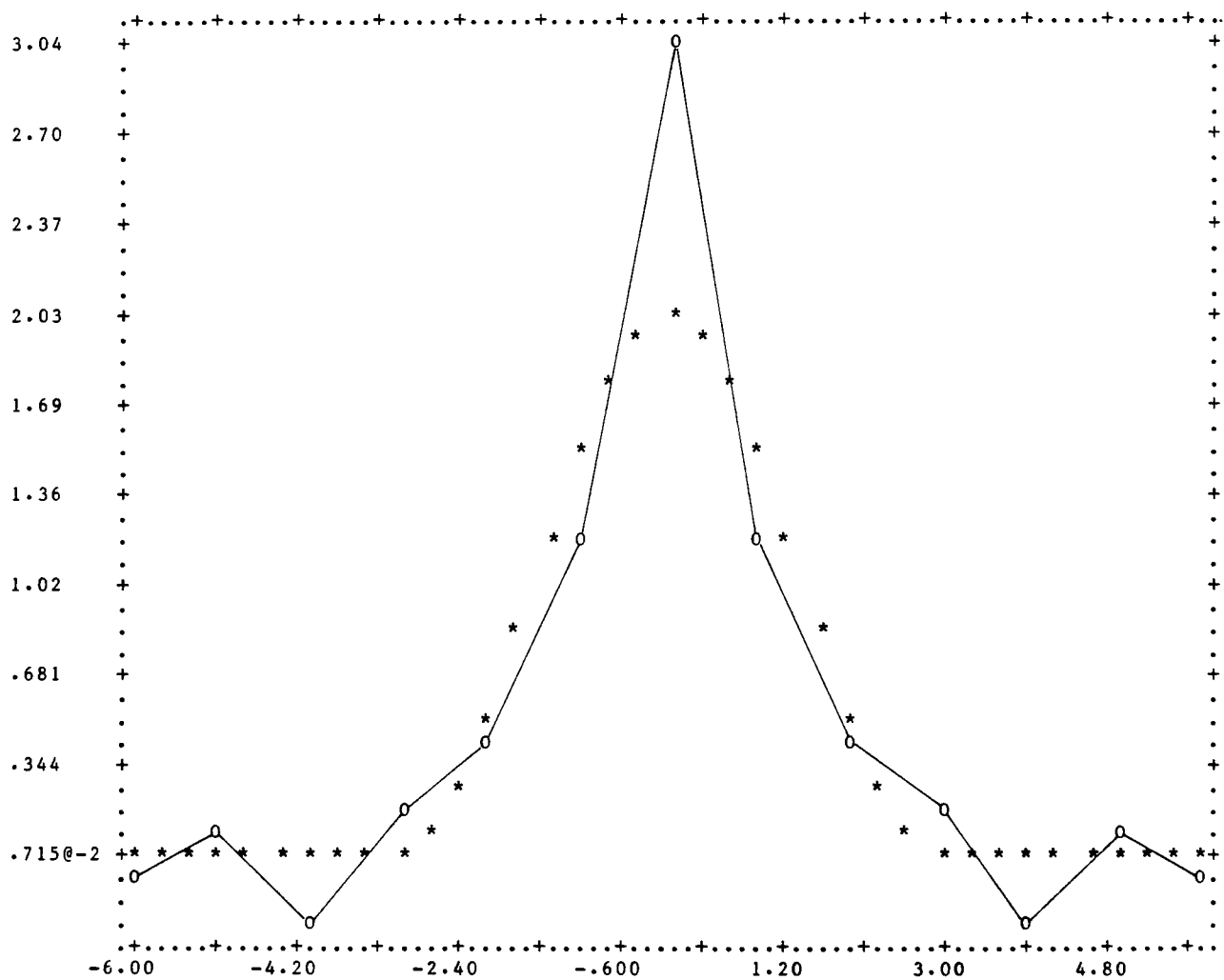
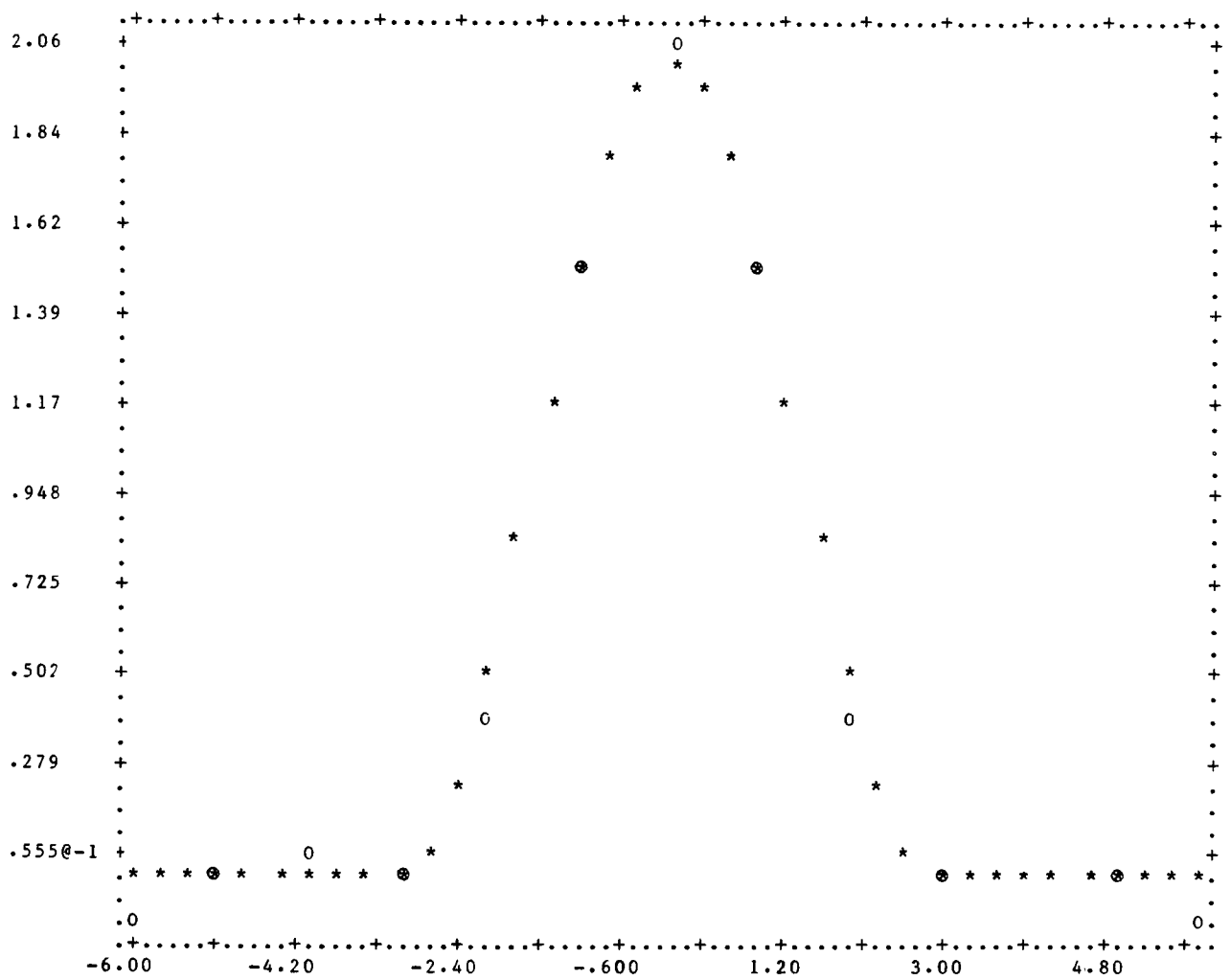


Figure 7.28 DER2 regularization with rounded data and Simpson's rule; $\lambda = .010$, $\epsilon = 1$.



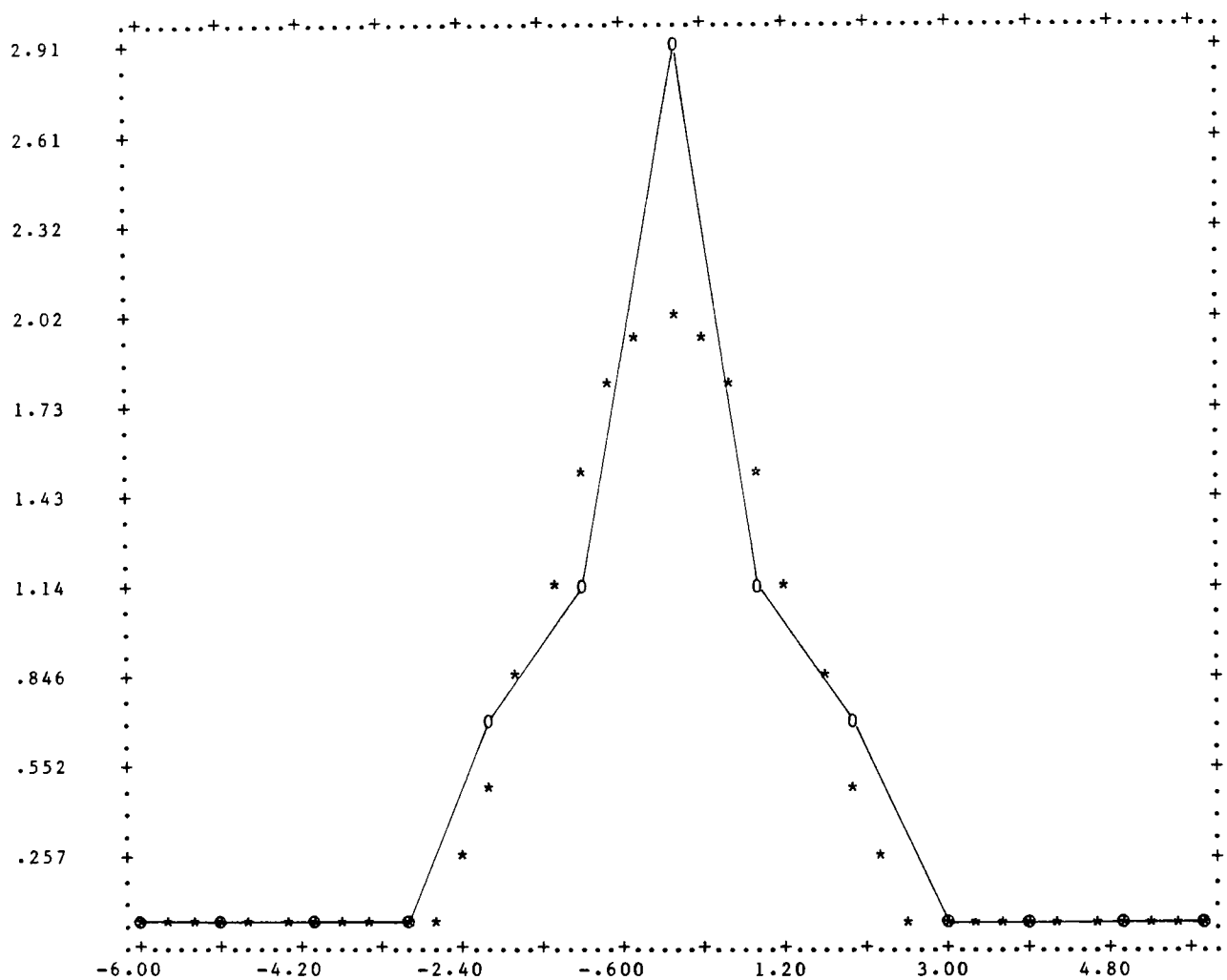


Figure 7.30 CDR regularization with exact data and Simpson's rule; $\lambda = 0$.

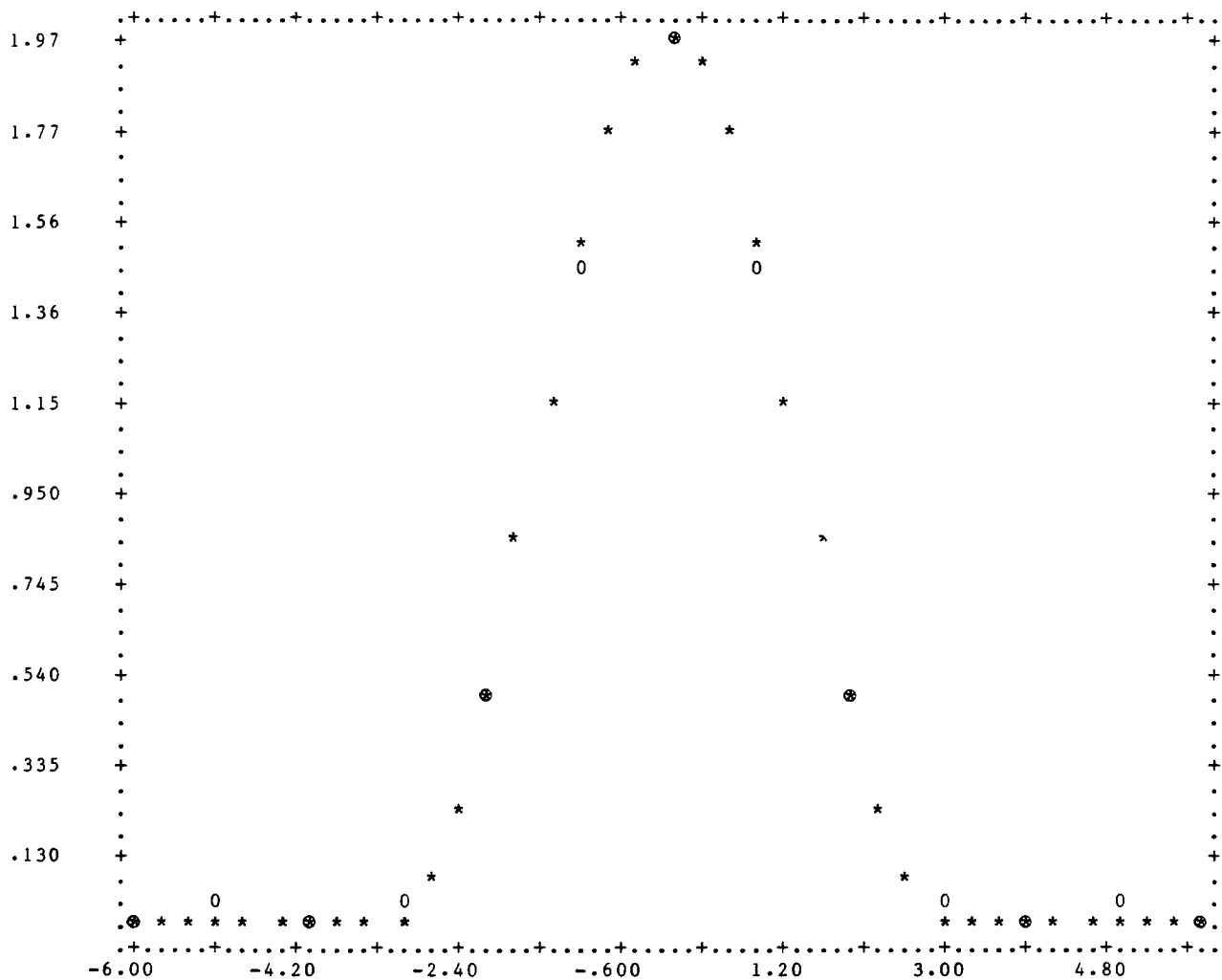


Figure 7.31 CDR regularization with exact data and Simpson's rule; $\lambda = .025$.

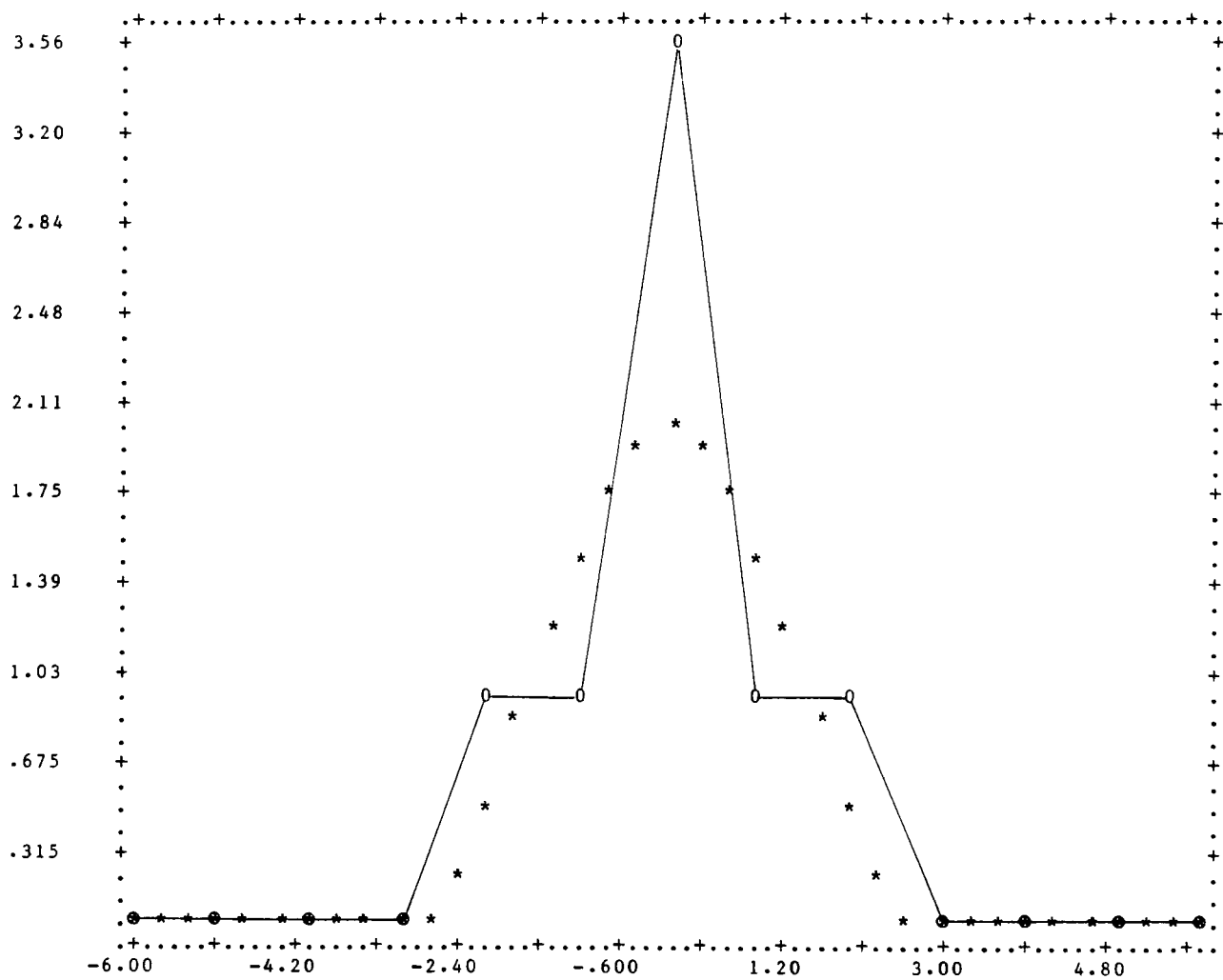


Figure 7.32 CDR regularization with rounded data and Simpson's rule; $\lambda = 0$

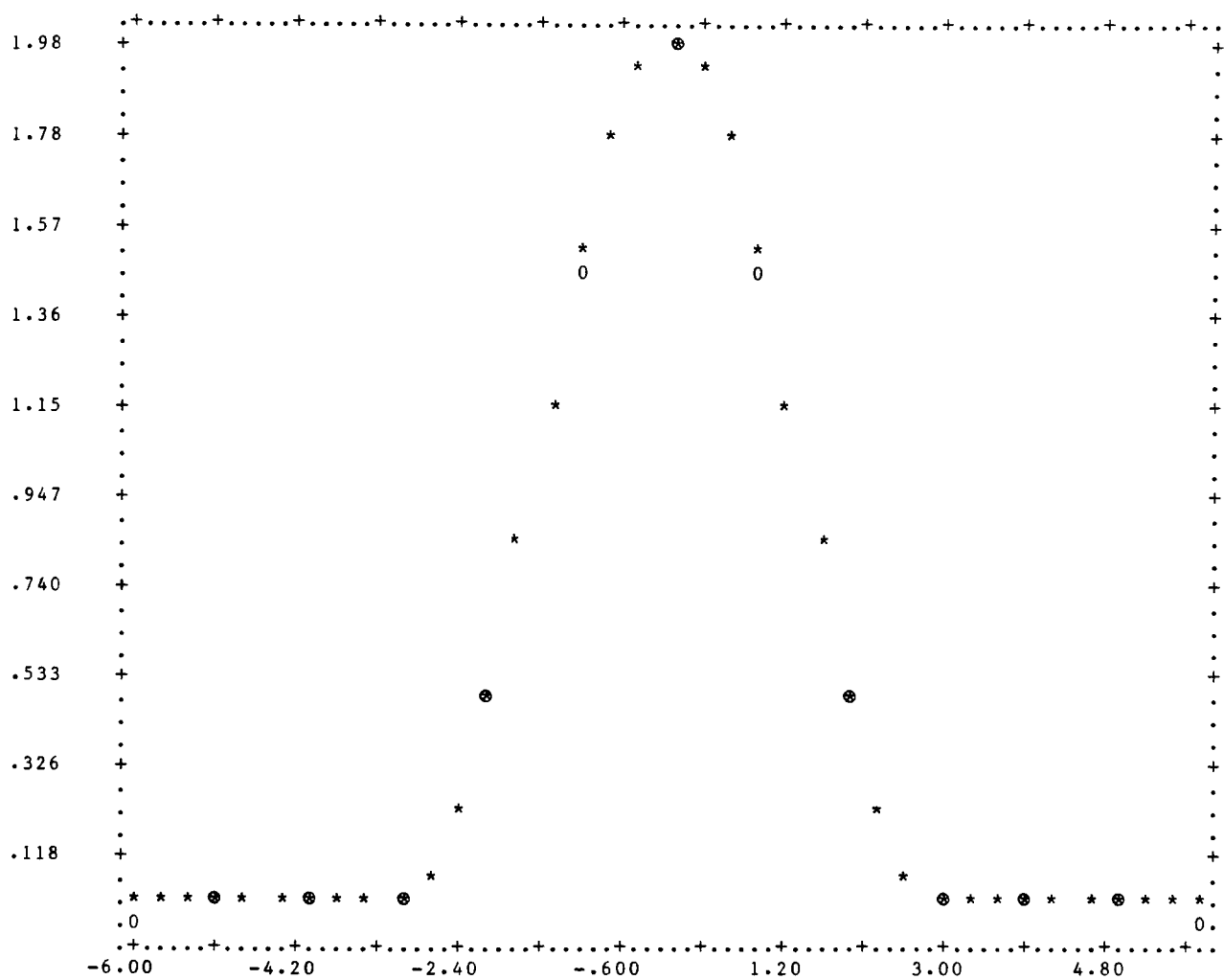


Figure 7.33 CDR regularization with rounded data and Simpson's rule; $\lambda = .030$.

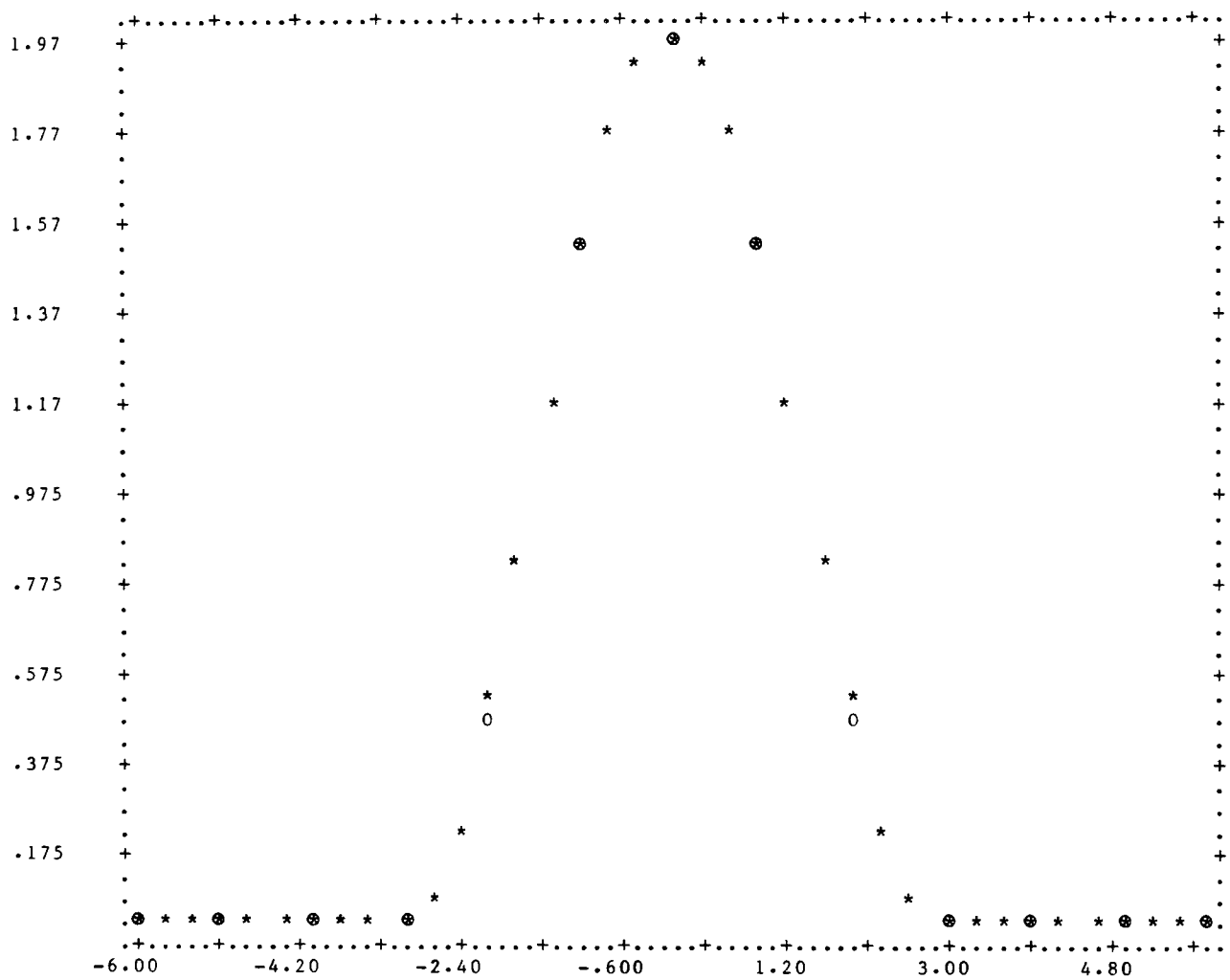


Figure 7.34 CDR regularization with exact data and rectangle rule; $\lambda = 0$.

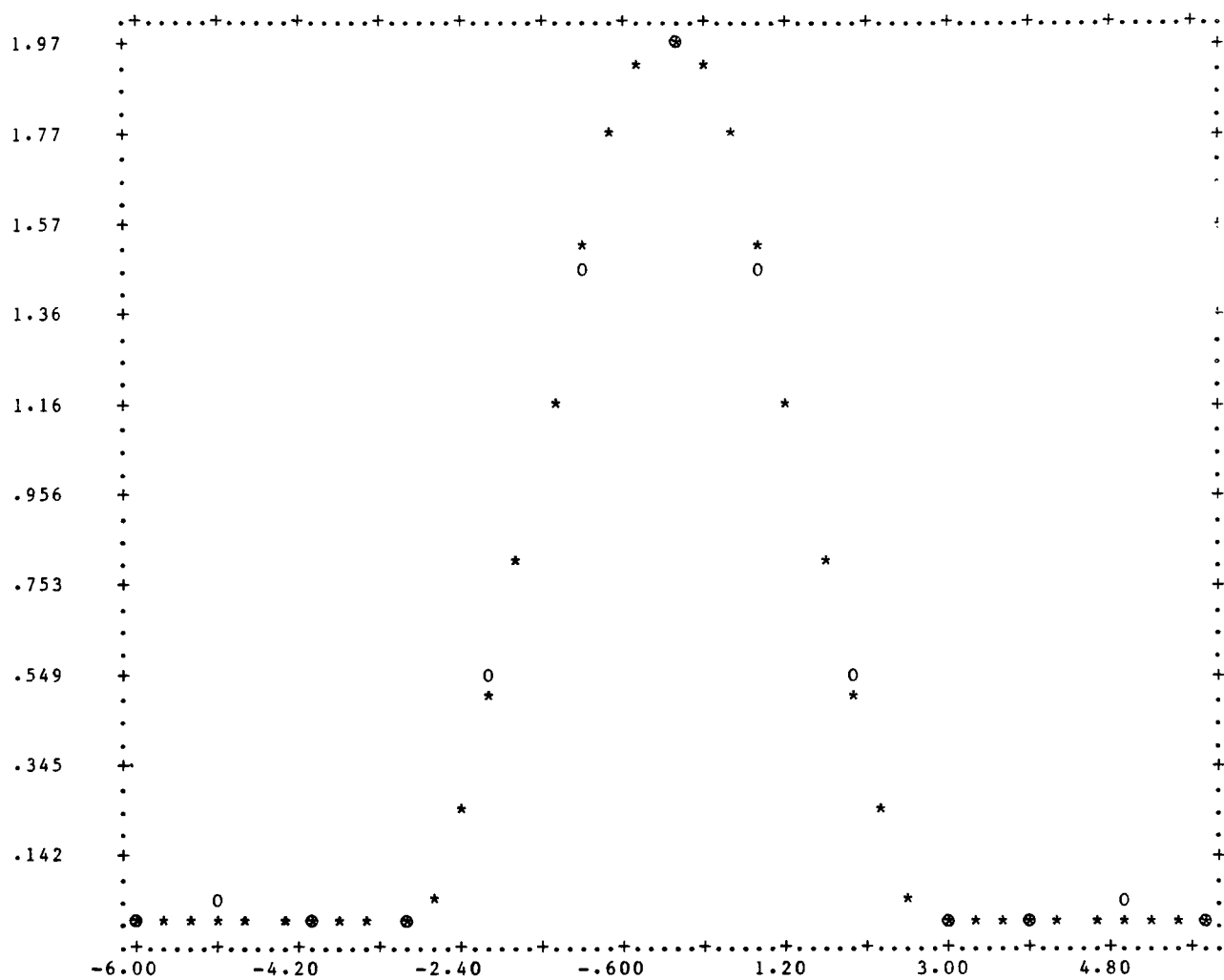


Figure 7.35 CDR regularization with exact data and rectangle rule; $\lambda = .025$.

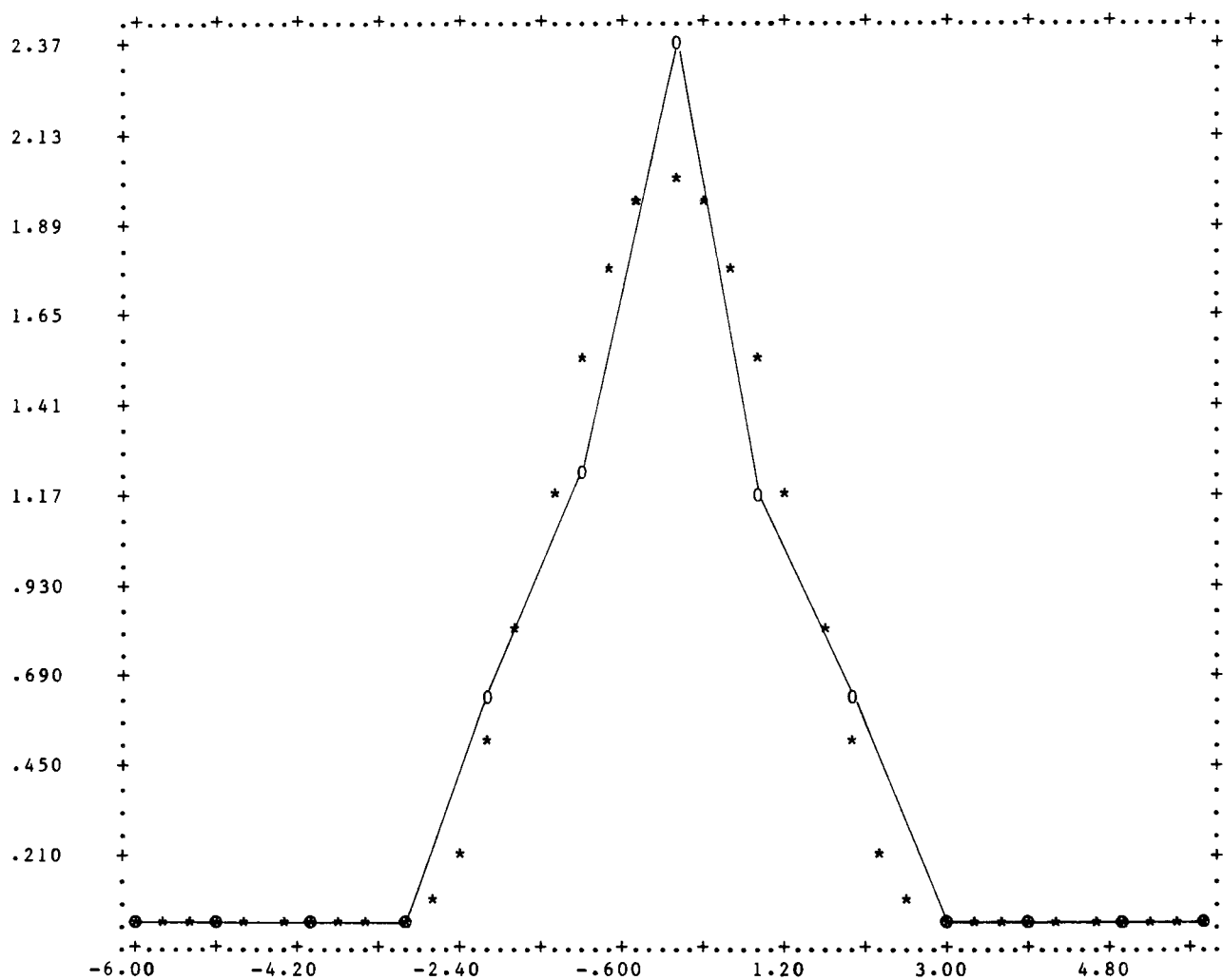


Figure 7.36 CDR regularization with rounded data and rectangle rule; $\lambda = 0$.

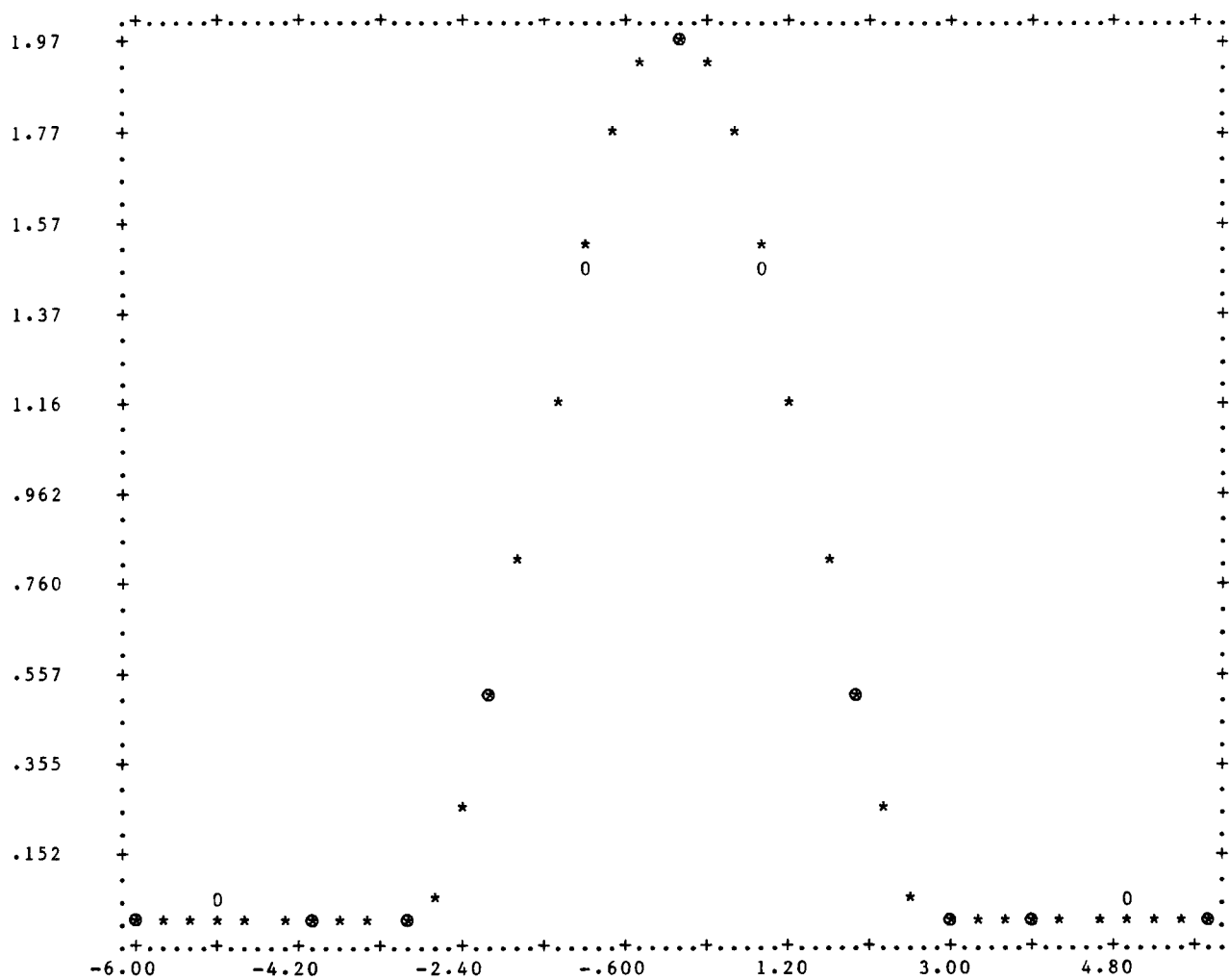


Figure 7.37 CDR regularization with rounded data and rectangle rule; $\lambda = .030$.

Section 8. Application to Ge(Li) Spectrometer Data

The final problems to which the methods developed under this contract were applied dealt with the attempt to achieve resolution improvement of actual spectral records recorded by a Nuclear Data ND100 spectrometer during an analysis of radium samples. In conducting these computations it was assumed that the model of (2.1) is valid and that h can be modeled as a difference kernel, as previously mentioned in the Summary. The recorded response of the instrument to a single radium peak was therefore accepted as comprising samples of the impulse response of the spectrometer; this record will hereafter be referred to as "PT4". The data used in the first series of these calculations was constructed by superposing 5% random noise on the PT4 data. (Throughout this discussion the records which are described all consist of 31 data points. In this section all curves are shown in normalized form.) This record was given the notation "PT4N05"; it is referred to as "spectral data" in the figures in this section. By dealing with data generated in this way it was possible to initially avoid any tendency of the spectrometer to violate the shift-invariant hypothesis and the resulting difficulty associated with such pathology of the instrument.

The results of the singular value analysis of the spectral data are shown in Figures 8.1 through 8.7. In these figures it can be observed that values of k large enough to yield any significant resolution improvement in the data yield also accompanying contamination by noise effects which is unacceptably large for many purposes. This situation is typical of the results obtained in all calculations with actual analyzer data using the singular value analysis approach.

Figures 8.8 through 8.12 indicate the type of results obtained with Euclidean regularization and various values of the smoothing parameter λ . Here some improvements over the results obtained using singular value analysis are noted. For example, Figure 8.11 ($\lambda = .001$) reveals a fairly significant level of resolution improvement with the degrading effects limited primarily to some "undershooting" of the zero count level in the immediate vicinity of the peak tip location.

The other figures indicating results obtained using the spectral data (Figures 8.13 through 8.21) show typical behavior of the differential and continuous/discrete regularization methods as applied to spectrometer data. No clear superiority of these methods (over Euclidean regularization) is apparent in these results and, due to the larger costs incurred with their use, there seems to be little to recommend them (in this type of problem).

The lower quality of the results observed to this point in this section (as compared with the previous one) seems to be due to an inherent instability in the process of attempting to deconvolve the analyzer peak data so as to produce the (theoretically correct) extremely sharp peak comprising the presumed incident data signal. One knows, of course, that deconvolution is normally an unstable process in any case, but the results obtained thus far (compared to those produced in Phillips' problem, for example) indicate that the problem at hand is especially unstable. The following compromise problem formulation was suggested by C. Nelson, Environmental Analysis Division, Office of Radiation Programs, as previously mentioned. With the viewpoint that the impulse response k of the analyzer is of an approximately Gaussian nature, one may select a Gaussian pulse p of half-width significantly less than that of k . Then a resolution improve-

ment calculation which yields the result p (with low superposed noise) from the spectral data would be a highly acceptable, though not ideal, achievement.

Continuing in the above vein, one may write (2.1) as $g = k*f$ where the star (*) denotes the operation of convolution. Convolving with p gives $g*p = k*f*p$ or

$$k*f_p = g_p \quad (8.1)$$

where, through the rest of this section, a subscripting with the name of a function will be used to indicate the result of convolution with that function. (Since convolution is commutative there is no need to insist on a given order in which the operands are listed.) If one replaces the problem of solving (2.1) for f with that of solving (8.1) for f_p then the compromise mentioned above has been conceptually effected. From the theoretical point of view one may regard the compromise problem in the following manner. The problem of solving (2.1) for f (as stated) has proven to be a quite ill-conditioned one so that significant levels of resolution improvement are being found extremely difficult to obtain (in the absence of such a priori information as will be mentioned momentarily) without unacceptable contamination due to noise effects. Therefore one has now replaced the original problem with that of determining the moment f_p given by

$$f_p(E) = \int_0^v f(x)p(E-x)dx. \quad (8.2)$$

The tacit hope, of course, is that the solution of (8.1) for the moment f_p defined by (8.2) will prove to be a significantly more stable problem (when discretized for actual computation, as usual) than that of solving (2.1) for f , as originally posed.

The pulse p chosen for the data being considered in this section is a Gaussian of standard deviation $4/3$. The convolution required to produce the data g_p for the problem of (8.1) was, of course, implemented in a discrete fashion. Although it is perhaps possible to obtain some reduction in computational costs on the ADP, Inc. system through the use of the Fourier approach to convolution outlined in Section 1, the savings would not be significant enough in the present problem to justify the additional time required for software development and so the straight-forward approach was taken. Specifically, a matrix PM with entries given by $PM_{ij} = p(E_i E_j)$ was generated; then the product of PM and the vector \vec{g} consisting of samples from g yields the sample vector \vec{g}_p appropriate for a discrete implementation of (8.1). The approximate solution of the resulting discrete version of (8.1) was then approached using the Euclidean regularization method. (Other methods of solution were not considered due to cost considerations and the prior indications that no significant improvement in the results obtained is likely.)

When the data g consisted of the previously considered spectral data PT4N05 the \vec{g}_p resulting was referred to as the "spread spectral data"; the results obtained are indicated in Figures 8.22 through 8.26. A comparison of these plots with the previously obtained Figures 8.8 through 8.12 (in which Euclidean regularization was used with the same spectral data) shows that very significant improvement of the stability of the problem has been achieved by using the data spreading technique while only very minimal losses of resolution level have been incurred.

The remaining consideration of interest in this section has to do with the application of these methods to other actual photopeak data taken

from the analyzer (as opposed to the previous spectral data which was generated by superposing random noise on the impulse response "PT4" of the analyzer). This second data, which will be called the "cross spectral" data, resulted from the recorded response of the spectrometer to a second radium peak; it will be denoted as "PT3". For reasons previously indicated, only the Euclidean regularization method was applied to the approximate solution of equations (2.1) and (8.1) with the data $g = \text{PT3}$. (The impulse response $k = \text{PT4}$ and the choice of the Gaussian pulse p remained as before.)

The results obtained with this cross spectral, and spread cross spectral, data are shown by a comparison of Figures 8.27 through 8.31 with Figures 8.32 through 8.36, respectively. The greatly increased stability of the latter group of solutions is most vivid and, in particular, Figure 8.34 shows that acceptable quality results are beginning to become available through the combined use of the regularization and data spreading techniques, whereas the regularization methods alone (Figure 8.29) do not yield results of stability sufficient for many purposes. One further consideration of gamma spectral data resolution improvement was studied, however, and found to be of great potential.

One knows, of course, that the solutions f of the problems being considered in this section are necessarily nonnegative ones. It has become obvious, however, that the effects of small amounts of noise and large tendency toward instability combine to give computed results f_λ having significantly large negative values. It is therefore very reasonable to hope that one might obtain some improvement in the results of solving both (2.1) and (8.1) by using the constraint $f(x) \geq 0$ for all x . Computationally this was effected by reconsidering the problem of (2.1) in the

Euclidean regularization framework where the a priori information of non-negativity was now imposed through the appropriate constraints. Thus the statement of the problem of (5.1) was modified to:

$$\text{Minimize } \left\| \vec{g} - A\vec{f} \right\|_E^2 + \lambda^2 \left\| \vec{f} \right\|_E^2 \text{ subject to } f_j \geq 0 \quad (8.3)$$

In solving (8.3) computationally an approach analogous to that indicated in Section 5 (following (5.1)) was taken; the well-known subroutine NNLS of Lawson and Hanson [19] was used in conjunction with a "driver program" written* for the EERF computer system. Again considering both the spectral data PT4N05 and the cross-spectral data PT3, resolution improvement calculations were carried out; the results of these computations are indicated by Figures 8.37 through 8.40. These final results appear most promising. It is very evident that a great increase in the stability and sharpness of the enhancements has been obtained in these sample calculations and, in fact, even setting $\lambda = 0$ (no regularization at all) appears to be a completely reasonable alternative. Using the usual FWHM criterion one finds that in Figure 8.37, for example, resolution improvement by a factor of approximately five is in evidence. Due to lack of time there were no further calculations conducted with this "ERNN" approach but it is clear that larger scale investigation of this method should be a high priority item in the second phase of work under this contract effort.

*Juanita Coley of EERF provided a great deal of expert assistance with programming and systems analysis during the course of this work.

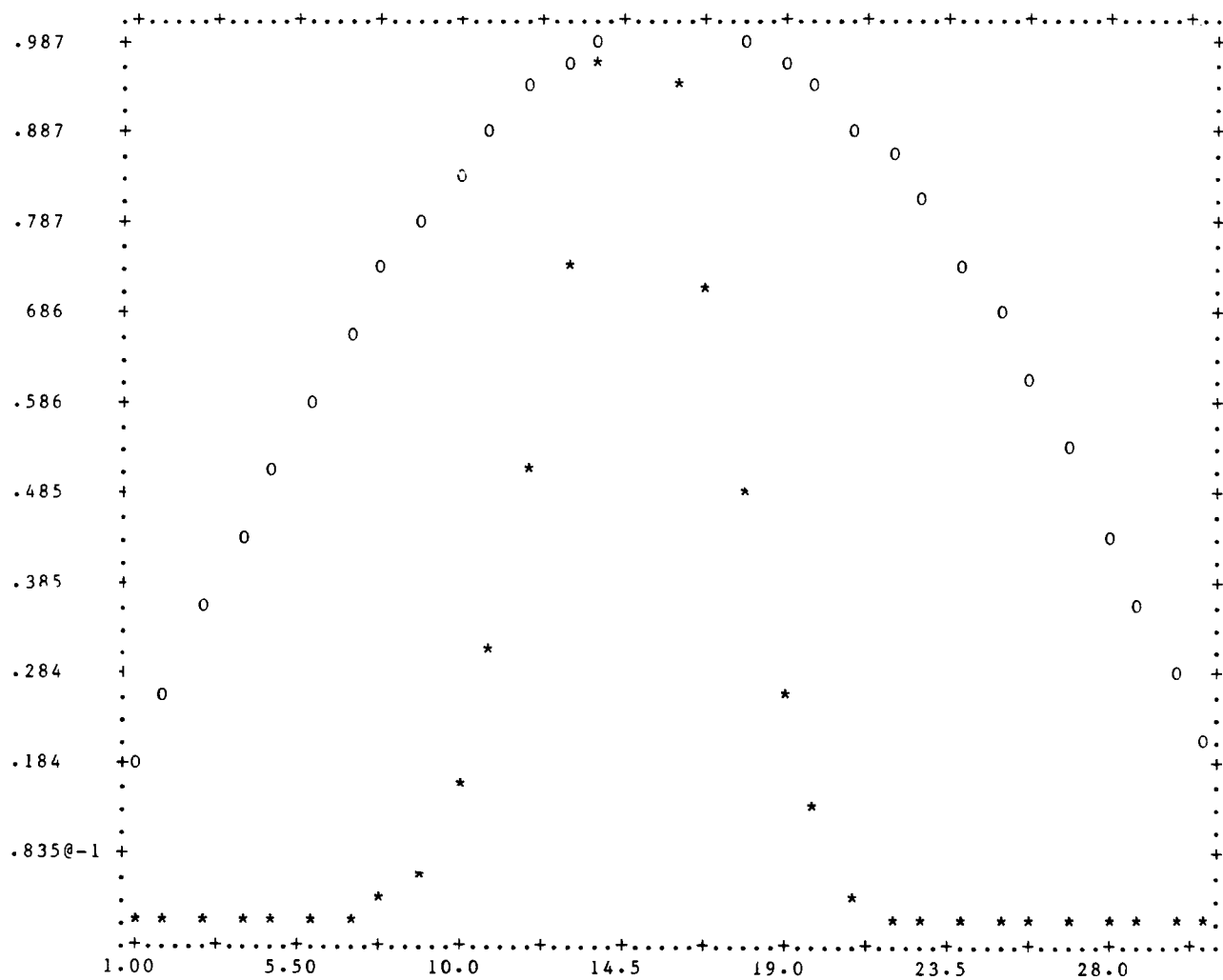


Figure 8.1 Singular value analysis with spectral data; $k = 1$.

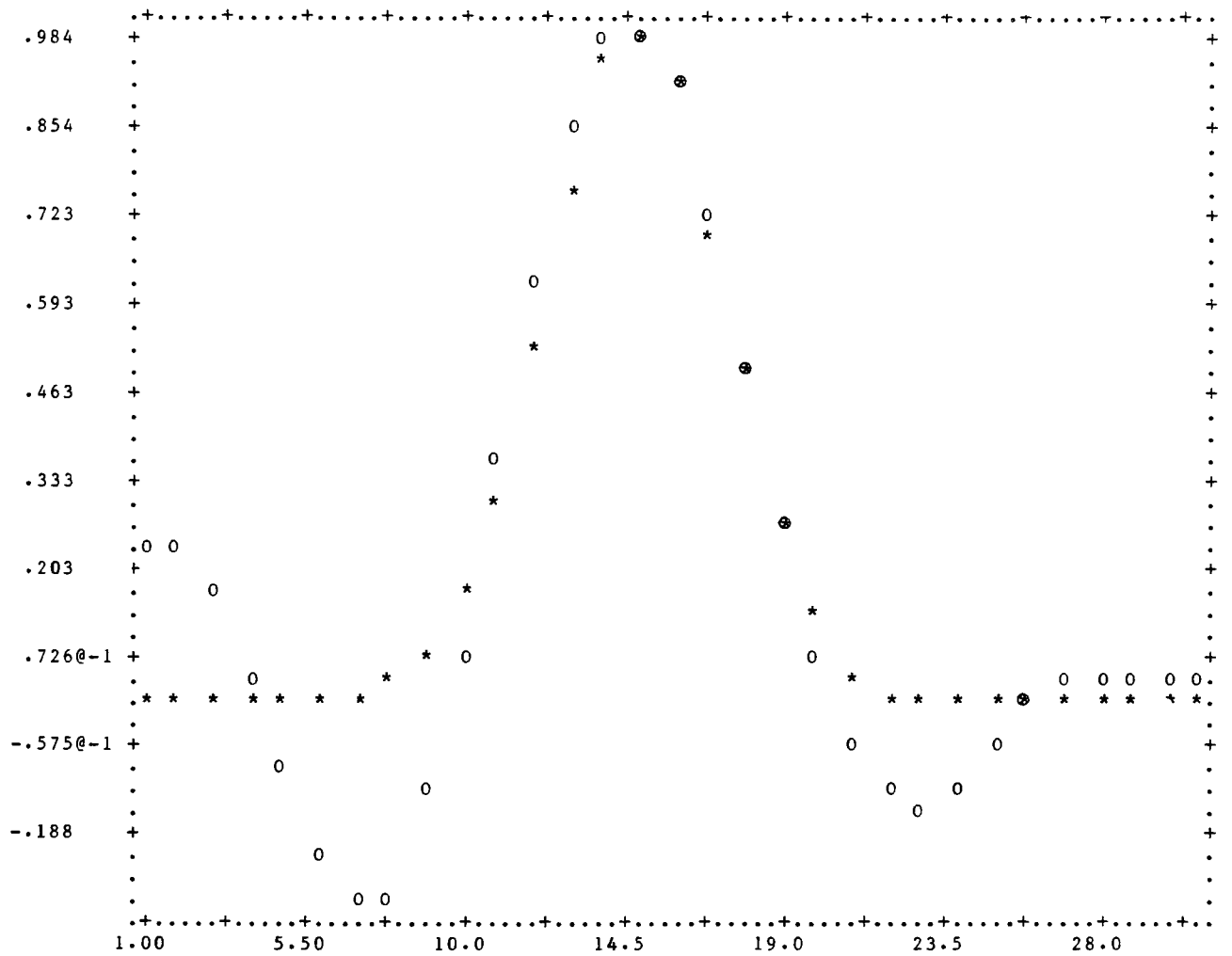


Figure 8.2 Singular value analysis with spectral data; $k = 6$.

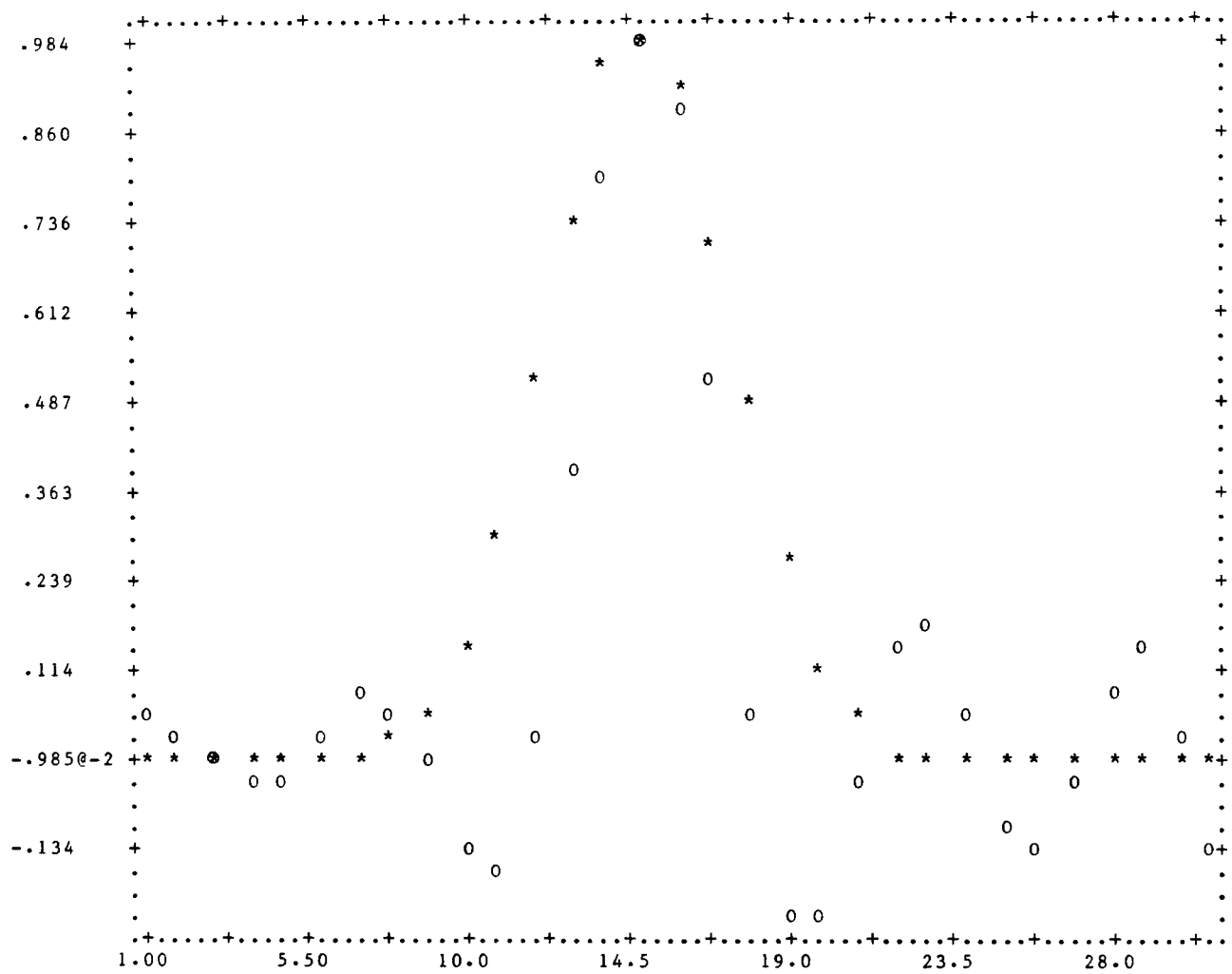


Figure 8.3 Singular value analysis with spectral data; $k = 11$.

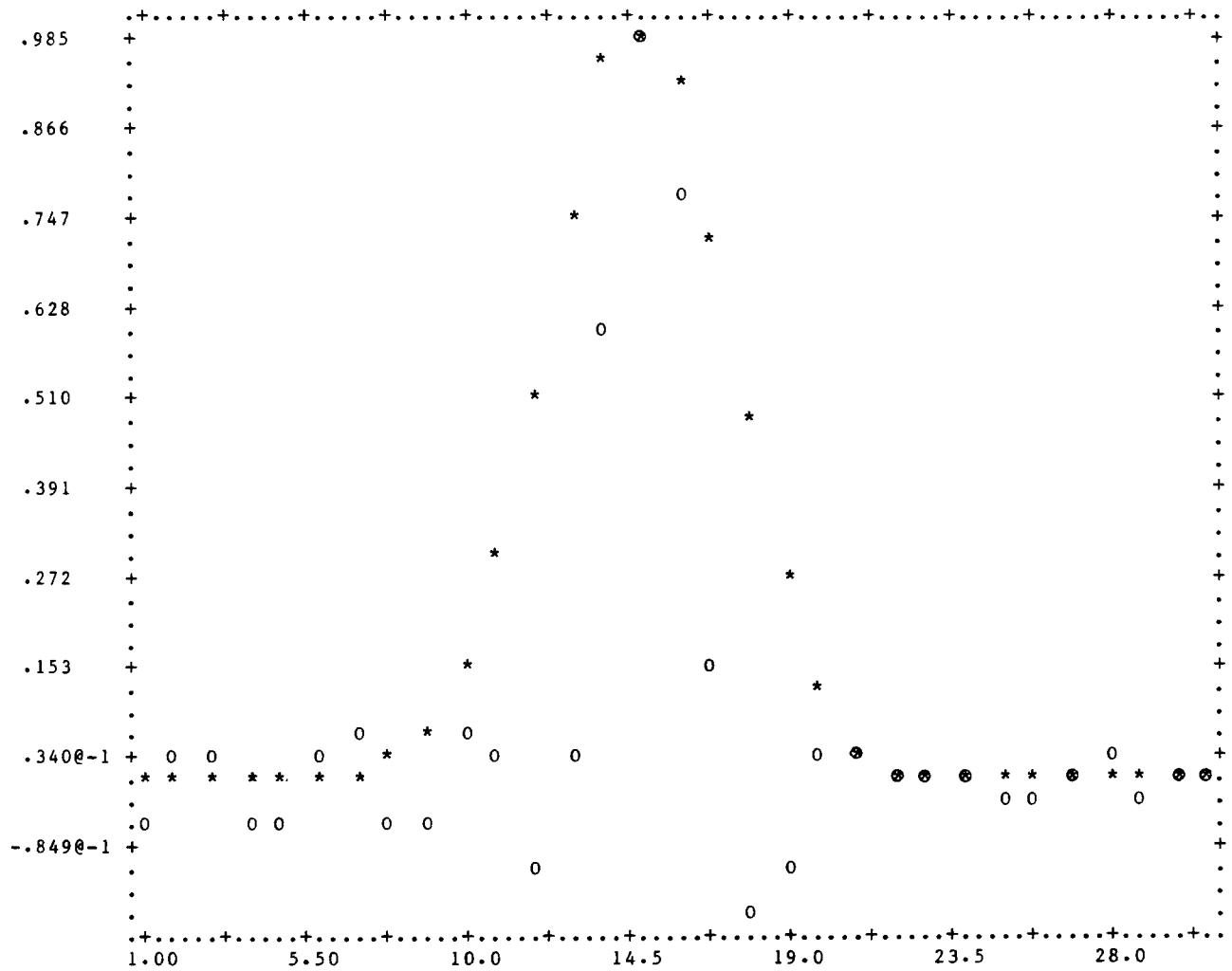


Figure 8.4 Singular value analysis with spectral data; $k = 16$.

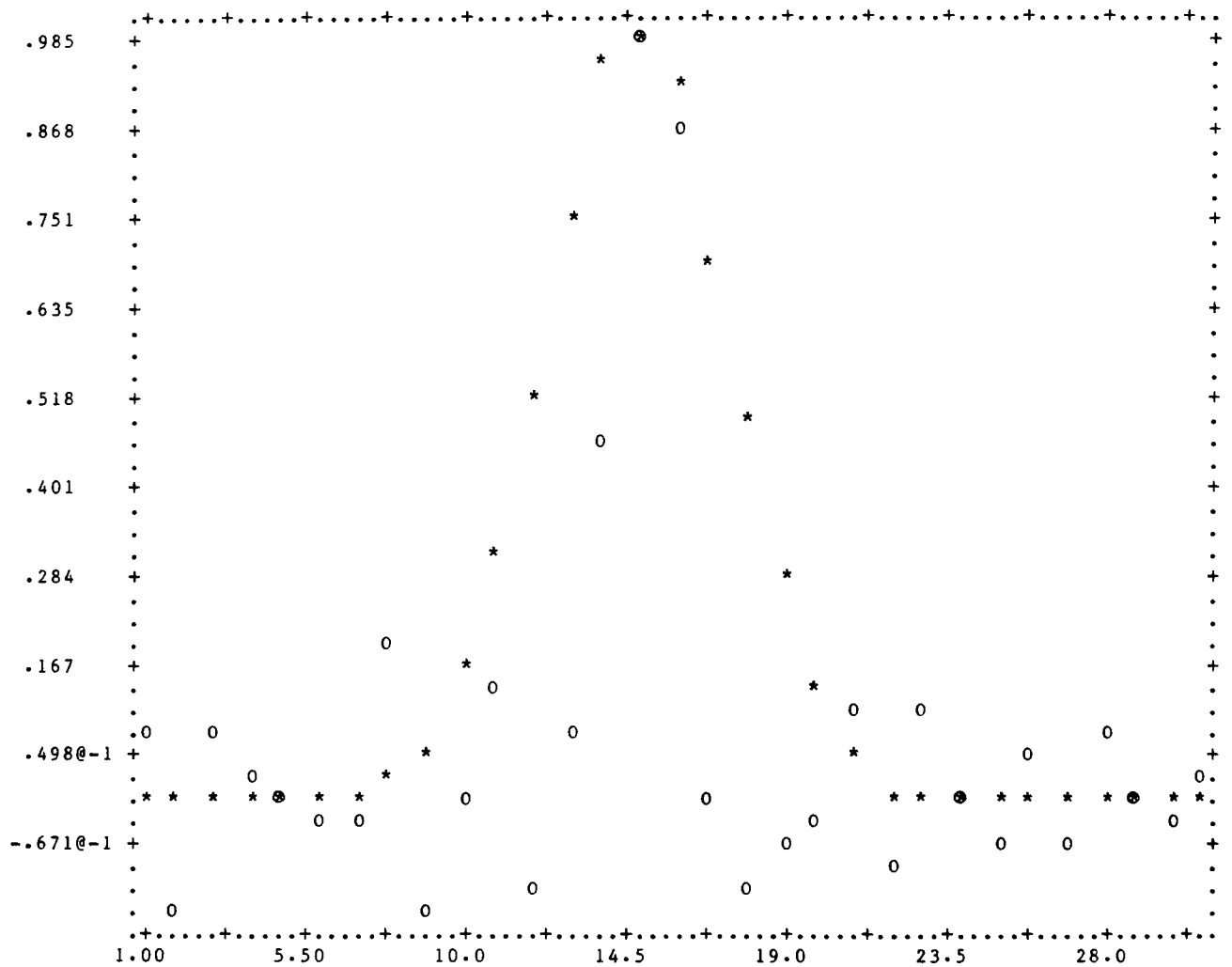


Figure 8.5 Singular value analysis with spectral data; $k = 21$.

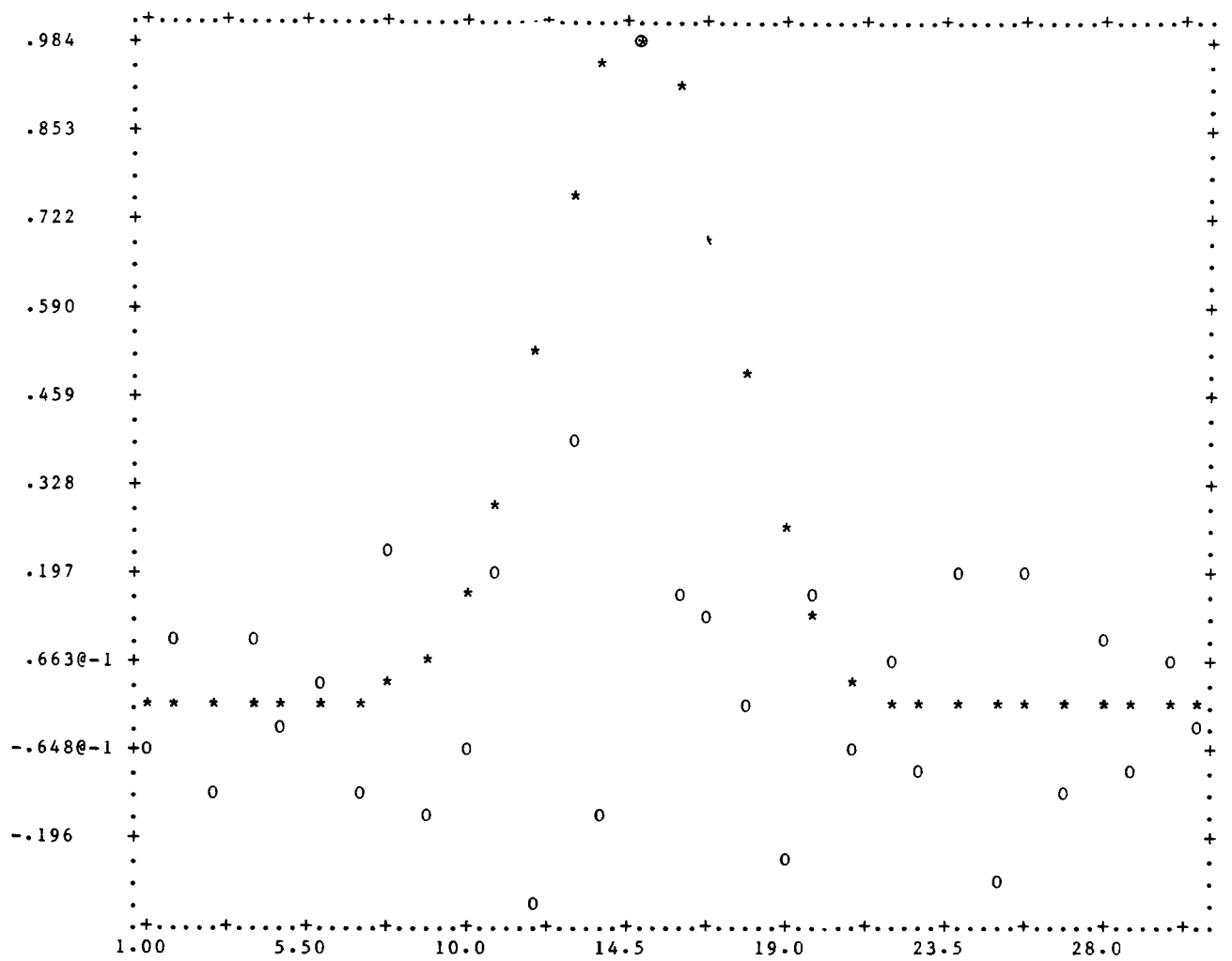


Figure 8.6 Singular value analysis with spectral data; $k = 26$.

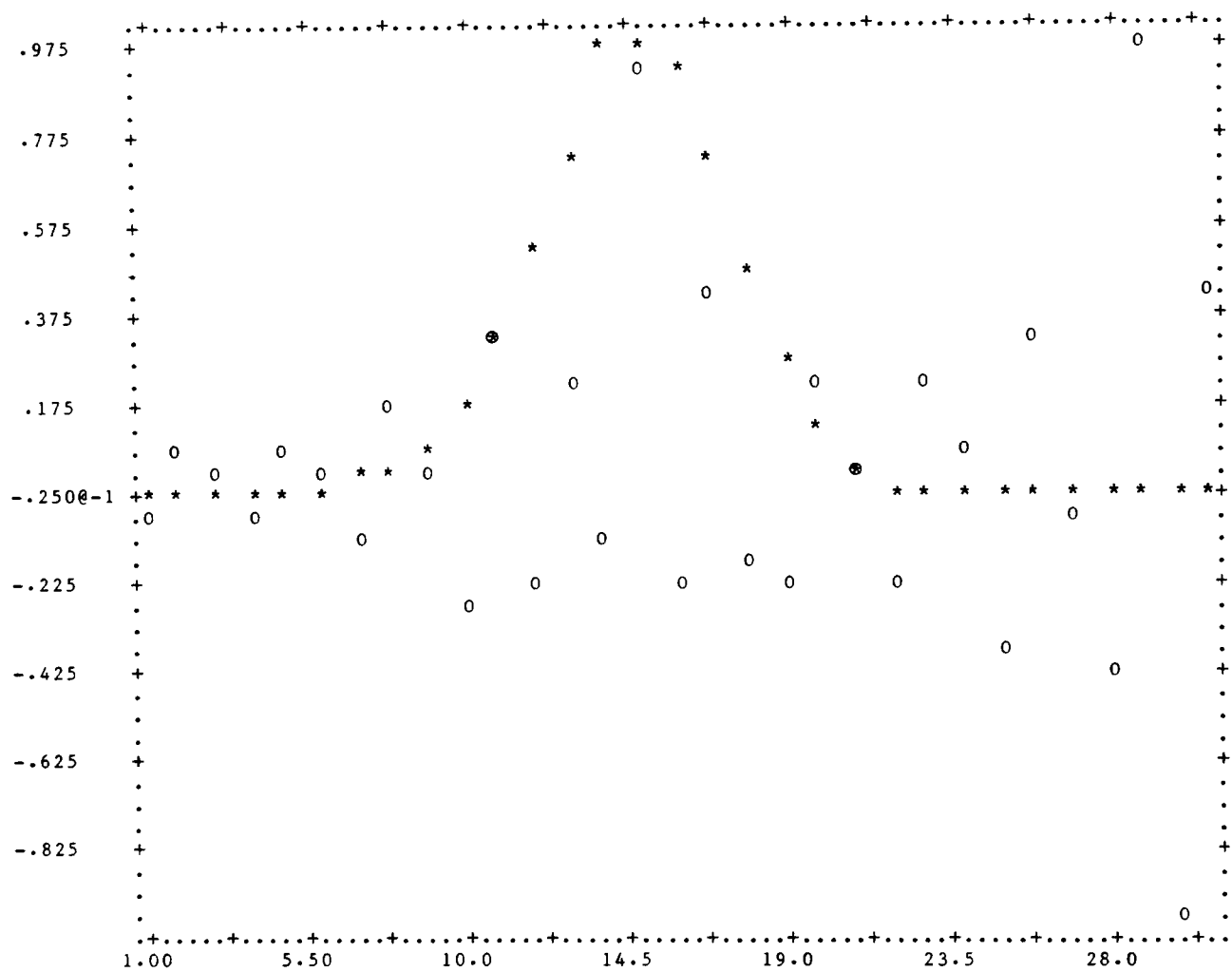


Figure 8.7 Singular value analysis with spectral data; $k = 31$.

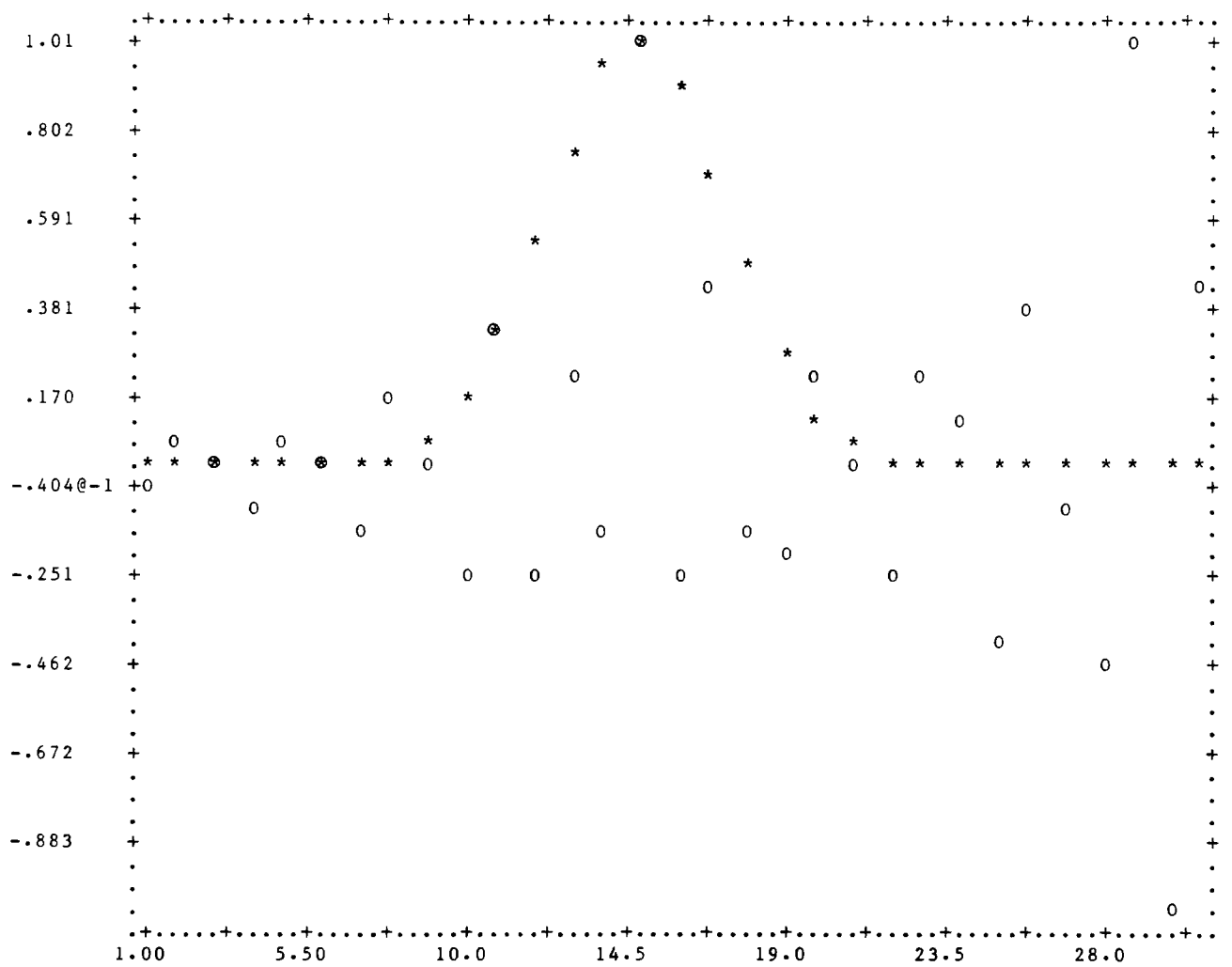


Figure 8.8 Euclidean regularization with spectral data; $\lambda = 0$.

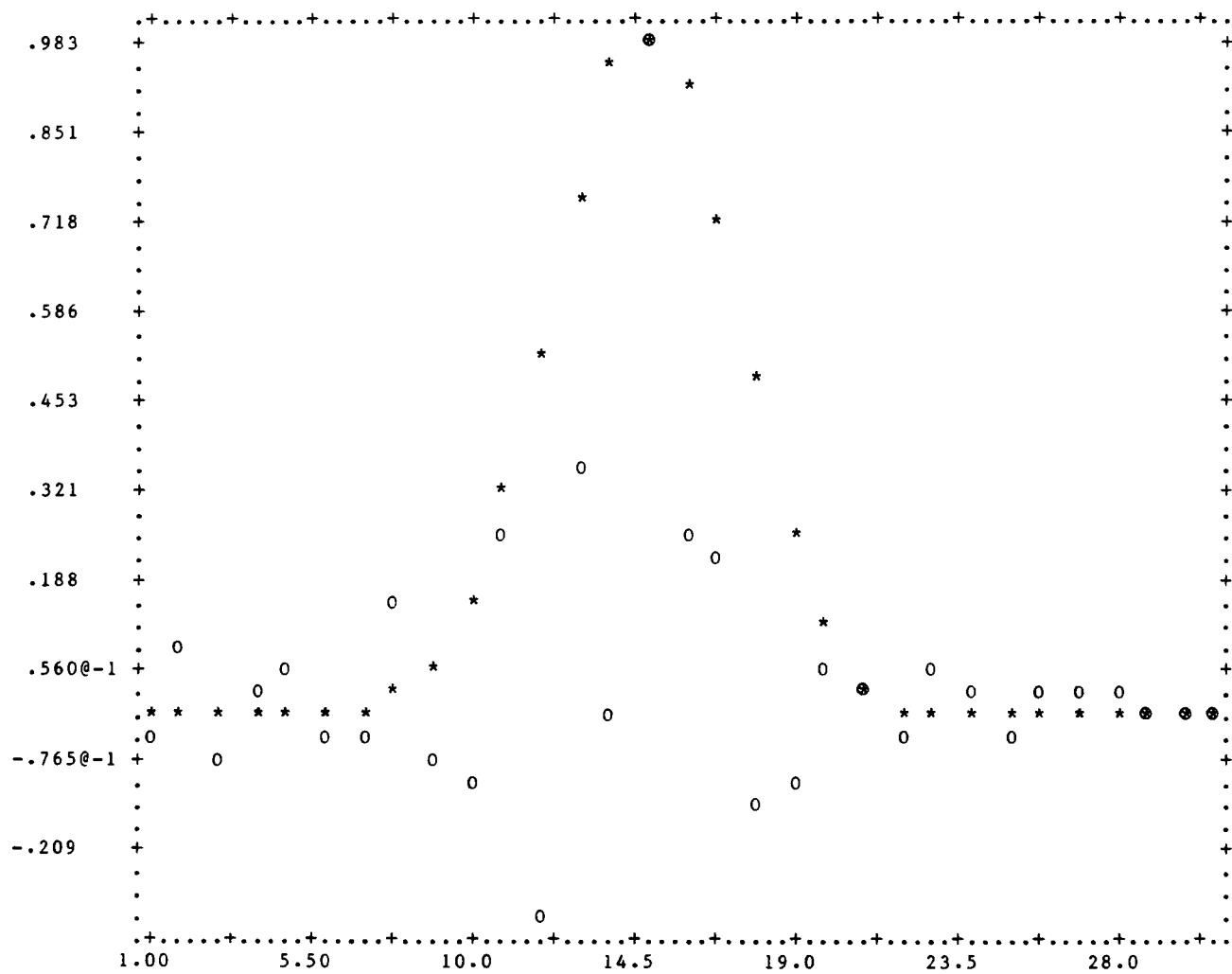


Figure 8.9 Euclidean regularization with spectral data;
 $\lambda = .00001$.

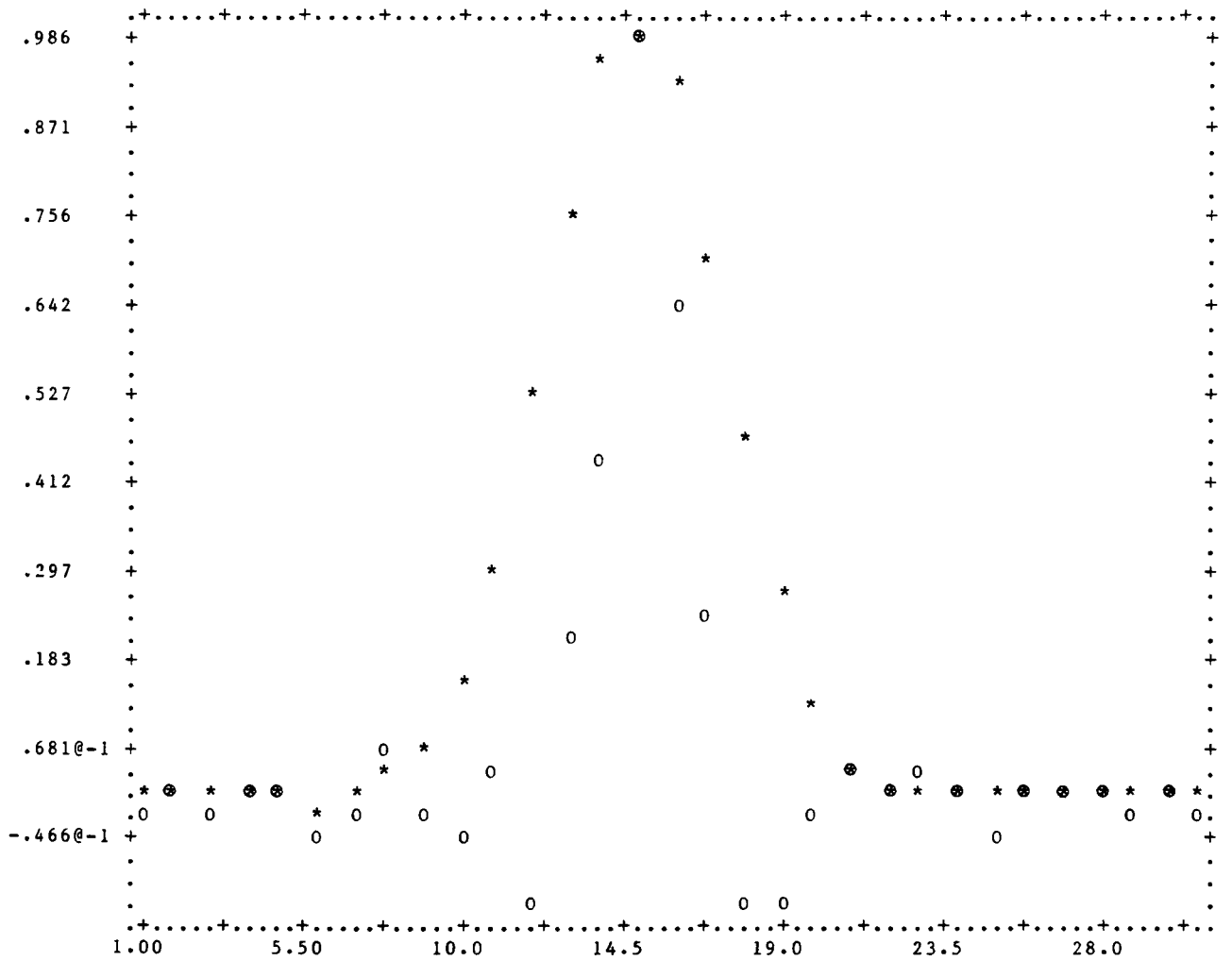
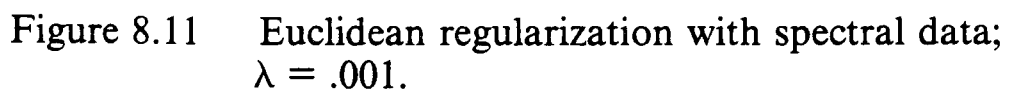


Figure 8.10 Euclidean regularization with spectral data;
 $\lambda = .0001$.



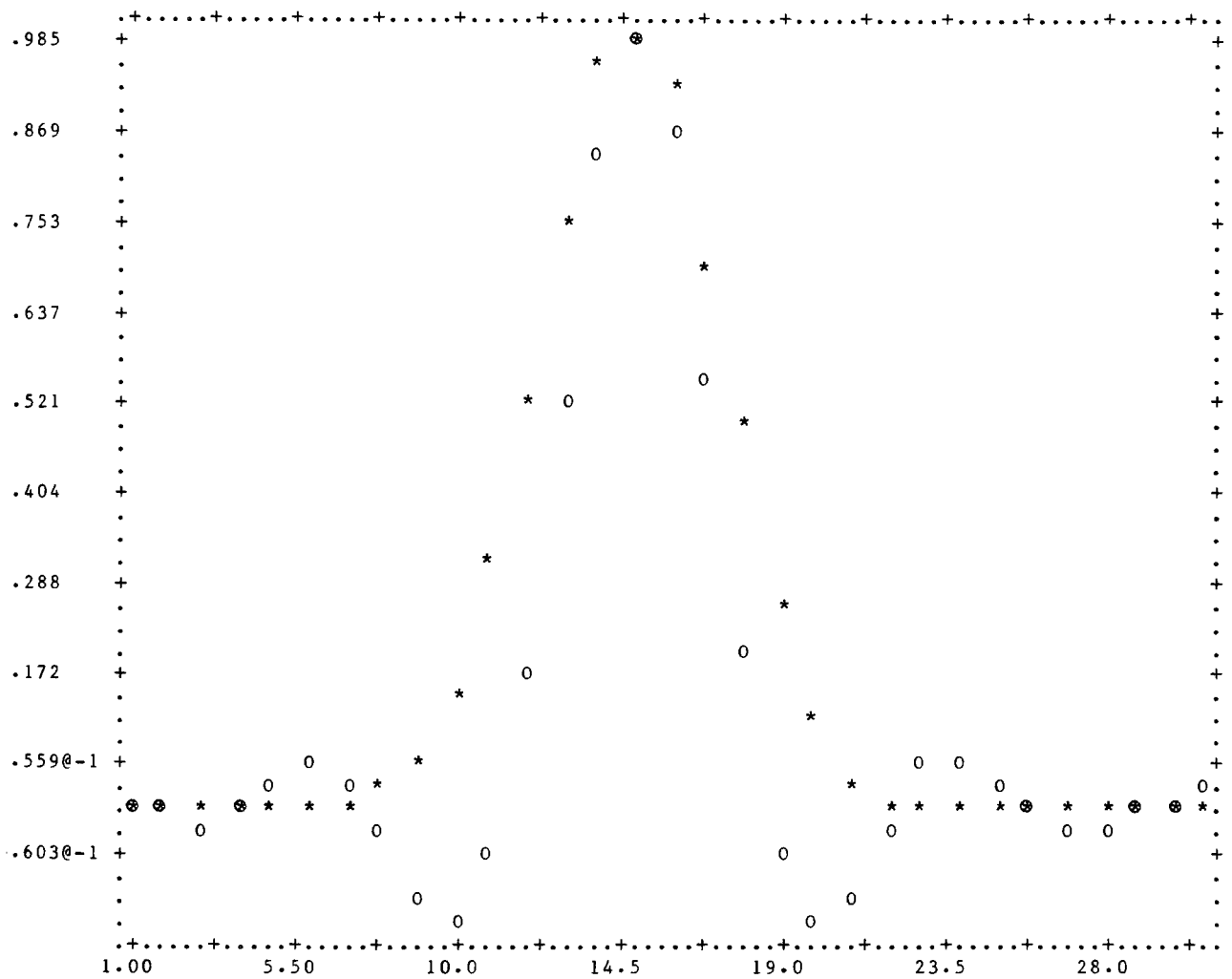


Figure 8.12 Euclidean regularization with spectral data;
 $\lambda = .010$.

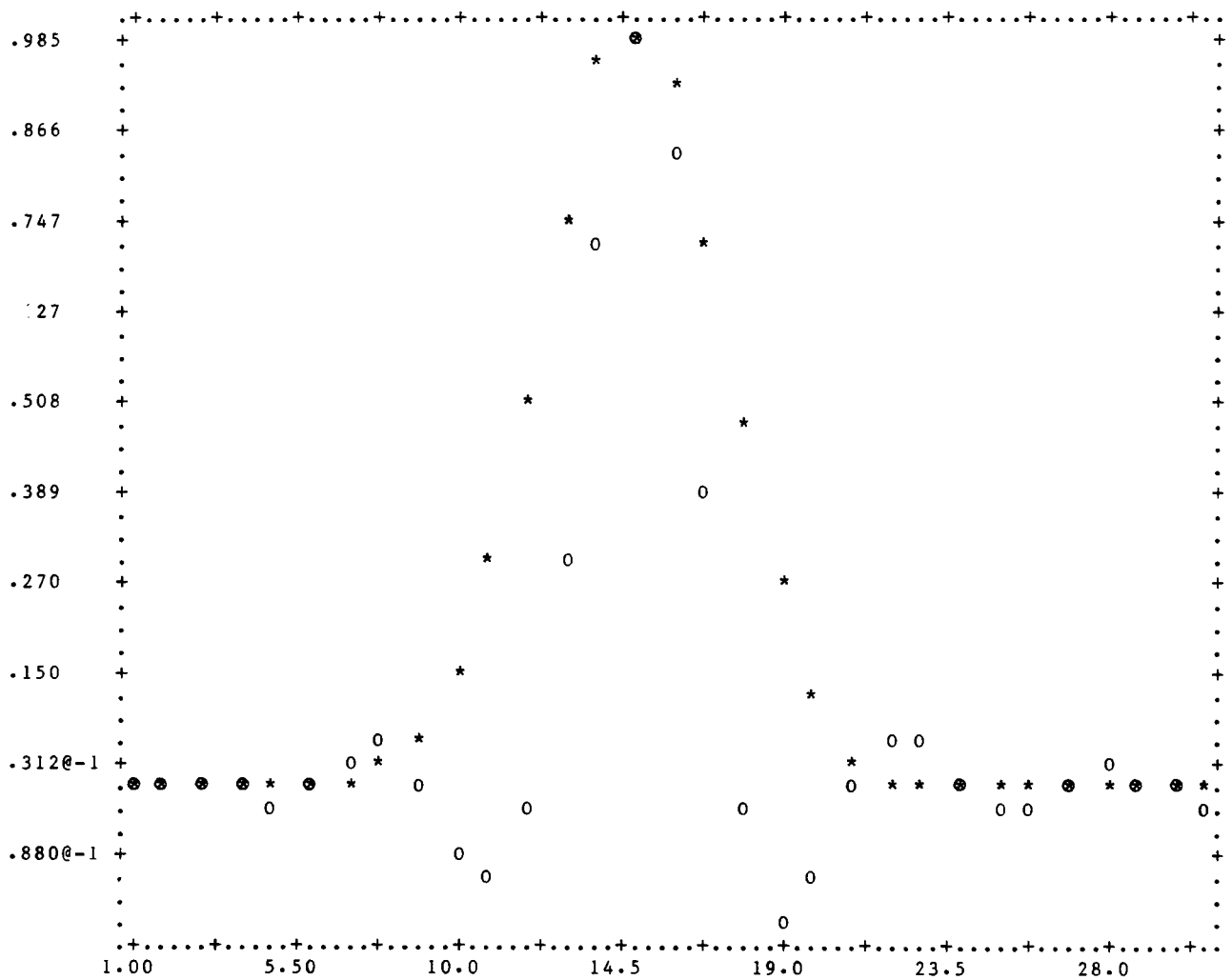


Figure 8.13 DER1 regularization with spectral data;
 $\lambda = .100$, $\delta = 1$.

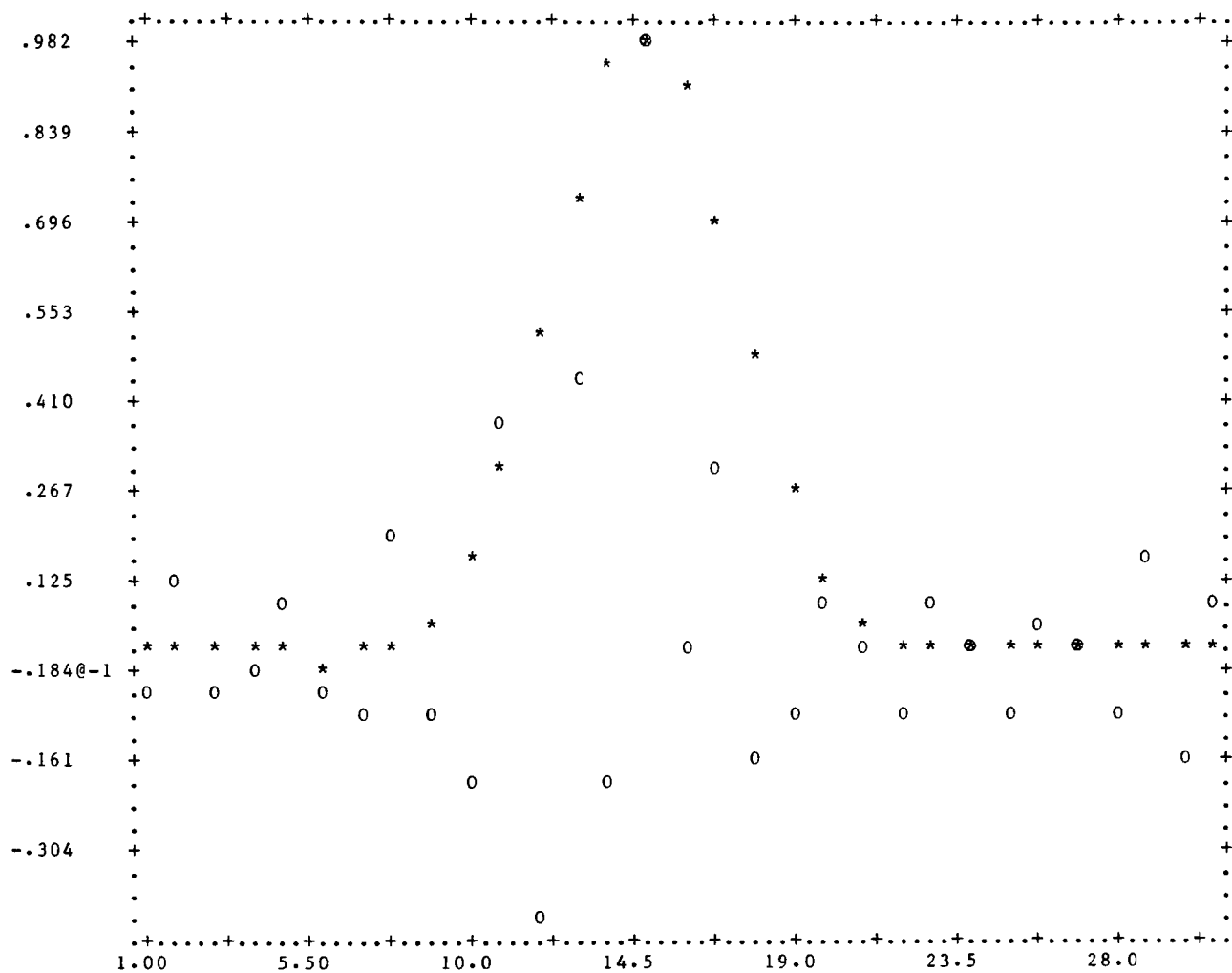


Figure 8.14 DER2 regularization with spectral data;
 $\lambda = .001$, $\epsilon = 1$.

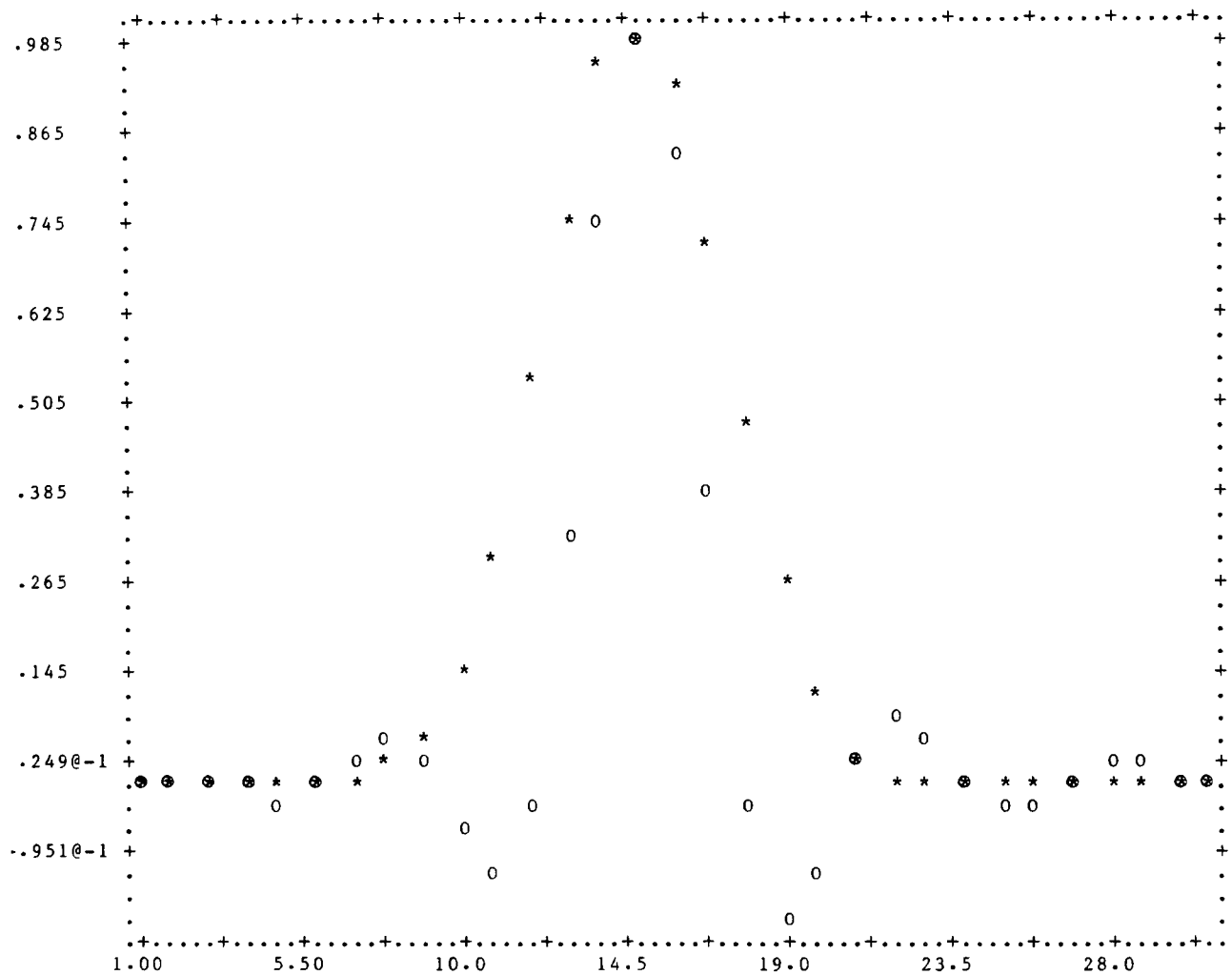


Figure 8.15 DER2 regularization with spectral data;
 $\lambda = .100, \epsilon = 1$.

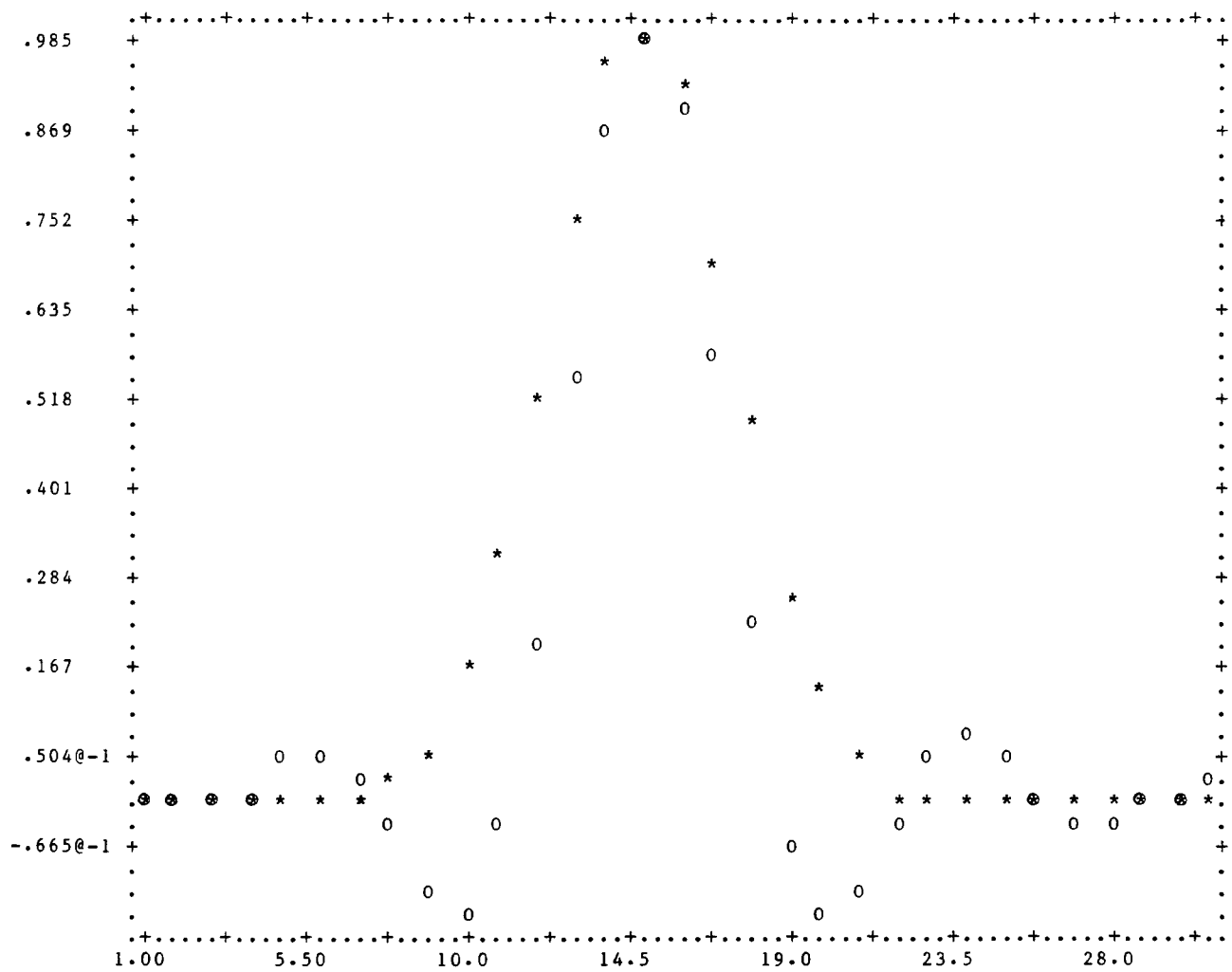


Figure 8.16 DER2 regularization with spectral data;
 $\lambda = .500$, $\epsilon = 1$.

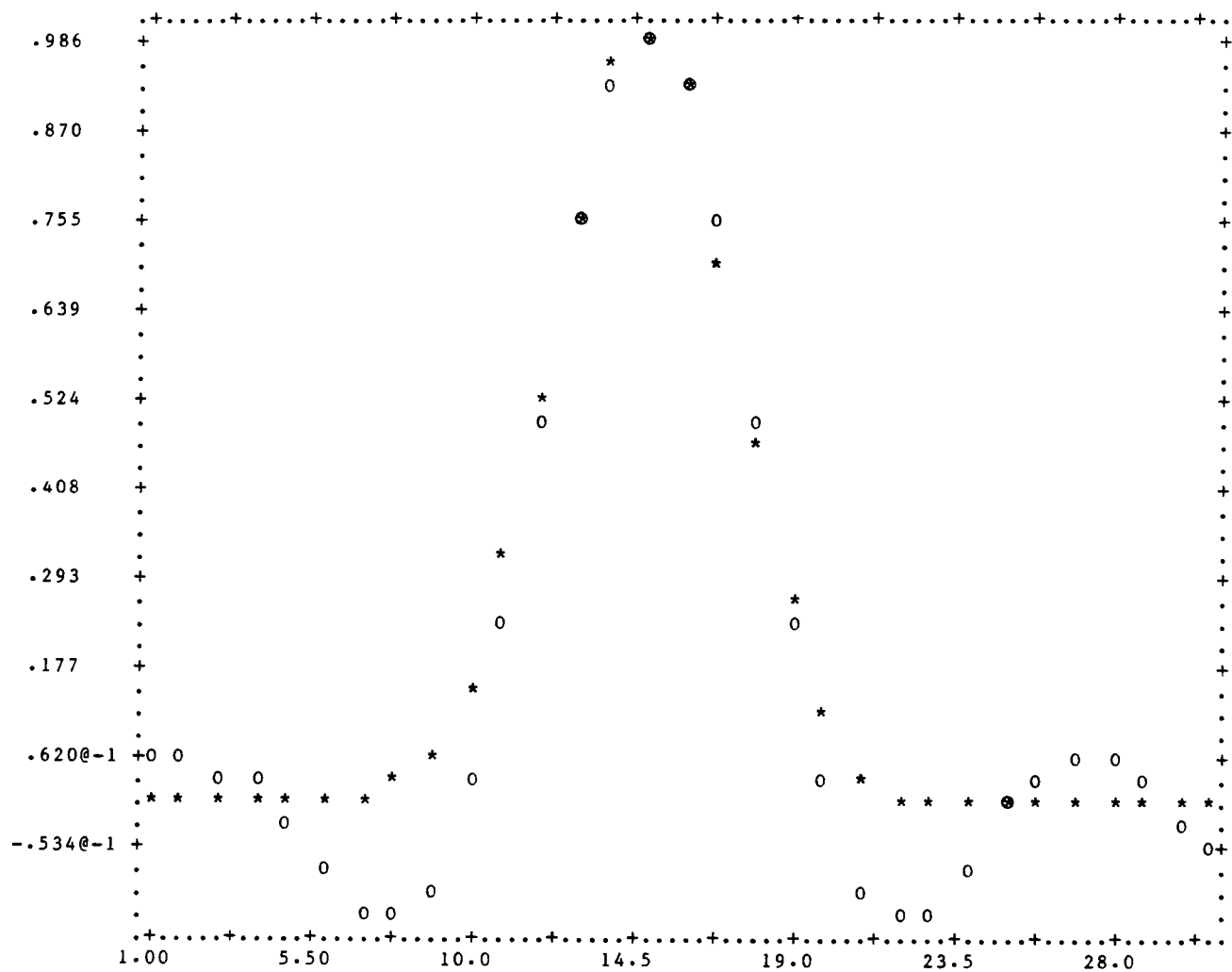


Figure 8.17 DER2 regularization with spectral data;
 $\lambda = .001$, $\epsilon = 5000$.

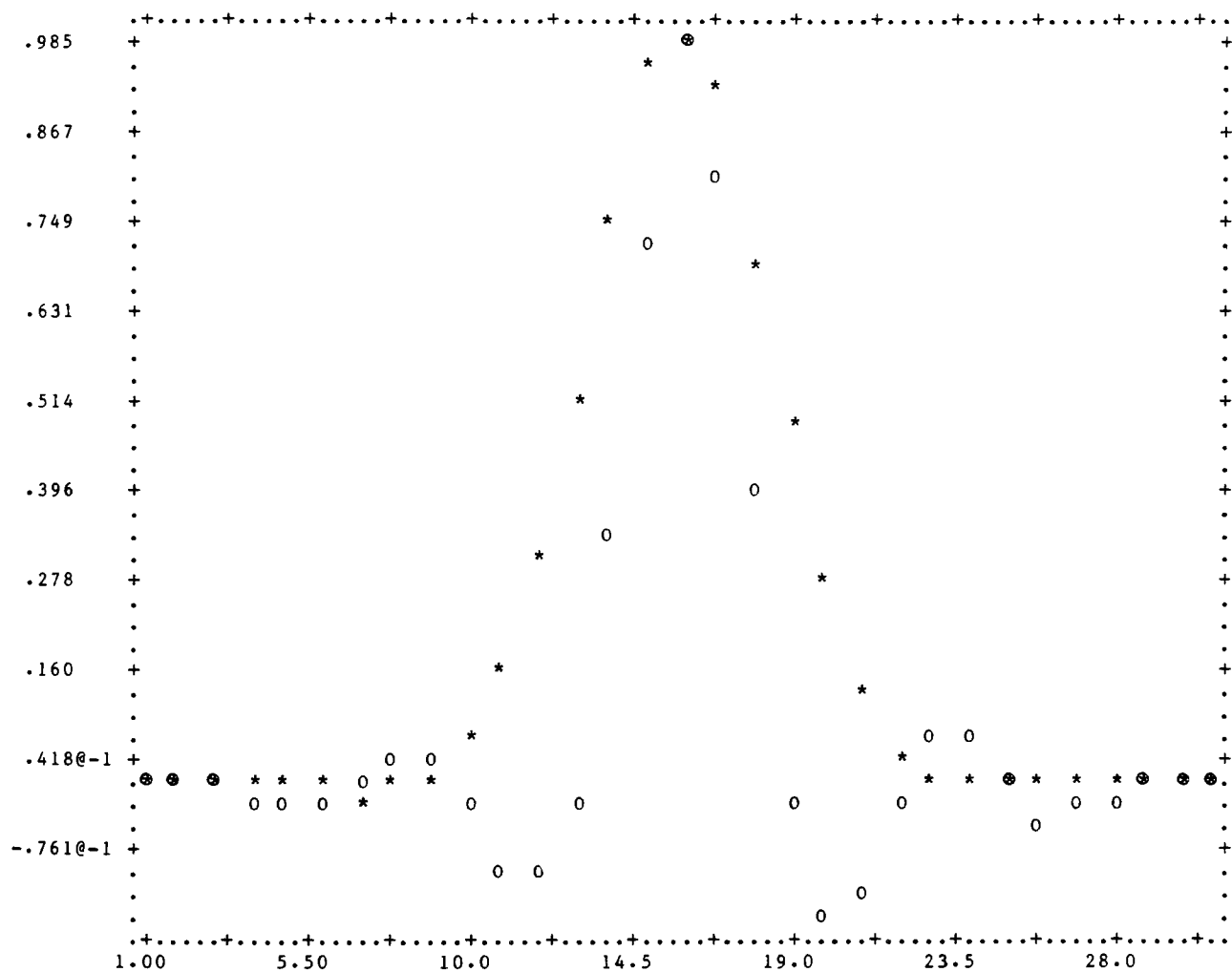


Figure 8.18 CDR regularization with spectral data; $\lambda = .001$.

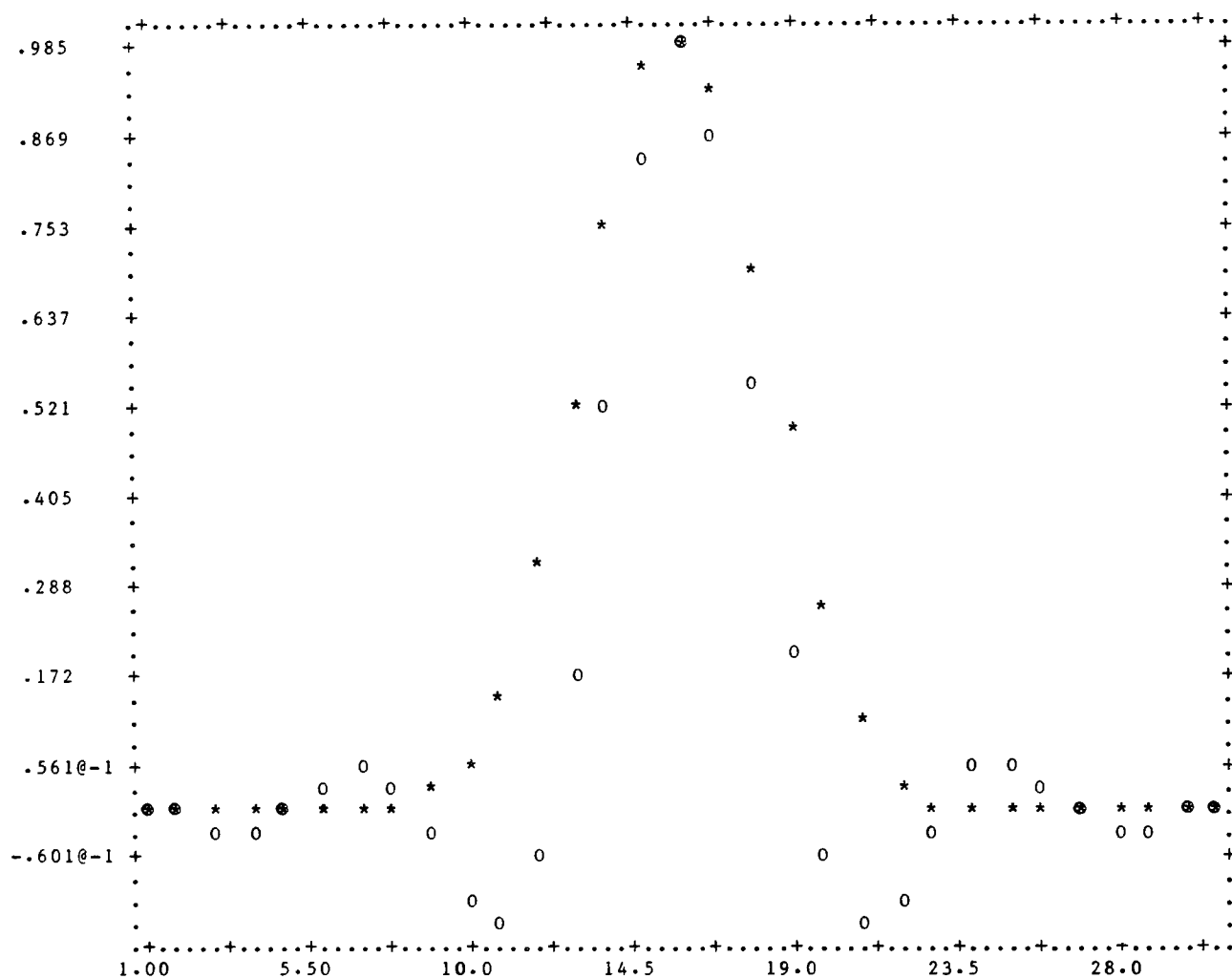


Figure 8.19 CDR regularization with spectral data;
 $\lambda = .010$.

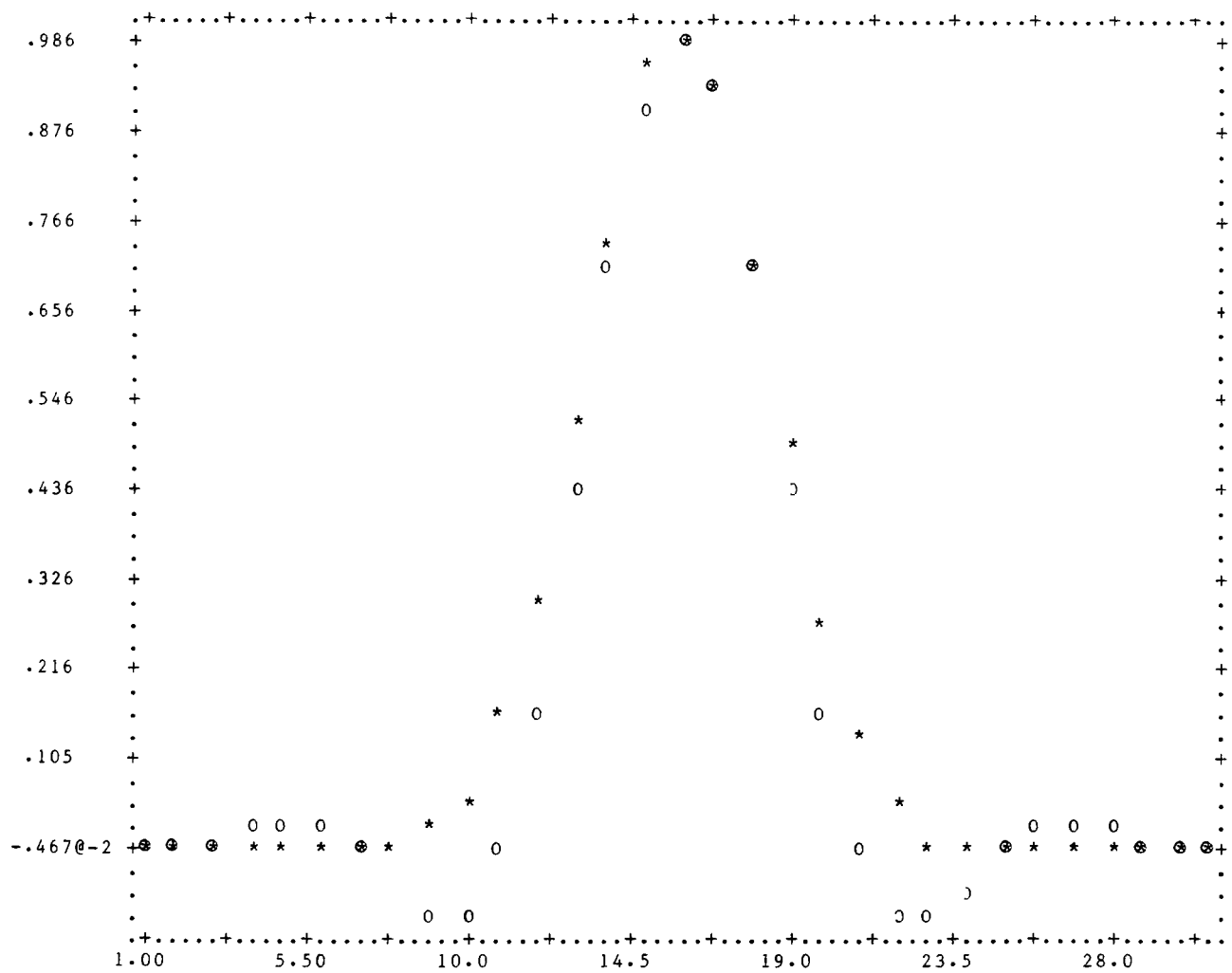


Figure 8.20 CDR regularization with spectral data; $\lambda = .100$.

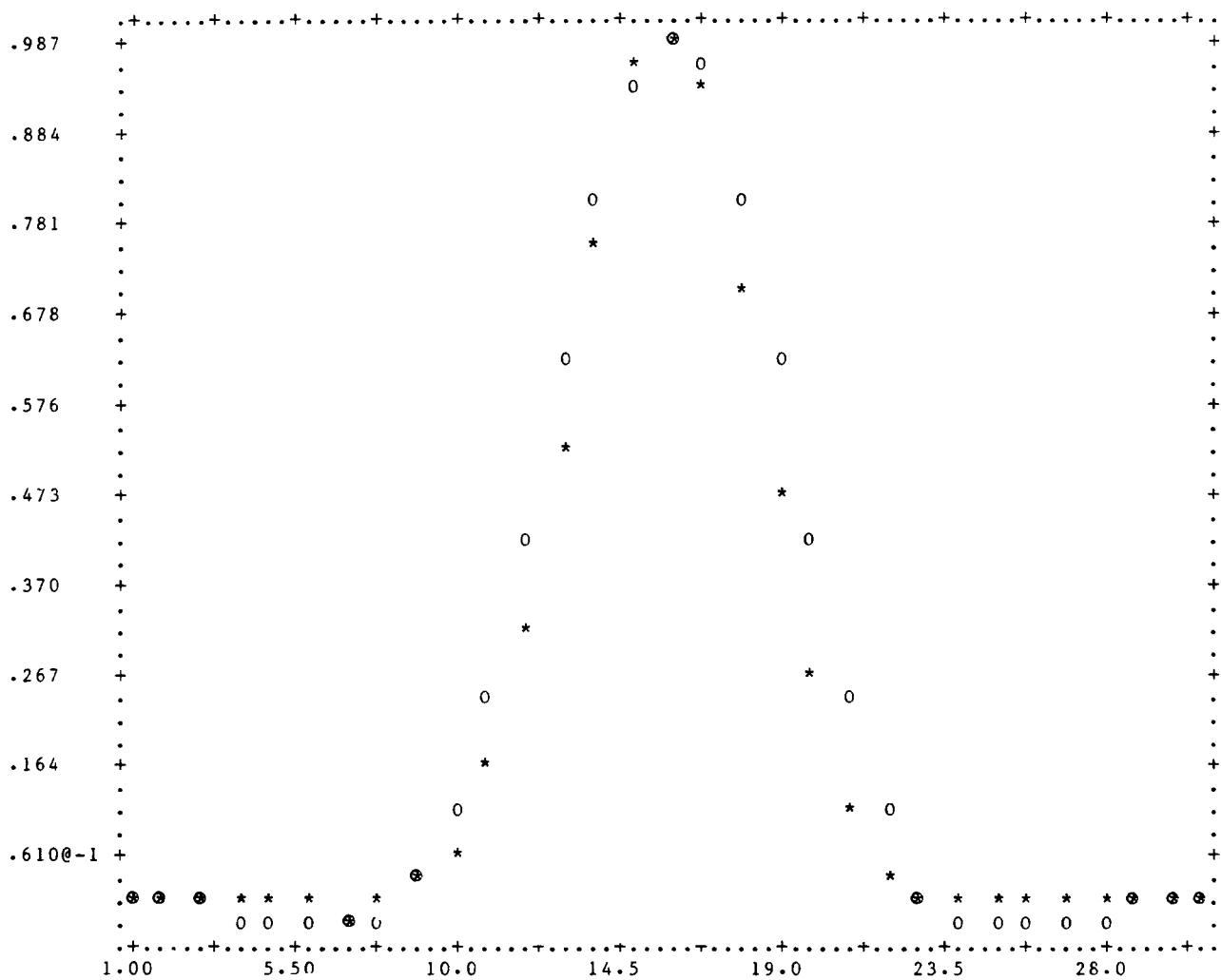


Figure 8.21 CDR regularization with spectral data; $\lambda = 1.00$.

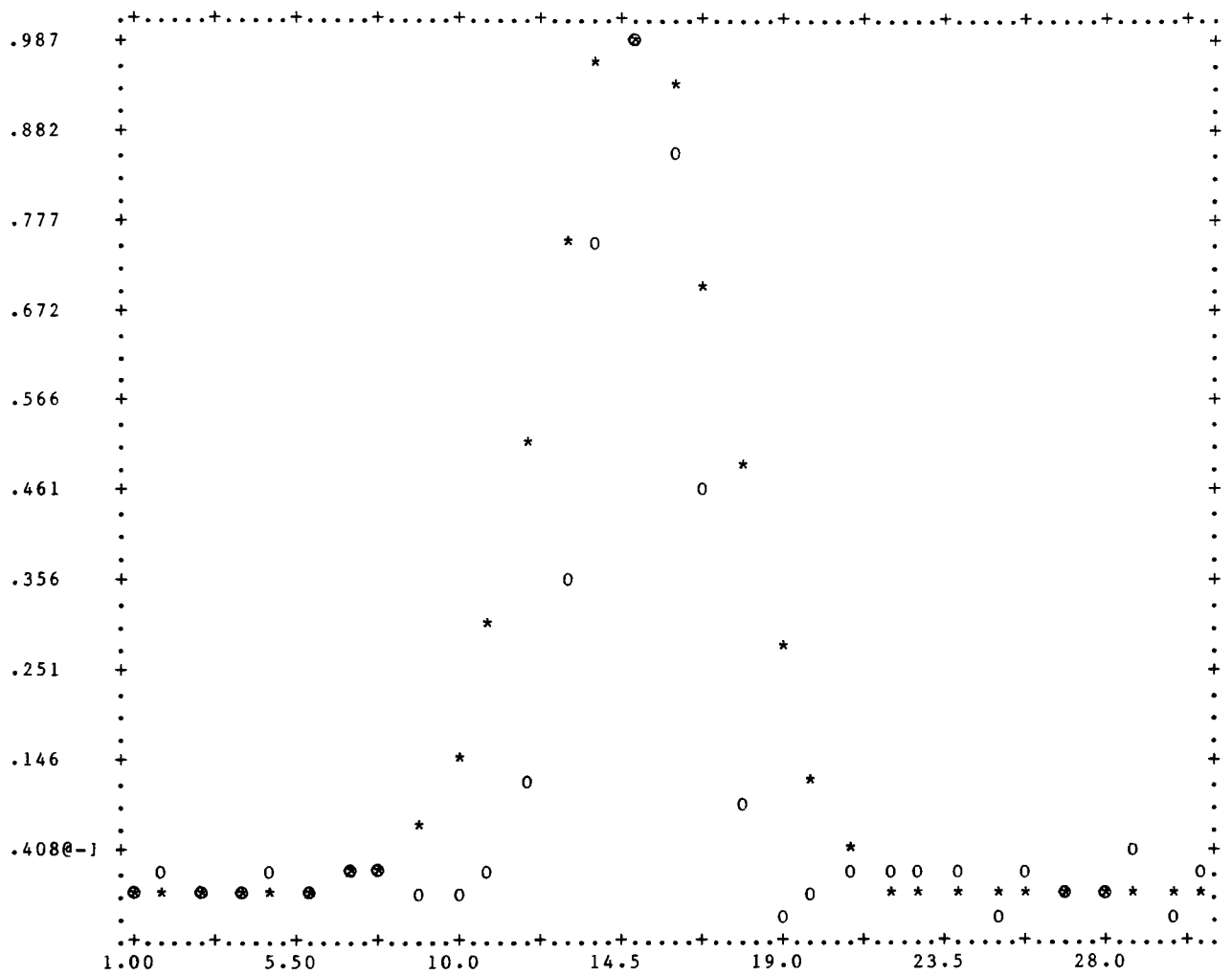


Figure 8.22 Euclidean regularization with spread spectral data; $\lambda = 0$.

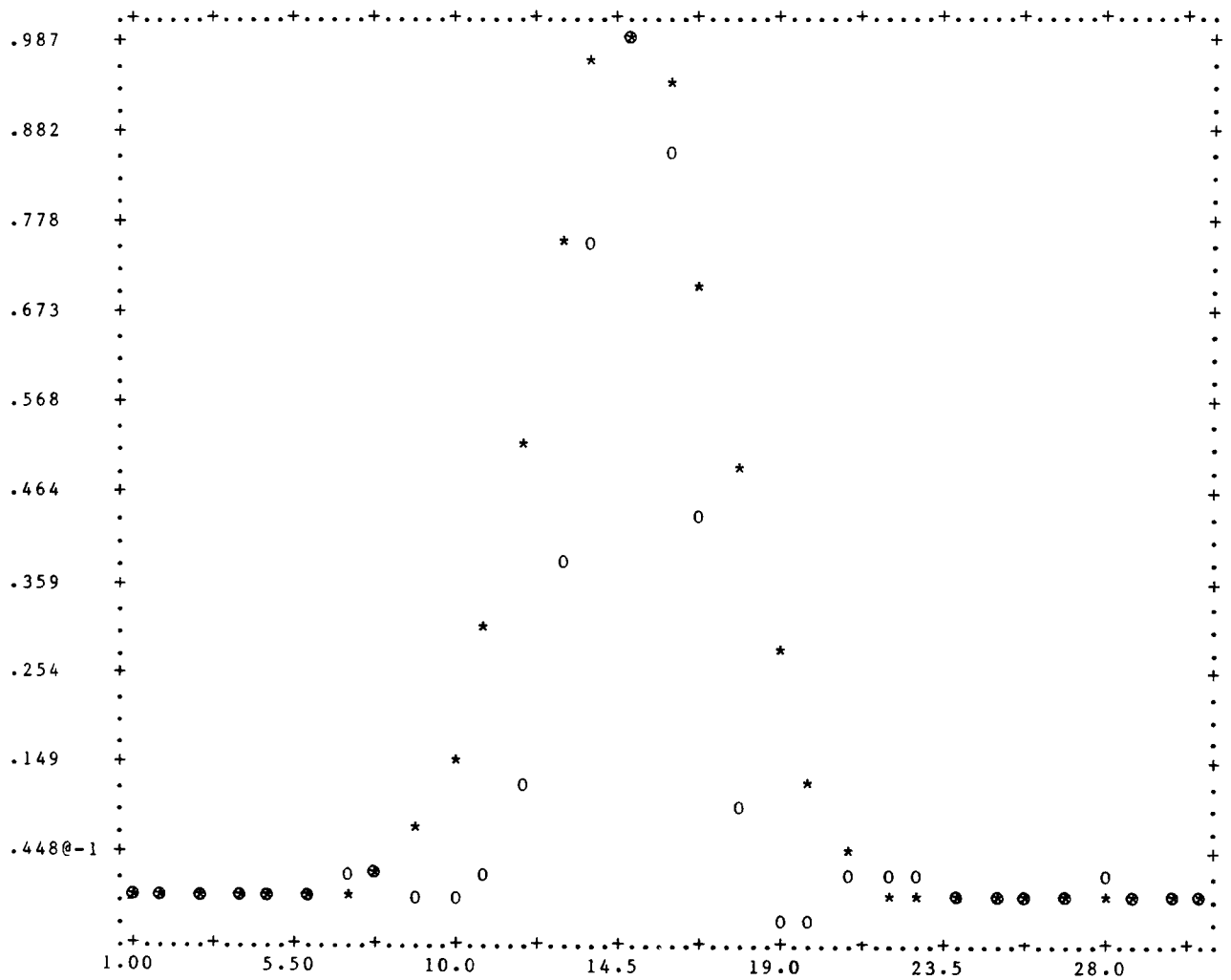


Figure 8.23 Euclidean regularization with spread spectral data; $\lambda = .00001$.

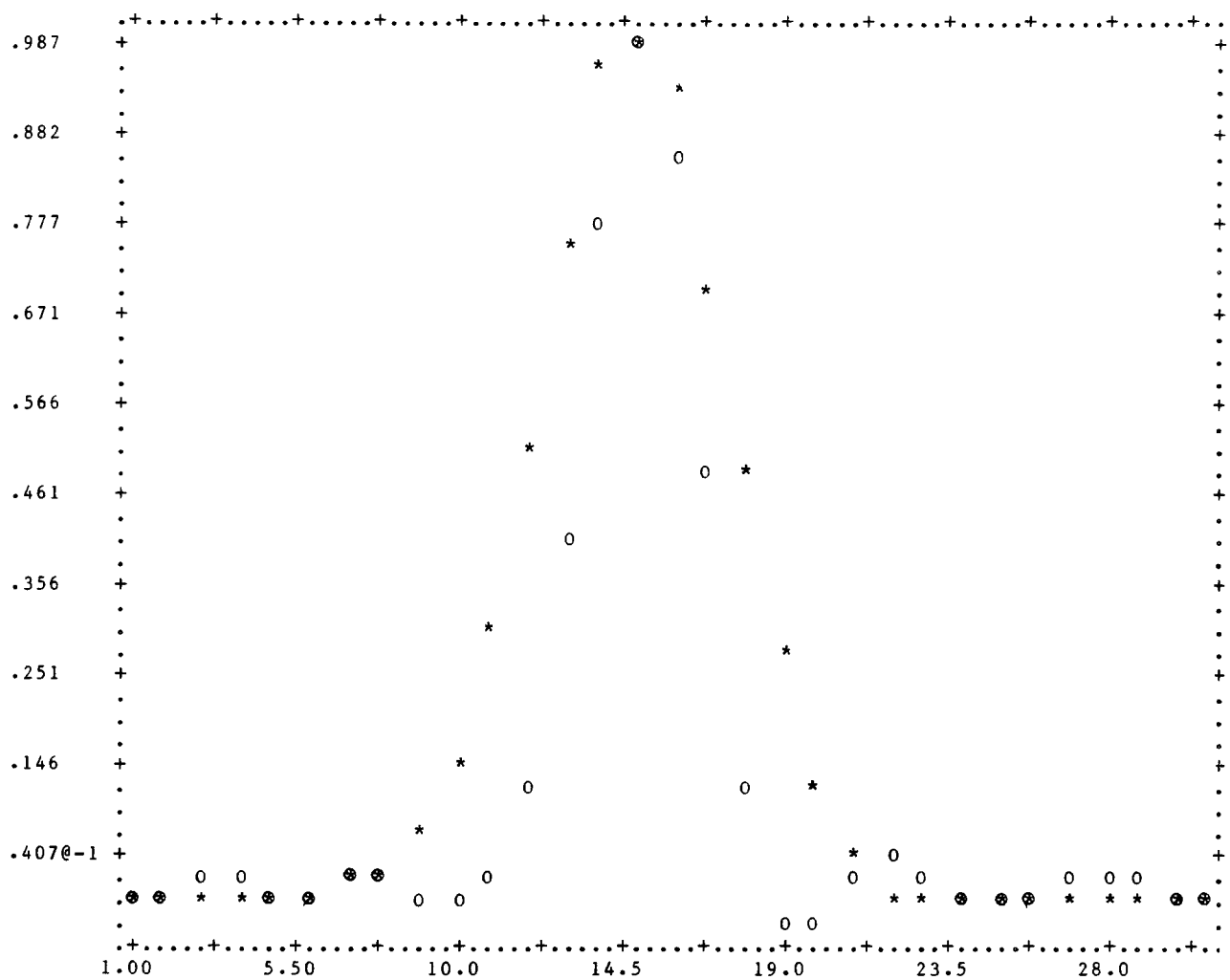


Figure 8.24 Euclidean regularization with spread spectral data; $\lambda = .0001$.

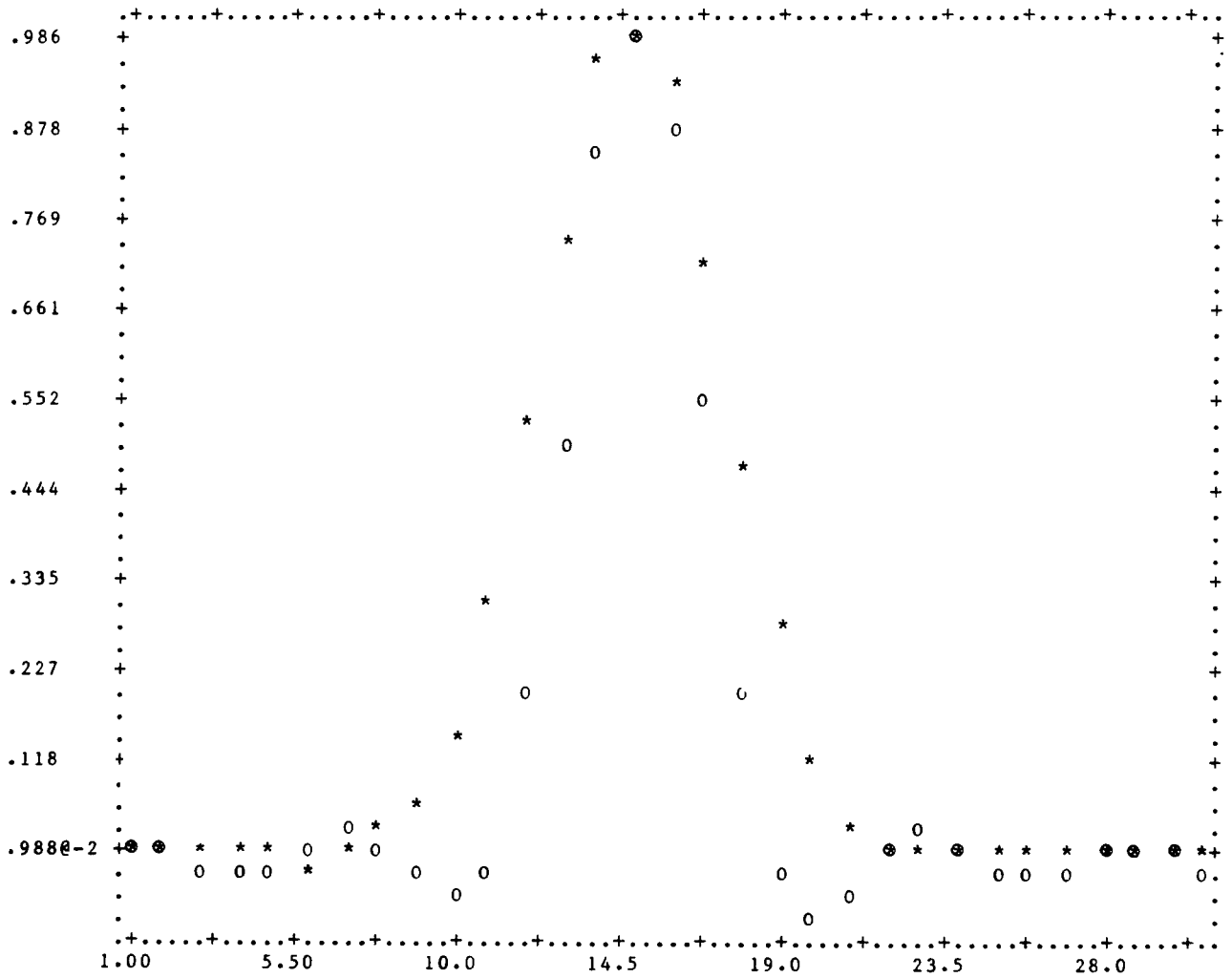
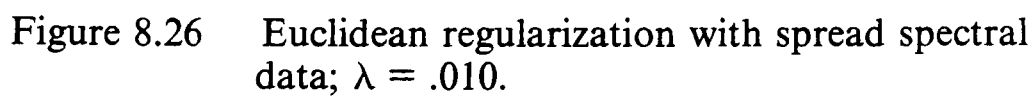


Figure 8.25 Euclidean regularization with spread spectral data; $\lambda = .001$.



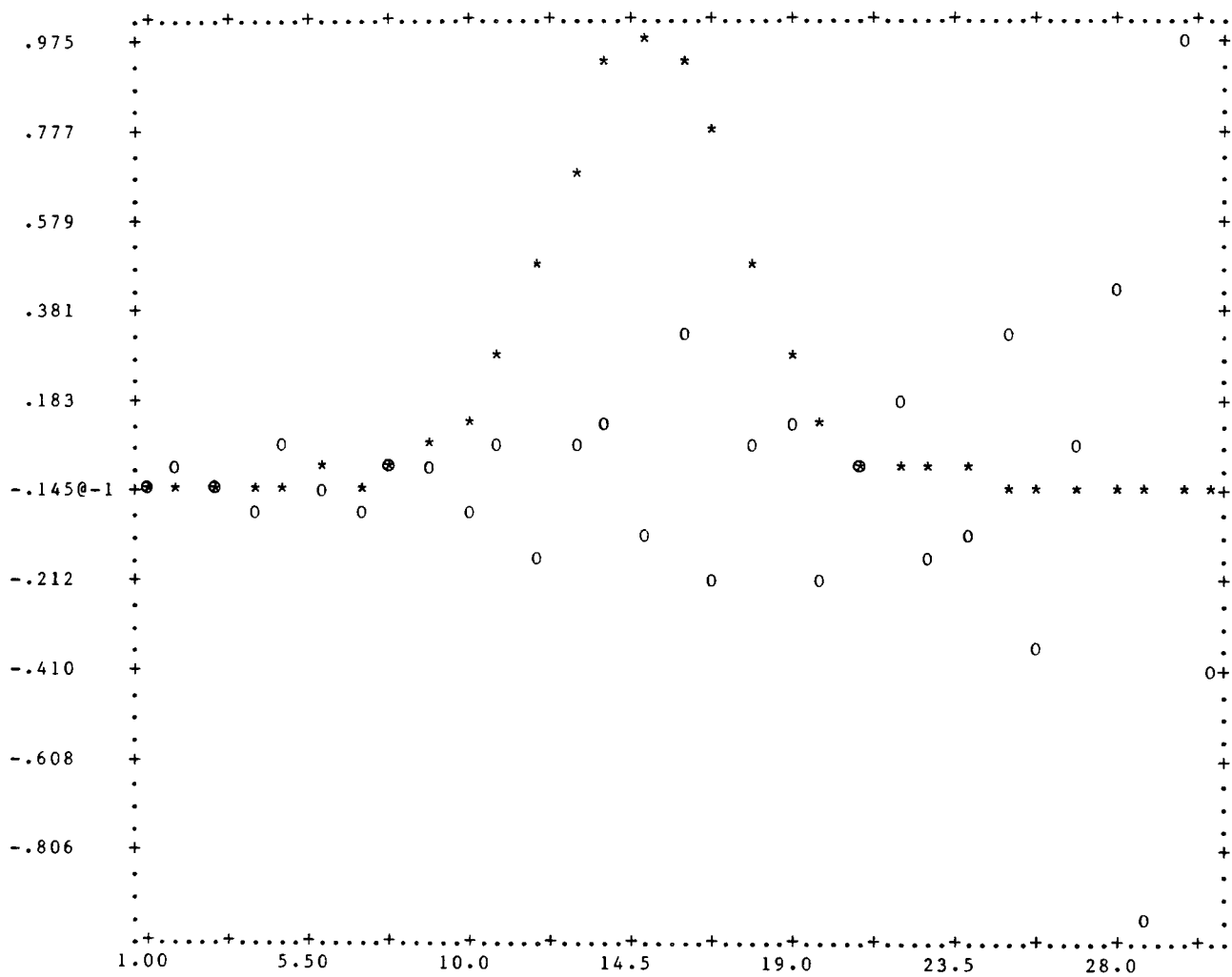


Figure 8.27 Euclidean regularization with cross-spectral data; $\lambda = 0$.

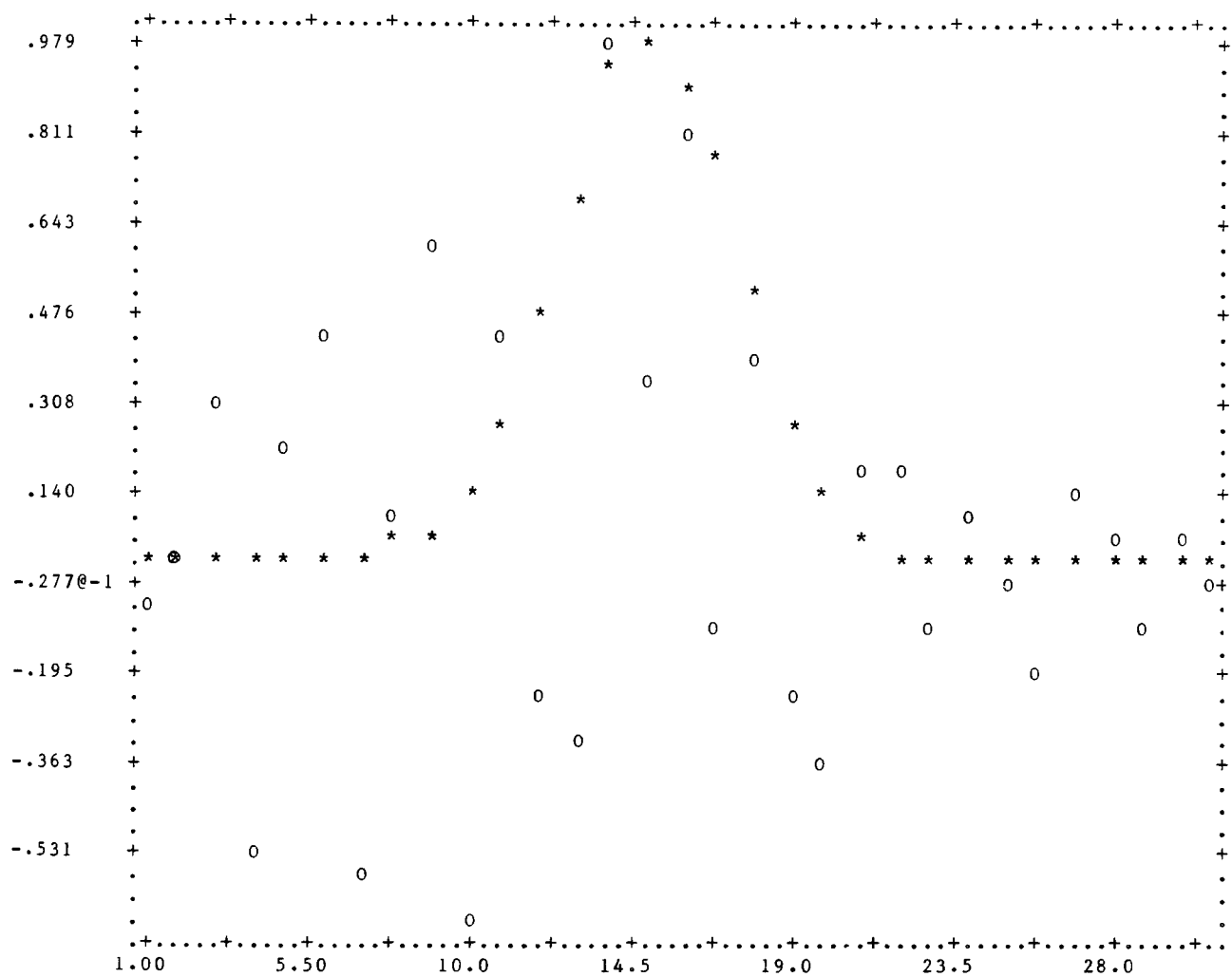


Figure 8.28 Euclidean regularization with cross-spectral data; $\lambda = .00001$.

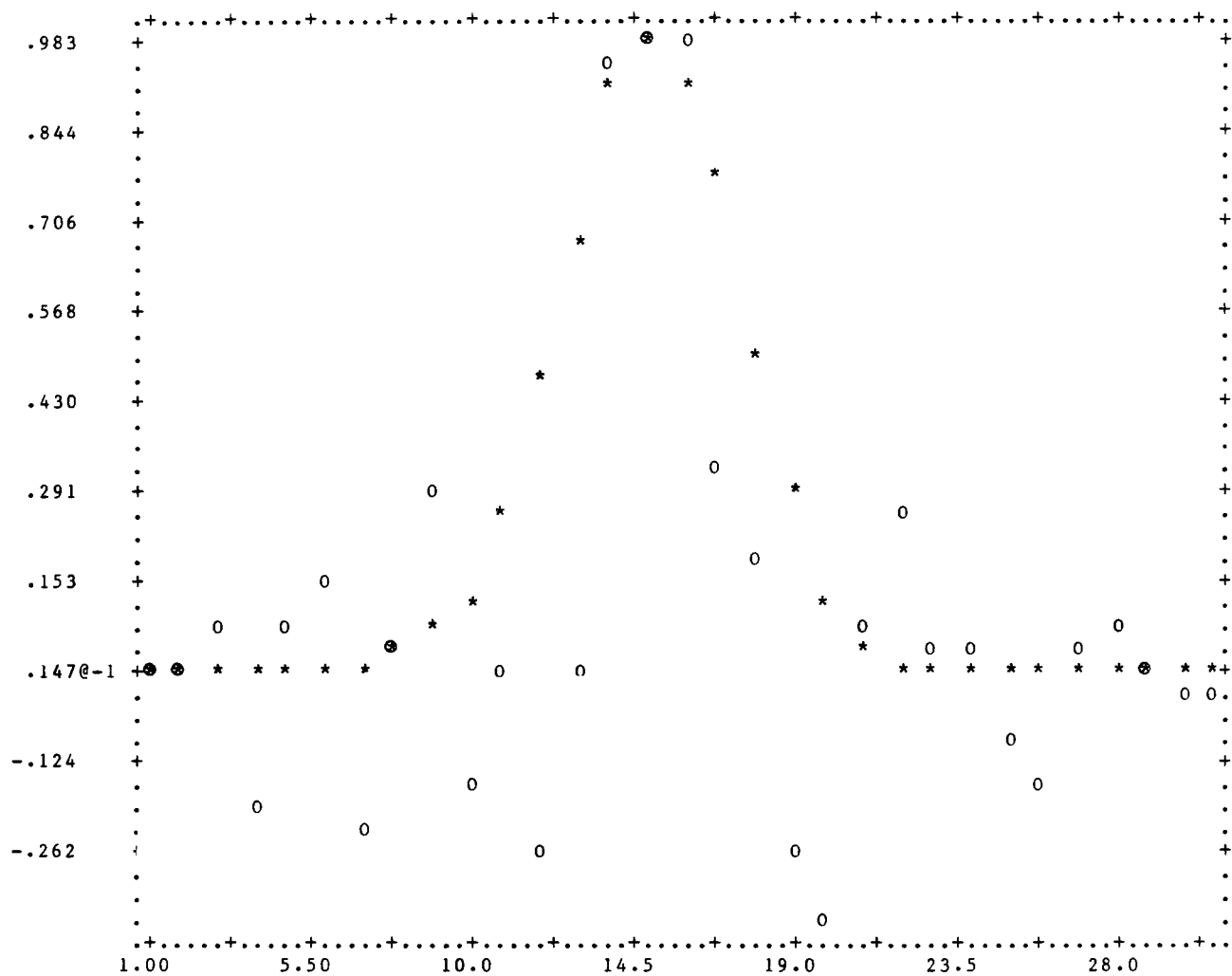


Figure 8.29 Euclidean regularization with cross-spectral data; $\lambda = .0001$.

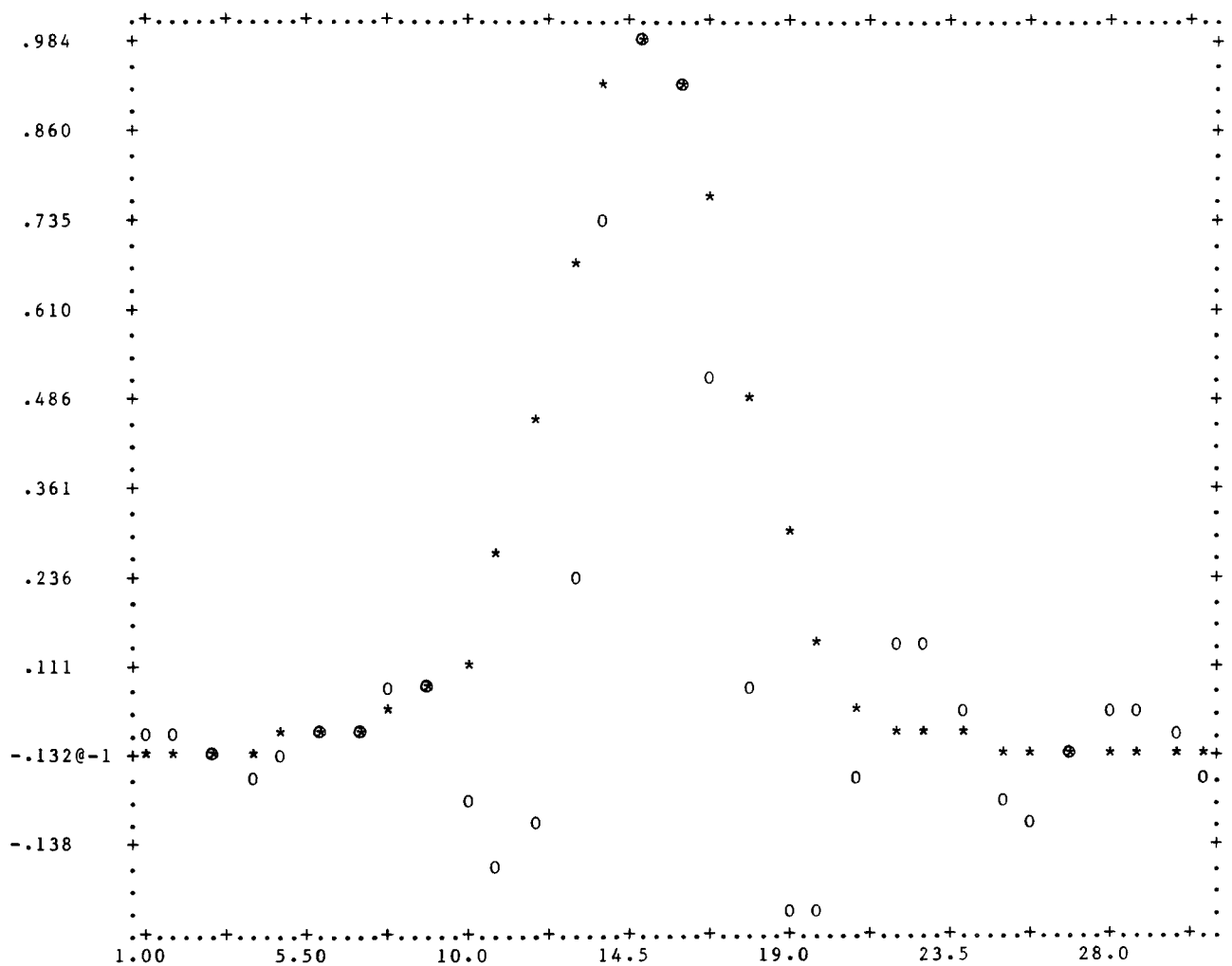


Figure 8.30 Euclidean regularization with cross-spectral data; $\lambda = .001$.

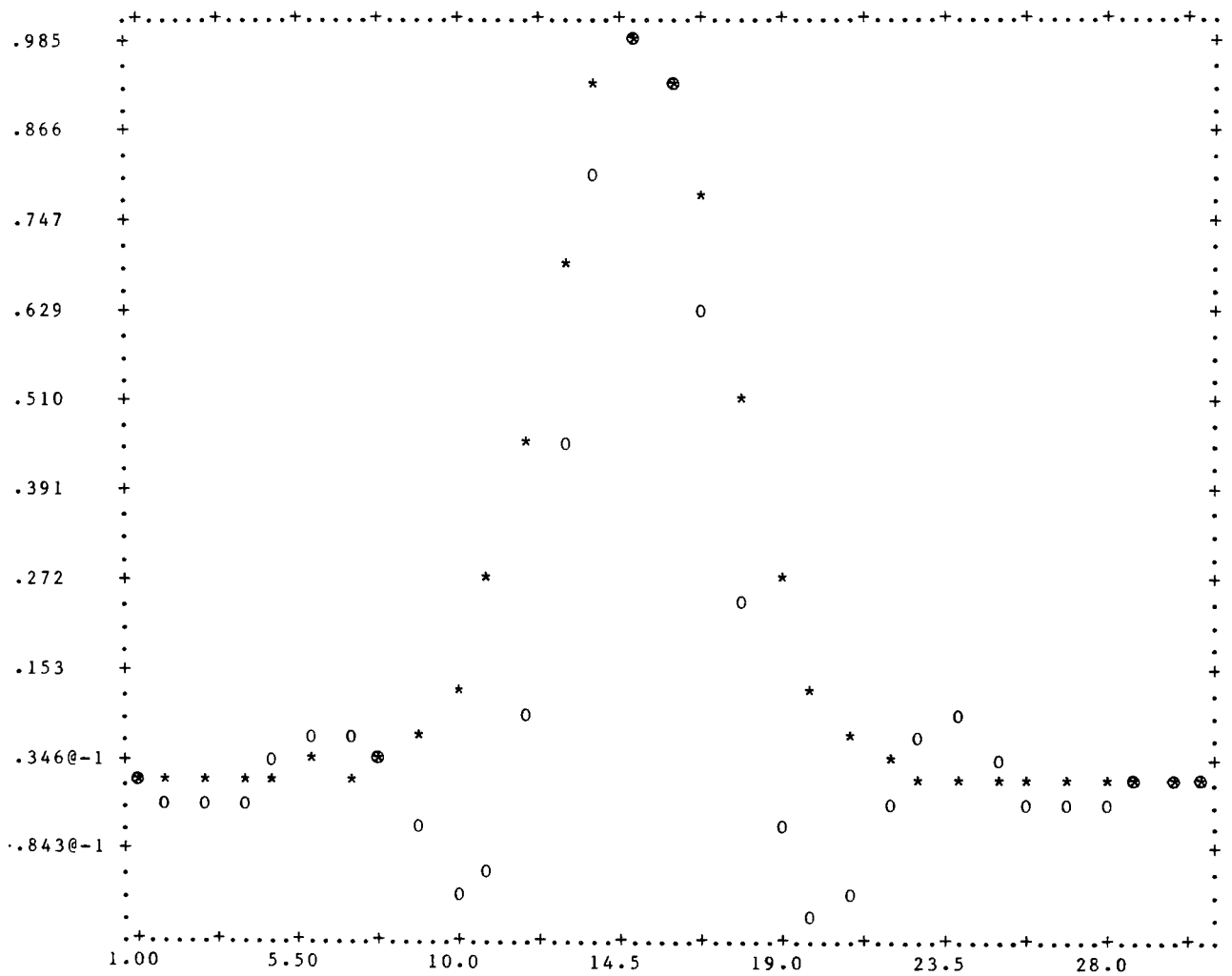


Figure 8.31 Euclidean regularization with cross-spectral data; $\lambda = .010$.

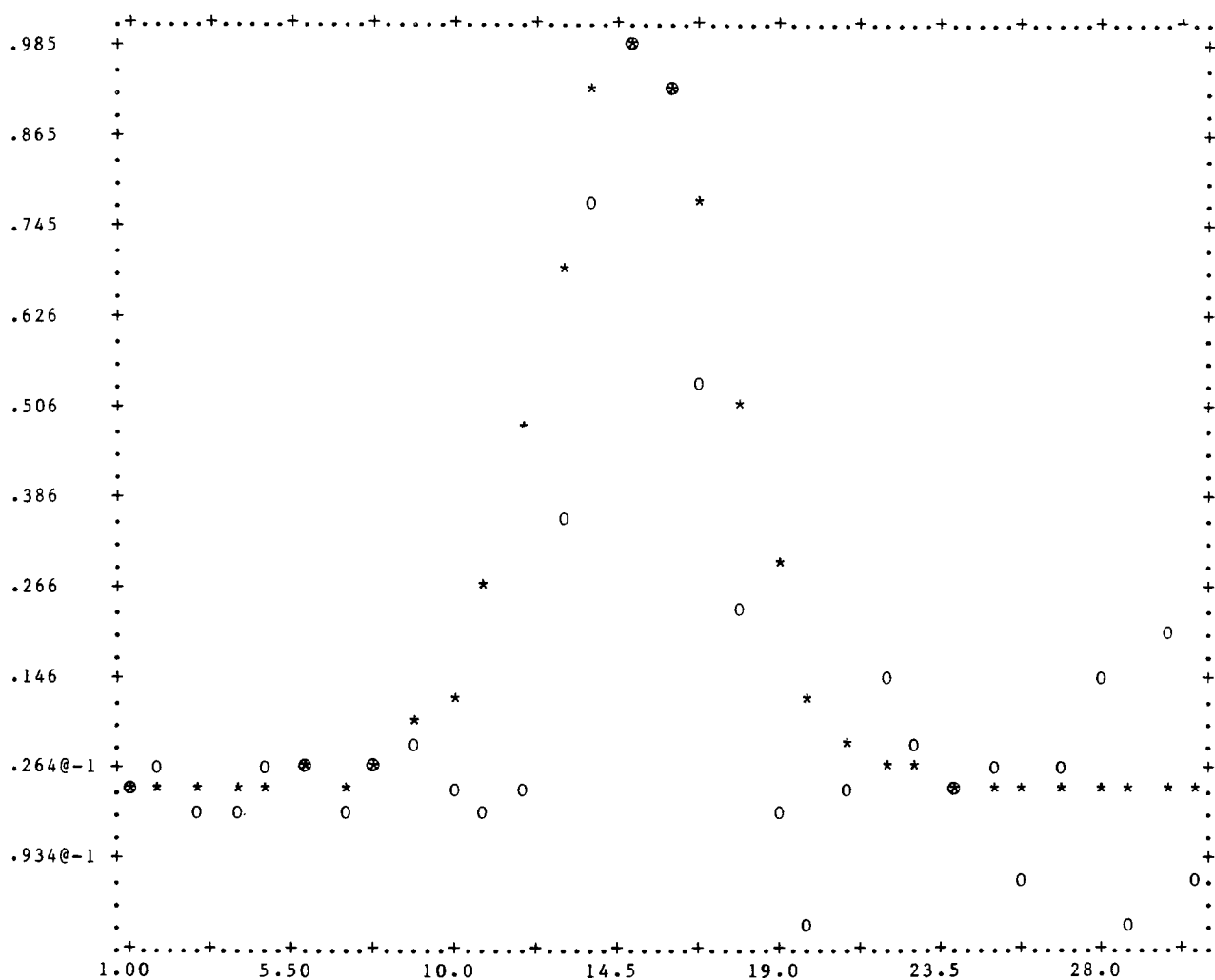


Figure 8.32 Euclidean regularization with spread cross-spectral data; $\lambda = 0$.

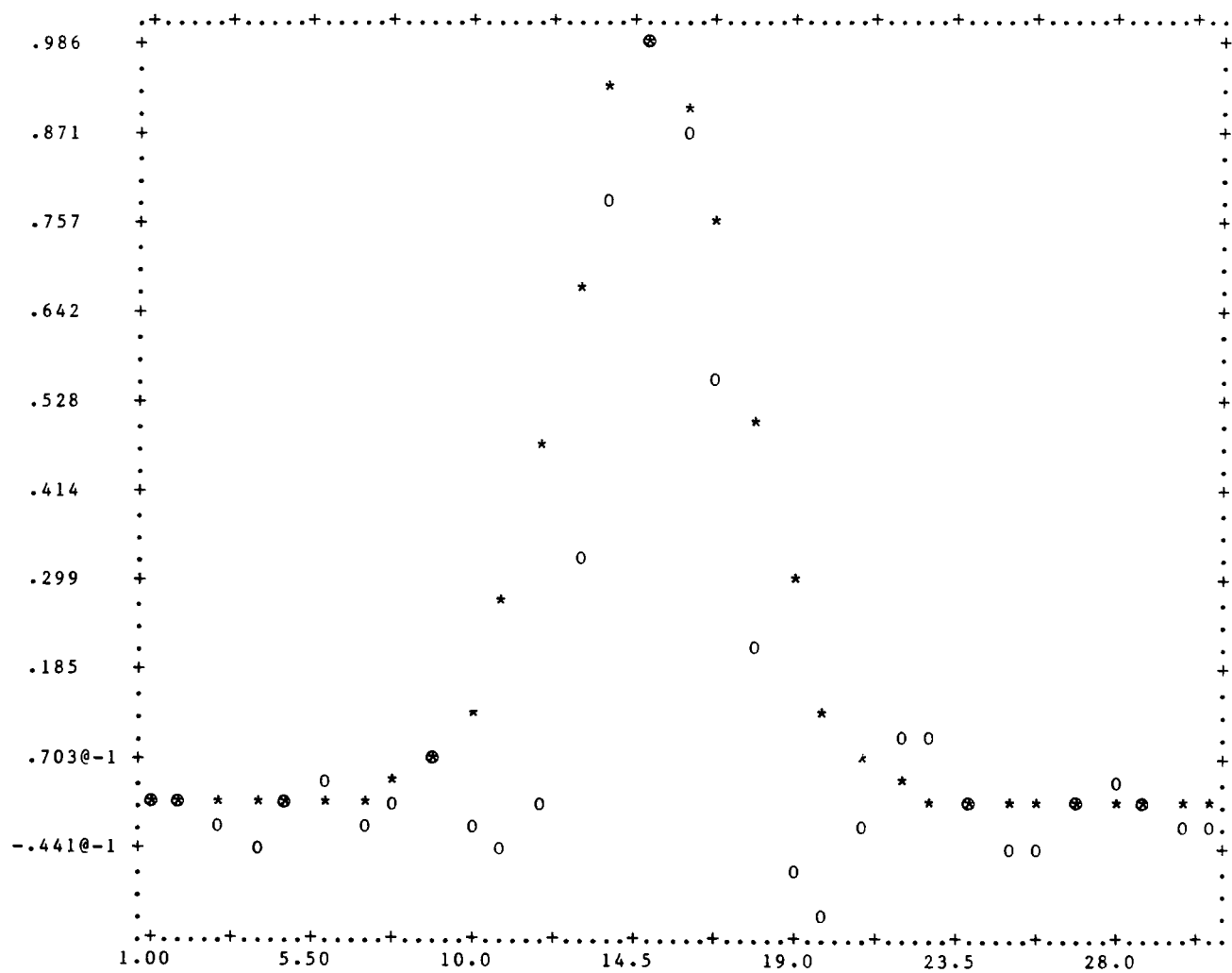


Figure 8.33 Euclidean regularization with spread cross-spectral data; $\lambda = .00001$.

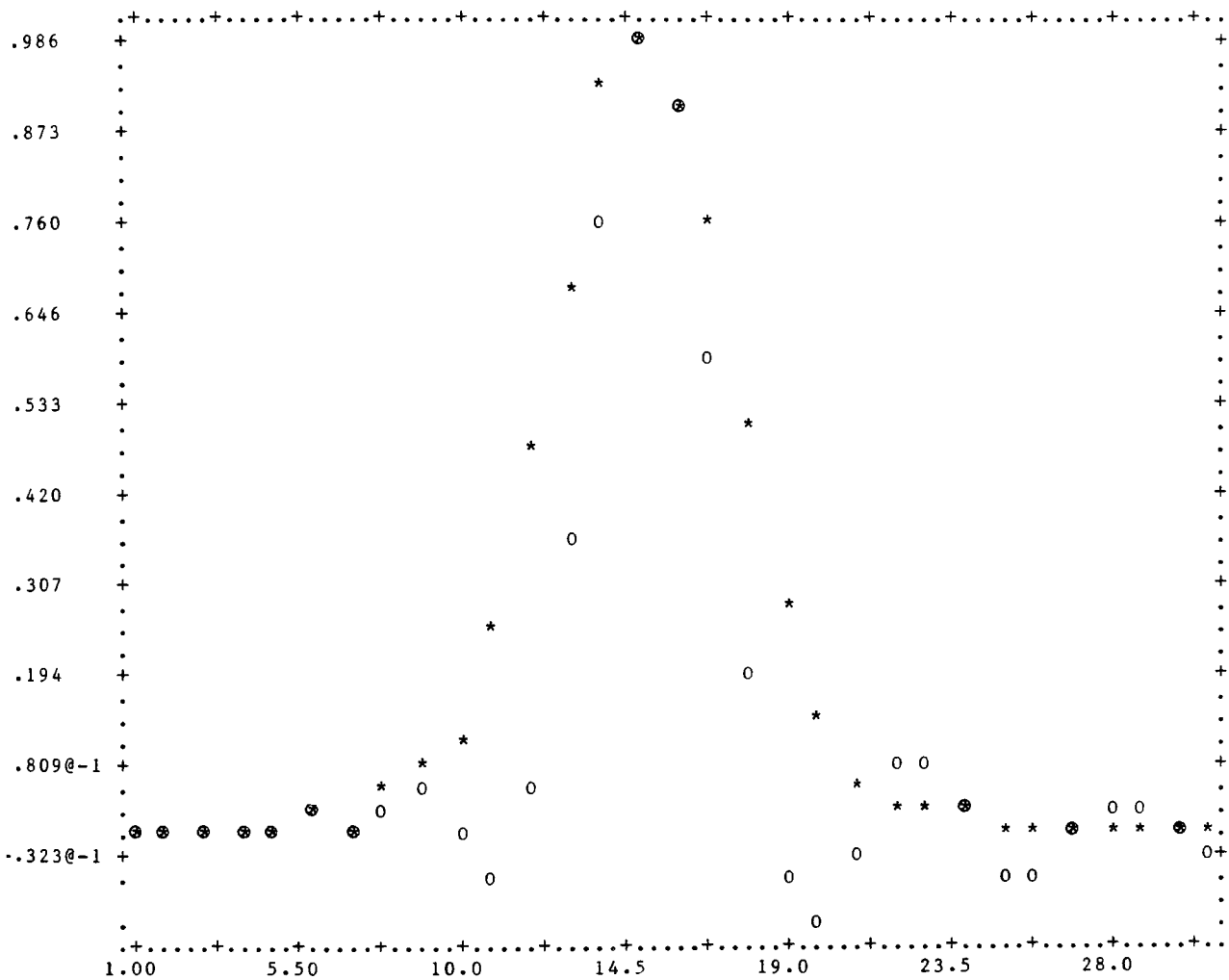


Figure 8.34 Euclidean regularization with spread cross-spectral data; $\lambda = .0001$.

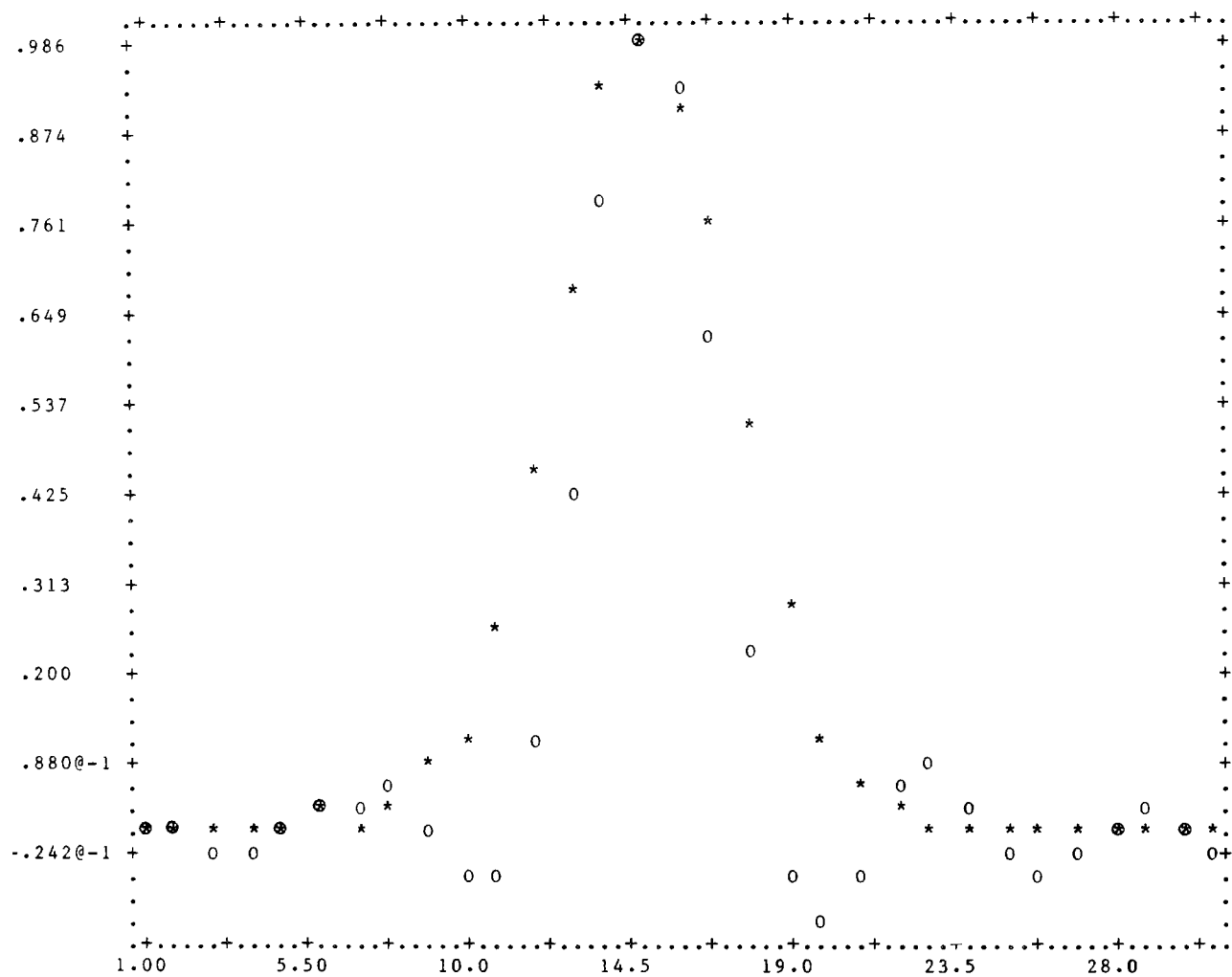
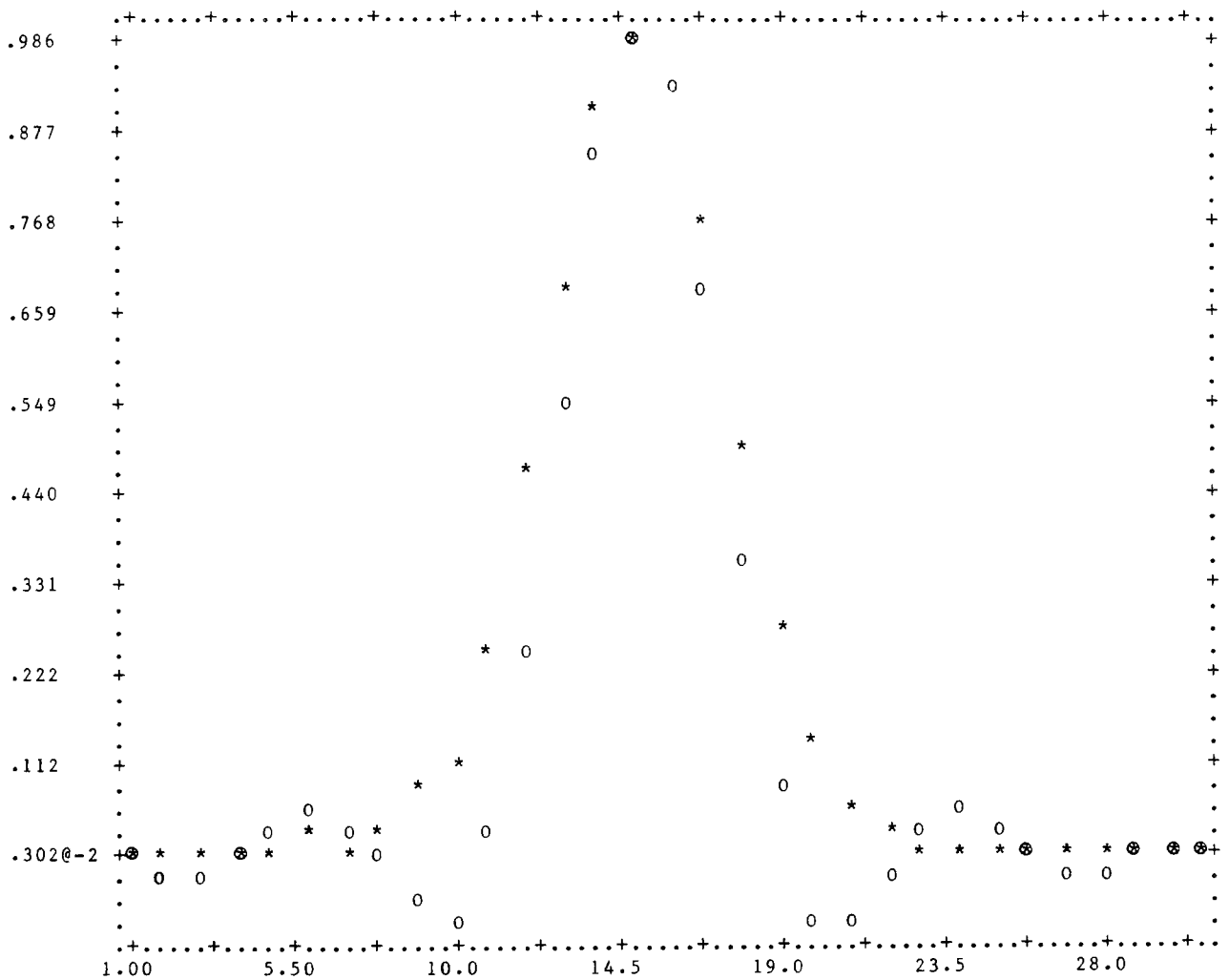


Figure 8.35 Euclidean regularization with spread cross-spectral data; $\lambda = .001$.



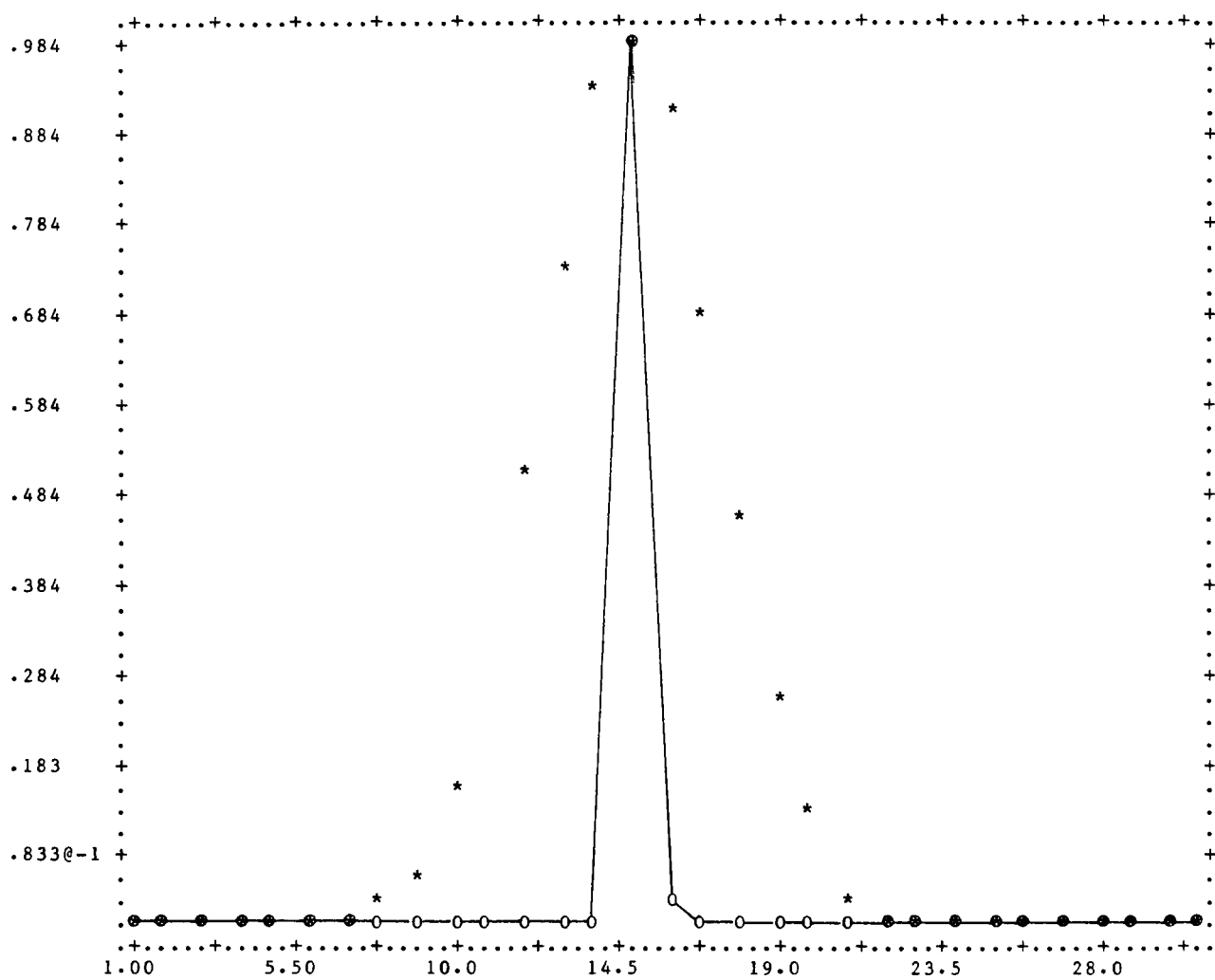


Figure 8.37 ERNN regularization with spectral data; $\lambda = 0$.

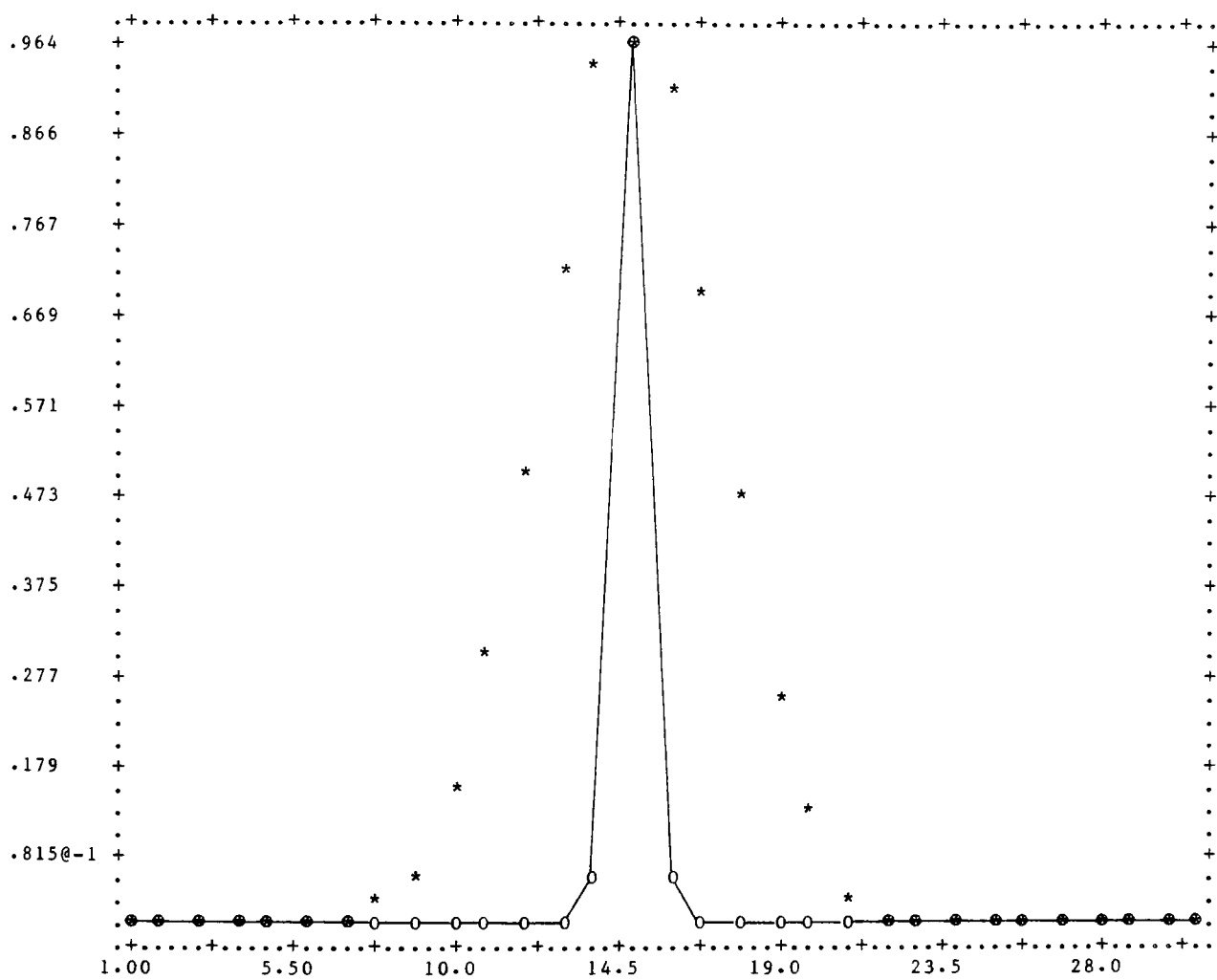


Figure 8.38 ERNN regularization with spectral data; $\lambda = .001$.

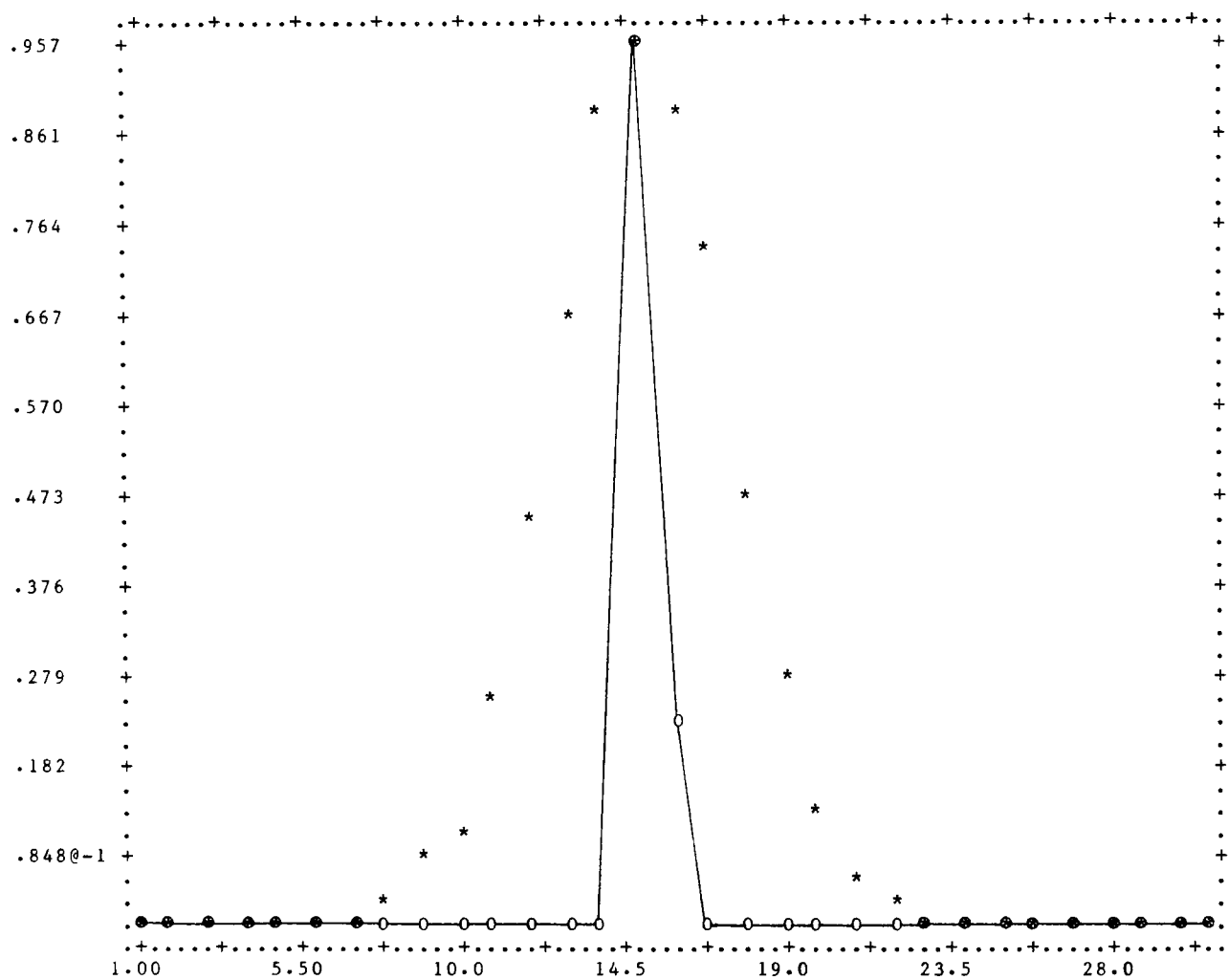


Figure 8.39 ERNN regularization with cross-spectral data;
 $\lambda = 0$.

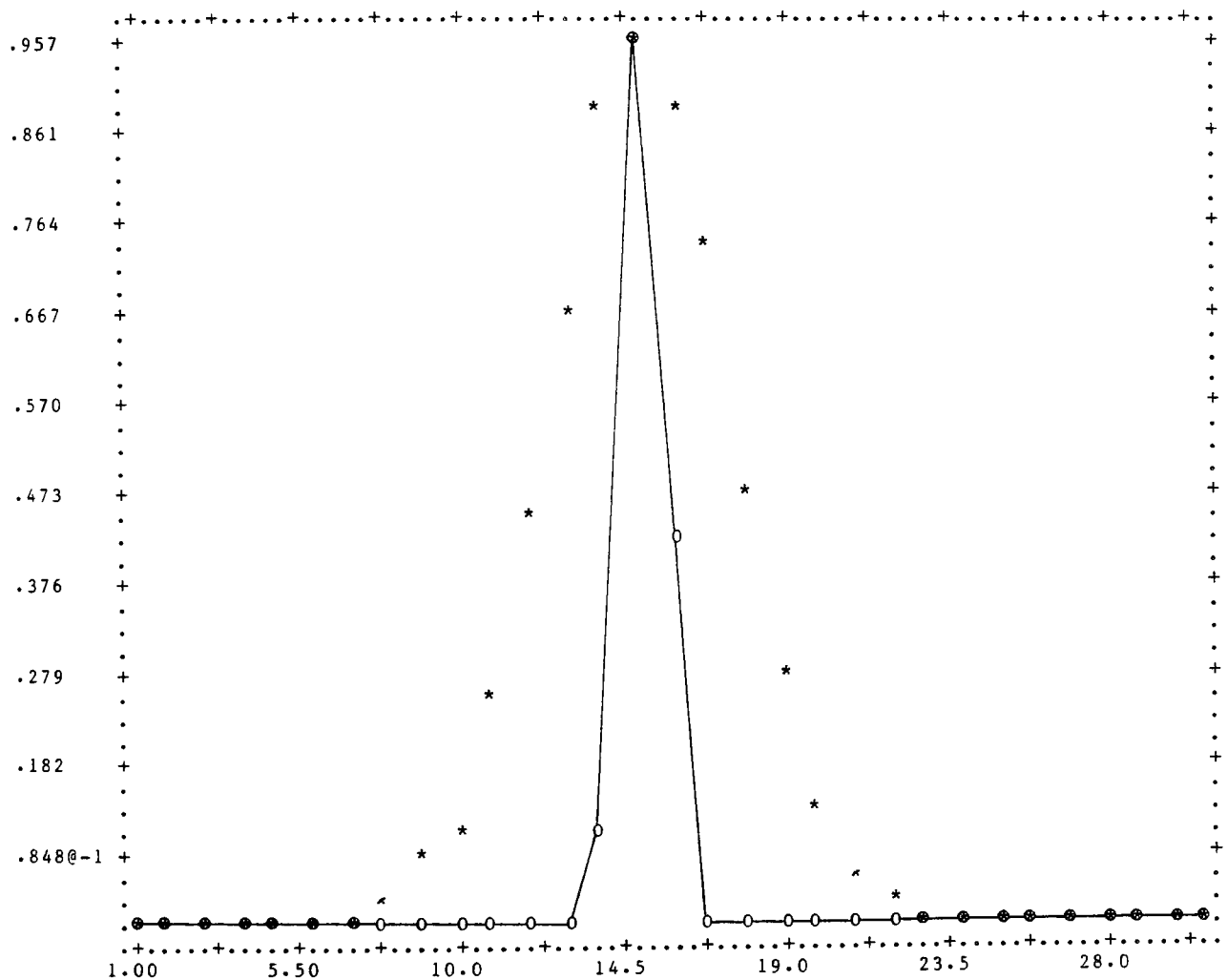


Figure 8.40 ERNN regularization with cross-spectral data;
 $\lambda = .003$.

BIBLIOGRAPHY

1. Baker, C.T., Fox, L., Mayers, D.F. and Wright, K., Numerical Solution of Fredholm Integral Equations of First Kind, Comput. J. 7 (1964) 141-148.
2. Bendat, J.S. and Piersol, A.G., Random Data: Analysis and Measurement Procedures, Wiley-Interscience, 1971.
3. Blinowska, K.J. and Wessner, E.F., A Method of On-Line Spectra Evaluation by Means of a Small Computer Employing Fourier Transforms, Nucl. Inst. and Meth. 118(1974) 597-604.
4. Bloomfield, P., The Fourier Analysis of Time Series, John Wiley and Sons, 1977.
5. Brillinger, D.R., Time Series: Data Analysis and Theory, Holt, Rinehart and Winston, 1975.
6. Chambless, D.A. and Broadway, J.A., Digital Filtering of Speckle-photography Data, Experimental Mechanics 19 (1979) 286-289.
7. Clark, E.L., Jr. and Croll, R.H., Jr., Applications of Digital Spectral Analysis and Filtering to Aerodynamic Testing, Technical Report SLA-73-7048A, Sandia Laboratories, Albuquerque, NM.
8. Cooley, T.W. and Tukey, J.W., An Algorithm for Machine Calculation of Complex Fourier Series, Math. Comp. 19, (1965) 297-301.
9. Cullum, Jane, Numerical Differentiation and Regularization, SIAM J. Numer. Anal. 8 (1971) 254-265.
10. Dines, K.A. and Kak, A.D., Constrained Least Squares Filtering, IEEE Trans. Acoust., Speech, Signal Processing ASSP-25 (1977) 346-350.

11. Ekstrom, M.P., A Numerical Algorithm for Identifying Spread Functions of Shift Invariant Imaging Systems, IEEE Transactions on Computers C-22 (1973) 322-328.
12. Golub, G.H. and Reinsch, C., "Singular Value Decomposition and Least Squares Solutions" in J.H. Wilkinson and C. Reinsch (editors) Handbook for Automatic Computation, Vol. II: "Linear Algebra", Springer, 1971.
13. Hanson, R.J., A Numerical Method for Solving Fredholm Integral Equations of the First Kind Using Singular Values, SIAM J. Numer. Anal. 8 (1971) 616-622.
14. Hilgers, J.W., On the Equivalence of Regularization and Certain Reproducing Kernel Hilbert Spaces Approaches for Solving First Kind Problems, SIAM J. Numer. Anal. 13 (1976) 172-184.
15. Inouye, T., The Super Resolution of Gamma-Ray Spectrum, Nucl. Inst. and Meth. 30 (1964) 224-228.
16. Inouye, I., Harper, T. and Rasmussen, N.C., Application of Fourier Transforms to the Analysis of Spectral Data, Nucl. Inst. and Meth. 67 (1969) 125-132.
17. Koopmans, L.H., The Spectral Analysis of Time Series, Academic Press, 1974.
18. Lanczos, C., Applied Analysis, Prentice Hall, 1961.
19. Lawson, C.L. and Hanson, R.J., Solving Least Squares Problems, Prentice Hall, 1974.
20. Perry, W.L., Approximate Solution of Inverse Problems with Piecewise Continuous Solutions, Radio Science 12 (1977) 637-642.

21. Peterson, G.E. et. al., Singular Value Decomposition and Boron NMR Spectra in Glass, *Journal of Non-Crystalline Solids* 23 (1977) 243-259.
22. Phillips, David L., A Technique for the Numerical Solution of Certain Integral Equations of the First Kind, *J. Assoc. Comput. Mach* 9 (1962) 84-87.
23. Rosenfeld, A., *Picture Processing by Computer*, Academic Press, 1969.
24. Rosenfeld, A. and Kak, A.C., *Digital Picture Processing*, Academic Press, 1976.
25. Schaeffel, J., Mullinix, B., Ranson, W. and Swinson, W.F., "Computer Aided Optical Nondestructive Flaw Detection System for Composite Materials", U.S. Army Missile Research and Development Command, Redstone Arsenal, AL, Technical Report T-78-5.
26. Singleton, R.C., An Algorithm for Computing the Mixed Radix Fast Fourier Transform, *IEEE Trans. Audio Electroacoust.* AU-17 (1969) 93-103.
27. Tihonov, A.N., Regularization of Incorrectly Posed Problems, *Soviet Math.* 4 (1963) 1624-1627.
28. Tihonov, A.N., Solution of Incorrectly Formulated Problems and the Regularization Method, *Soviet Math* 4 (1963) 1035-1038.
29. Tihonov, A.N. and Glasko, V.B., An Approximate Solution of Fredholm Integral Equations of the First Kind, *USSR Comp. Math, and Math. Phys.* 4 (1964) 236-247.
30. Twomey, S., On the Numerical Solution of the Fredholm Integral Equations of the First Kind by the Inversion of the Linear System Produced by Quadrature, *J. Assoc. Comput. Mach* 10 (1963) 97-101.

31. Varah, J.M., A Practical Examination of Some Numerical Methods for Linear Discrete Ill-Posed Problems, SIAM Review 21 (1979) 100-111.
32. Wahba, G., Practical Approximate Solutions to Linear Operator Equations When the Data are Noisy, SIAM J. Numer. Anal. 14 (1977) 651-667.
33. Wahba, G., "Optimal Smoothing of Density Estimates" in Classification and Clustering, Academic Press, 1977.
34. Wahba, G. and Wold, S., A Completely Automatic French Curve: Fitting Spline Functions by Cross Validation, Communications in Statistics 4 (1975) 1-17.
35. Yule, H.P., Mathematical Smoothing of Gamma Ray Spectra, Nucl, Inst. and Meth. 54 (1967) 61-65.

EJED EPA 520/5-80-003
Chambless, Donald A.
Radiological data analysis
in the time and...
- Due Name and Phone# Mcode

EJED EPA 520/5-80-003
Chambless, Donald A.
Radiological data analysis
in the time and...
Due Name and Phone# Mcode

U.S. ENVIRONMENTAL PROTECTION AGENCY
Office of Prevention, Pesticides & Toxic Substances
OPPTS Chemical Library (7407)
401 M Street SW
Washington DC 20460
(202) 260-3944

United States
Environmental Protection
Agency
Office of Radiation Programs

**Eastern Environmental
Radiation Facility**
P.O. Box 3009
Montgomery AL 36193

Postage and
Fees Paid
Environmental
Protection
Agency
EPA-G35



Official Business
Penalty for Private Use \$300

Third Class